

Newcastle University

Creating and Optimising a Fluid
Simulation For Use in Video Games

BSc Computer Science

Sakir Azimkar
200823588

Supervised by: Richard Davison

May 2025

Abstract

This dissertation explores the Navier-Stokes equations, which are used to describe the motion of fluids. It briefly looks at an Eulerian implementation introduced by Jos Stam[1], before shifting focus on to Lagrangian methods - specifically Smoothed Particle Hydrodynamics (SPH). Furthermore, this paper describes an implementation of this technique.

The main goal of this project is to produce a real-time fluid simulation that can be integrated into a video game, with minimal performance loss. It is an optimisation problem, motivated by an interest in the GPU and shader languages. The final project is a Smoothed Particle Hydrodynamics simulation that can reach 600 frames per second with over thirty-two thousand particles on modern hardware.

Declaration

“I declare that this dissertation represents my own work, unless explicitly stated otherwise.”

Acknowledgements

I would like to express my deepest gratitude to my supervisor, Richard Davison, for being reliable and helpful throughout the entire project. I'd also like to thank Gary Ushaw, my “second” supervisor, who was always encouraging and present at our meetings. Lastly, I'd like to thank my friends and family for supporting me during this time. This dissertation is dedicated to these people.

Contents

| | | |
|----------|---|-----------|
| 1 | Introduction | 10 |
| 1.1 | Motivation | 10 |
| 1.2 | Aim | 10 |
| 1.3 | Objectives | 11 |
| 1.4 | Changes | 11 |
| 1.5 | Dissertation Structure | 12 |
| 1.5.1 | Time Structure | 12 |
| 1.5.2 | Dissertation Outline | 12 |
| 2 | Background Review | 14 |
| 2.1 | Strategy | 14 |
| 2.2 | Exploring existing fluid simulations | 14 |
| 2.2.1 | WebGL Implementations | 14 |
| 2.2.2 | Unity Assets | 18 |
| 2.2.3 | Fluids in Video Games | 19 |
| 2.2.4 | Conclusion | 23 |
| 2.3 | Software Tools | 23 |
| 2.3.1 | Graphics API vs. Existing Game Engine | 23 |
| 2.3.2 | OpenGL vs. Vulkan | 24 |
| 2.4 | Fluid Simulation methods | 25 |
| 2.4.1 | Navier-Stokes Equations | 25 |
| 2.4.2 | Eulerian Implementations | 27 |
| 2.4.3 | Lagrangian Implementations | 29 |
| 2.4.4 | Chosen Implementation | 30 |
| 2.5 | Requirements | 31 |
| 2.5.1 | Functional Requirements | 31 |
| 2.5.2 | Non-Functional Requirements | 31 |
| 3 | What Was Done and How | 32 |
| 3.1 | Ethical Considerations | 32 |
| 3.2 | Software Development Model | 32 |
| 3.3 | Hardware | 32 |
| 3.4 | Graphics Rendering Pipeline | 33 |
| 3.4.1 | Vertex Shader | 33 |
| 3.4.2 | Geometry Shader | 34 |
| 3.4.3 | Shape Assembly | 35 |
| 3.4.4 | Rasterization | 35 |
| 3.4.5 | Fragment Shader | 35 |
| 3.4.6 | Tests and Blending | 35 |

| | | |
|----------|--|-----------|
| 3.5 | GLFW and GLAD | 36 |
| 3.6 | Learn OpenGL | 36 |
| 3.7 | Simulation Loop | 37 |
| 3.7.1 | Density and Pressure | 37 |
| 3.7.2 | Forces | 38 |
| 3.7.3 | Update Velocity and Position | 40 |
| 3.7.4 | Resolve Collisions | 41 |
| 3.8 | Spawn and Move Particles | 41 |
| 3.8.1 | CPU | 42 |
| 3.8.2 | GPU | 43 |
| 3.9 | Spatial Hashing | 44 |
| 3.9.1 | Spatial Hash CPU | 44 |
| 3.9.2 | Spatial Hash GPU | 45 |
| 3.9.3 | Cell Calculation | 46 |
| 3.9.4 | Hash Key Calculation | 47 |
| 3.9.5 | Storing the Hash Keys | 47 |
| 3.9.6 | Bitonic Sort | 48 |
| 3.9.7 | Update Lookup Table | 51 |
| 3.9.8 | Using the Spatial Hash | 51 |
| 3.10 | More Forces | 52 |
| 3.10.1 | Surface Tension | 52 |
| 3.10.2 | External Forces | 54 |
| 3.10.3 | Performance | 54 |
| 3.11 | Pre-Computed Constants | 55 |
| 3.12 | Circles | 56 |
| 4 | Results and Evaluation | 59 |
| 4.1 | Agile Development | 59 |
| 4.2 | OpenGL Simulation | 59 |
| 4.3 | Unity CPU Simulation | 60 |
| 4.4 | Unity GPU Simulation | 61 |
| 4.5 | Requirements | 65 |
| 4.6 | Hardware Statistics | 66 |
| 4.6.1 | Idle | 66 |
| 4.6.2 | CPU | 68 |
| 4.6.3 | GPU | 70 |
| 4.6.4 | Hardware Evaluation | 72 |

| | |
|--|------------|
| 5 Conclusion | 73 |
| 5.1 Aim and Objectives | 73 |
| 5.1.1 Aim | 73 |
| 5.1.2 Objectives | 73 |
| 5.2 What Was Learned | 74 |
| 5.3 Future Work | 75 |
| 6 References | 77 |
| A Unity Asset Store | 81 |
| B Learn OpenGL and graphics | 83 |
| C CPU Implementation with Unity | 86 |
| D GPU Implementation with Unity | 91 |
| D.1 Rendering Logic | 91 |
| D.2 Sphere Collider Logic | 93 |
| D.3 Collision Resolution | 94 |
| D.4 Rewritten Shader | 95 |
| D.5 Final Result | 98 |
| E Kernel Derivations | 103 |
| E.1 Spiky Kernel Gradient | 103 |
| E.2 Poly6 Gradient | 103 |
| E.3 Poly6 Laplacian | 104 |

List of Figures

| | | |
|----|---|----|
| 1 | Gantt chart of project timeline [2] | 12 |
| 2 | <i>WebGL</i> Fluid Simulation by PavelDoGreat on GitHub [3] . . . | 15 |
| 3 | <i>WebGL</i> Fluid Simulation by Grant Kot. [4] | 16 |
| 4 | <i>Interplanetary Postal Service</i> by Sebastian Macke [5] | 17 |
| 5 | <i>Obi Fluid</i> , Unity Asset [6] | 18 |
| 6 | <i>KWS Water System Standard</i> [7] | 19 |
| 7 | <i>From Dust</i> Gameplay [8] | 20 |
| 8 | A screenshot of water blocked by an invisible wall in Clair Obscur: Expedition 33 | 21 |
| 9 | Helicopter physics in Far Cry 6 [9] | 22 |
| 10 | Empty Unity[10] scene | 23 |
| 11 | Computational grid with densities and velocities defined in their centres [1] | 27 |
| 12 | Density exchange through diffusion between neighbours [1] . . | 28 |
| 13 | Eulerian simulation [11] | 29 |
| 14 | Graphics Rendering Pipeline [12] | 33 |
| 15 | Rainbow Triangle rendered with OpenGL | 35 |
| 16 | Final progress with OpenGL | 36 |
| 17 | Particle instantiation | 42 |
| 18 | First frame of the simulation using prefabs | 42 |
| 19 | First frame of the simulation using GPU instancing | 43 |
| 20 | Visualisation of neighbour array for pink particle | 45 |
| 21 | Spatial Hash Visualisation [13] | 46 |
| 22 | FindCell HLSL | 47 |
| 23 | FindHash HLSL | 47 |
| 24 | HashParticles HLSL | 48 |
| 25 | C# parallelisation | 50 |
| 26 | Bitonic Sort computation HLSL | 50 |
| 27 | FillLookupTable HLSL | 51 |
| 28 | Pre-computed Variables [14] | 55 |
| 29 | Camera Logic Vertex Shader [14] | 56 |
| 30 | Circle Logic Fragment Shader [14] | 57 |
| 31 | Colour Palette Formula [15] | 57 |
| 32 | Rainbow gradient and circle particles | 58 |
| 33 | First Frame Small Box | 62 |
| 34 | First Frame Big Box | 63 |
| 35 | Particle Count vs. Frame Rate [16] | 63 |
| 36 | Grid Simulation Issues | 64 |
| 37 | CPU core usage IDLE | 66 |

| | | |
|----|---|-----|
| 38 | CPU core temperatures IDLE | 67 |
| 39 | GPU statistics IDLE | 67 |
| 40 | CPU core usage CPU IMPL | 68 |
| 41 | CPU core temperatures CPU IMPL | 69 |
| 42 | GPU statistics CPU IMPL | 69 |
| 43 | CPU core usage GPU IMPL | 70 |
| 44 | CPU core temperatures GPU IMPL | 71 |
| 45 | GPU statistics GPU IMPL | 71 |
| 46 | Most popular results for "fluid simulation" [17] | 81 |
| 47 | Cheapest results for "fluid simulation" [17] | 82 |
| 48 | Example of surface-only Unity asset [18] | 83 |
| 49 | Initial Triangle Rendering | 83 |
| 50 | Rainbow Triangle and Colour-changing triangle | 84 |
| 51 | Textures | 84 |
| 52 | Graphics moving with time | 84 |
| 53 | Phong Lighting and moveable light source | 85 |
| 54 | More lighting | 85 |
| 55 | Rendering Object Files | 85 |
| 56 | CPU collision detection C# | 86 |
| 57 | Simulation Loop | 87 |
| 58 | Neighbour Table | 88 |
| 59 | Density and Pressure | 88 |
| 60 | Get Neighbours | 89 |
| 61 | Pressure and Viscosity Forces | 90 |
| 62 | Particle struct sent to shader | 91 |
| 63 | Update loop to render the particles | 91 |
| 64 | Buffer setup for shaders | 92 |
| 65 | Render the grid of particles with slight jitter | 93 |
| 66 | Sphere Collider Logic | 93 |
| 67 | Particle movement and collision resolution in the same method | 94 |
| 68 | setup and Particle struct | 95 |
| 69 | appdata, v2f structs and vertex shader | 96 |
| 70 | Fragment Shader and Palette method | 97 |
| 71 | Small box, first few seconds | 98 |
| 72 | Small box, slowed down | 98 |
| 73 | Box X-dimension increase | 99 |
| 74 | Box X-dimension abruptly decreased | 99 |
| 75 | Box Z-dimension increase | 100 |
| 76 | Ripples as particles pushed away by sphere | 100 |
| 77 | Sphere displacement | 101 |
| 78 | No particles inside the sphere radius | 101 |

| | | |
|----|--|-----|
| 79 | Box X-dimension increase then Z-dimension increase | 102 |
| 80 | 3 FPS and instability with 884736 particles | 102 |

1 Introduction

This section highlights the motivations, aims and objectives of this project. It talks about the overall dissertation structure and compares the differences between this project and the initial proposal.

1.1 Motivation

Fluid dynamics are observed in all aspects of daily life and in research. It is crucial to be able to simulate and understand the behaviour of all fluids, including liquids and gases. There already exists a number of different techniques to achieve this, through utilisation of the Navier-Stokes equations. These methods have been crucial in research and in industry. For example in aerospace, which utilises Computational Fluid Dynamics (CFD) for aerodynamic analysis, aircraft design optimisation and thermal management, to name just a few. As our knowledge of fluids and CFD techniques improve, the global market is expected to increase by nearly triple its current value by 2033[19]. Simulations are also essential for cost reduction, as they reduce the need for physical prototypes, which are significantly more expensive to produce.

In the gaming industry, realistic fluid dynamics are essential to enhance immersion; being able to interact with the ocean in a beach environment is a lot more engaging than the common use of invisible barriers that prevent interaction with the water in many games. A fantastic example of excellent water physics is *Far Cry 6*[20], as it looks very realistic and is affected by external forces from objects such as vehicles and people swimming.

However, affordable options for advanced fluid simulation are quite difficult to come by for indie developers, who do not have the same funding as triple A companies like *Ubisoft*. As a result, the motivation for this project is to produce a free, lightweight simulation for all types of fluid (not just water). It will also aim to maintain a high performance, so it may be seamlessly implemented into an existing video game with minimal performance loss. This is essential in the gaming industry as lag and low frame rates hinder the overall gameplay experience.

1.2 Aim

The aim of this dissertation is to utilise the Navier-Stokes equations and Smoothed Particle Hydrodynamics to produce an accurate fluid simulation. The performance (specifically frame rate) of the simulation will be measured

and there will be attempts to optimise it. The resulting code should be a 3D fluid flow video game asset that works for Unity.

1.3 Objectives

1. **Explore Existing Fluid Simulations** - This dissertation will test and experiment with free and accessible simulations available on the internet. It will compare and identify issues with them from the perspective of a game developer searching for a tool to implement into their own game.
2. **Navier-Stokes and SPH** - This dissertation will explain what the Navier-Stokes equations are and describe two ways to utilise them in a fluid simulation.
3. **OpenGL and C++/GLFW** - This dissertation will briefly mention a graphics API that was used initially in this project and explain why it was chosen. It will then talk about the issues experienced with this API and why it was not utilised in the final project.
4. **Unity and Compute Shaders** - This dissertation will talk about the use of Unity and compute shaders to produce a fluid simulation that runs on the GPU.
5. **Frame Rate and Performance Investigations** - Throughout this dissertation, the main focus will be on improving the frame rate of the simulation. It will talk about what methods were used to improve the frame rate, such as reprogramming the simulation in shader languages. The overall goal will be to improve the performance of the simulation.

1.4 Changes

In the initial project proposal, it was stated that the simulation would be programmed in *C++*, using *GLFW*[21] to create windows and display the graphics created by the graphics API that I would be using, *OpenGL*[22]. However, later in development this decision was changed to utilising the *Unity* game engine[10] and compute shaders. Reasoning will be provided in the What was Done and How section.

Additionally, the project proposal stated that the simulation would be first created in two dimensions and later upgraded to three. It was decided to skip this step as the development process was mostly the same, the only difference being whether the vectors contained two or three values. This was to save development time and allow more focus on optimisation.

1.5 Dissertation Structure

1.5.1 Time Structure

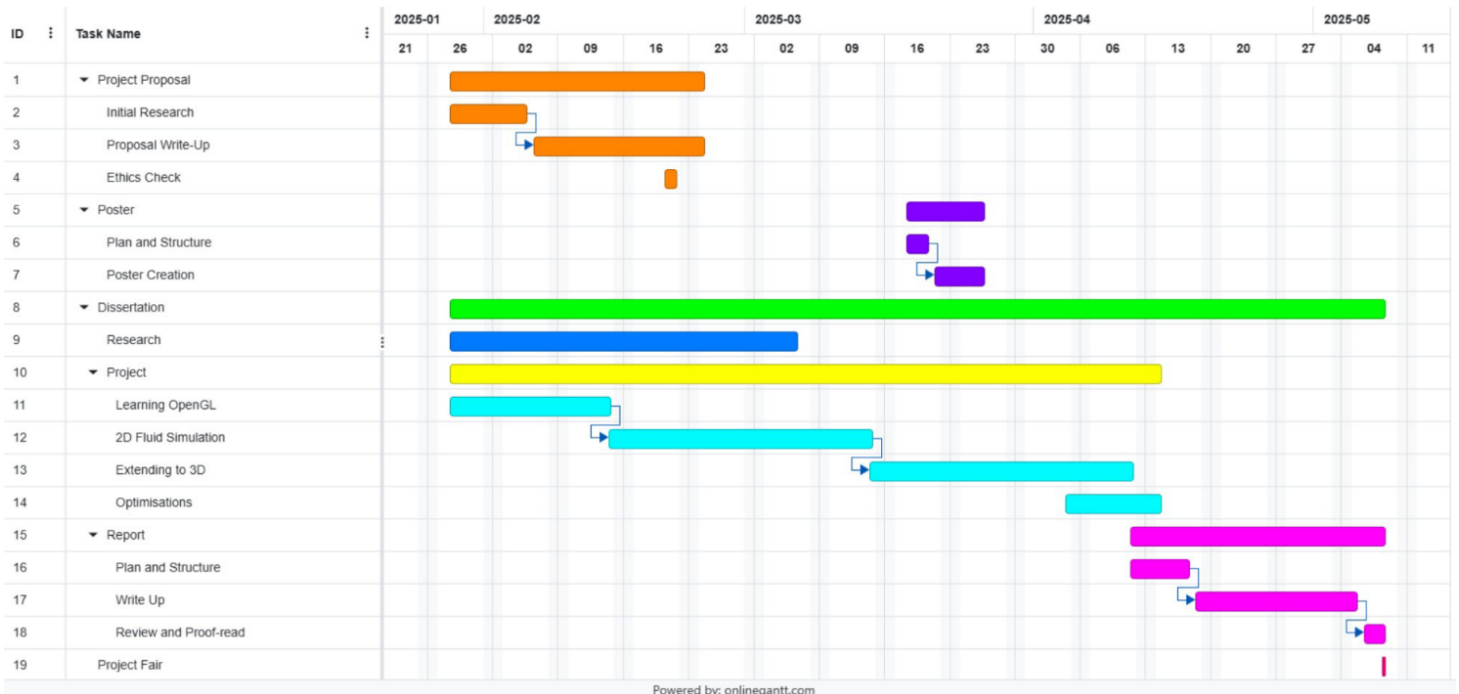


Figure 1: Gantt chart of project timeline [2]

1.5.2 Dissertation Outline

- **Introduction**

An introduction to the dissertation, outlining the motivation, aim, objectives and overall project structure.

- Motivation
- Aim
- Objectives
- Changes
- Structure

- **Background Review**

A breakdown of research performed before and during the project.

- Existing fluid simulations

- Software Tools
- Requirements

- **What was Done and How**

An explanation of how the simulation was implemented, including the methods learned and processes involved.

- Mathematics and Physics
- OpenGL
- Unity
- Compute Shaders
- GPU Instancing
- Optimisations

- **Results and Evaluation**

A complete analysis of frame rate improvements over the course of the project and results obtained.

- Frame Rate
- Simulation Types Produced
- Advantages and Disadvantages of Each Implementation
- Requirements

- **Conclusion**

A conclusion that describes fulfilment of objectives, what was learned and future work.

- Aims and Objectives
- Achievements
- What was Learned
- Future Work

2 Background Review

This section shows the research made on this dissertation. It talks about relevant background resources that were used for different parts of the development process.

2.1 Strategy

There are three main components that needed to be researched at the start of this project:

- Exploring existing fluid simulations
- Software Tools
- Fluid simulation methods

All three of these sections are integral in achieving a functional, lightweight simulation that is suitable for a video game. Below is an outline of the papers, videos and other resources that were used to understand these topics.

2.2 Exploring existing fluid simulations

It is important to understand current existing options that are available and describe their benefits and limitations in the context of video games.

2.2.1 WebGL Implementations

“WebGL (Web Graphics Library) is a JavaScript API for rendering interactive 2D and 3D graphics within any compatible web browser without the use of plug-ins. WebGL is fully integrated with other web standards, allowing GPU-accelerated usage of physics, image processing, and effects in the HTML canvas”.[23]

There are a lot of fantastic *WebGL* implementations of fluid motion that are easily accessible due to their availability in a web browser. An example is the one developed by PavelDoGreat on GitHub.

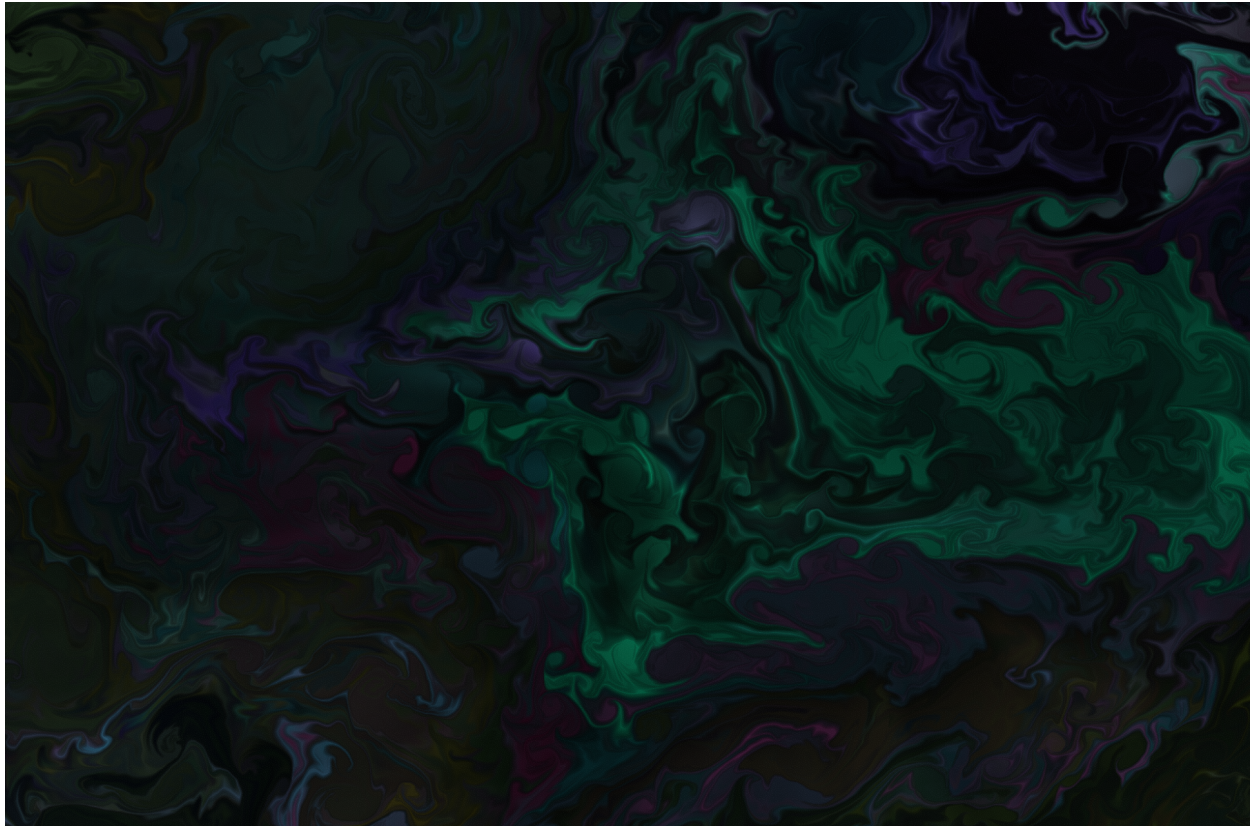


Figure 2: *WebGL* Fluid Simulation by PavelDoGreat on GitHub [3]

This simulation showcases a gaseous fluid made up of different, randomly-generated colours. They appear to mostly be for aesthetic purposes. The screen begins completely black and requires the user to input an external force by left-clicking and moving the cursor across the screen. There is a control panel on the top right corner, which allows the user to change various settings, such as density diffusion and vorticity. This is a great visual aid for educational purposes as it allows the user to see the visual impacts that these variables have on the fluid in real time. As an educational tool, this is an excellent visual aid; the immediate feedback and colourful representation make it easy to understand complex fluid dynamics concepts. In the context of video games, however, the colours are a bit unnecessary. This can be easily rectified if someone were to use it in their game, but they would need to make a number of modifications to the existing code to make it independent of user input (for the more common uses of fluids in games).

Here is another example of a *WebGL*-based fluid simulation available for free online, developed by Grant Kot.

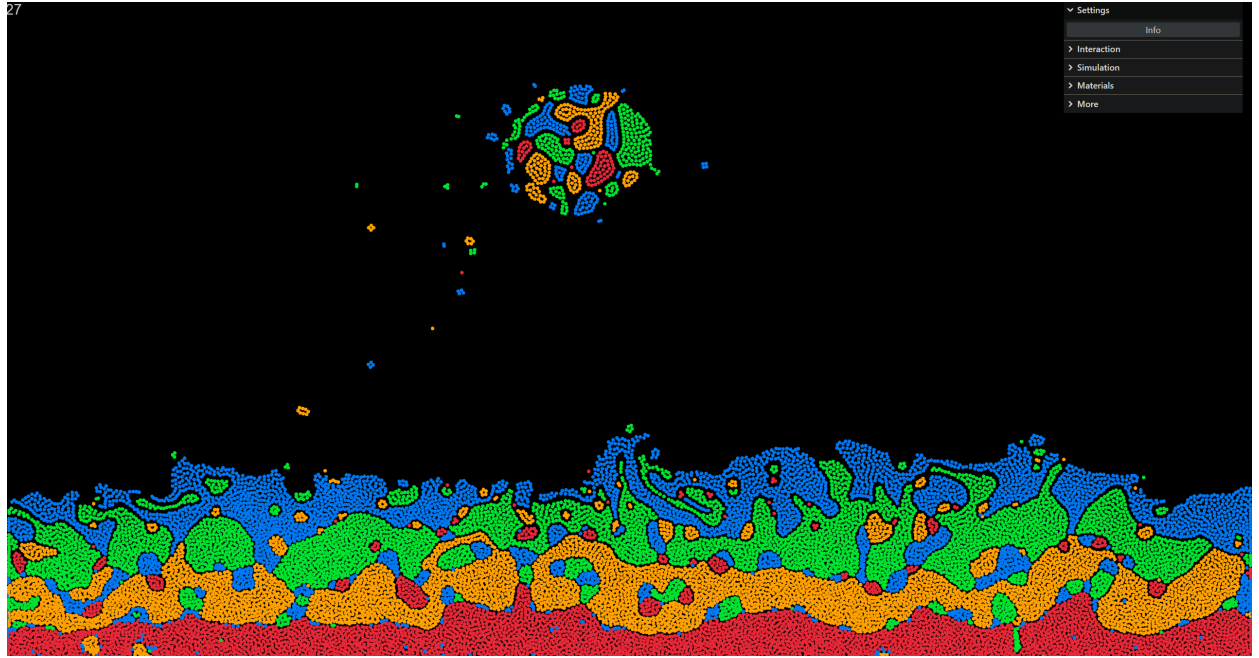


Figure 3: *WebGL Fluid Simulation* by Grant Kot. [4]

This simulation excels in visualising fluid interactions, particularly between liquids of varying masses - represented by four distinct colours. You can use the mouse and different key binds to manipulate the fluid with a range of forces, such as lifting a portion of it up (as shown in figure 3), or creating dynamic collision objects that follow the cursor. It behaves with realistic motion that is driven by gravity and internal pressure and user interaction is only optional.

Conversely, there is a performance issue with this project. During testing, the simulation peaked at around 50 frames per second. This is completely fine when exploring the fluid in a web browser or for educational demos, but becomes a much larger issue when using it as a video game asset, as video games prefer to be consistently above 60 frames per second - to maintain responsiveness and overall gameplay fluidity. Further optimisations would be required of this simulation in order to utilise it in a video game environment.

WebGL simulations, however, work exceptionally in very simple browser games. Here is an example called *Interplanetary Postal Service*[5], which was created by Sebastian Macke, for a coding competition with a strict 13KB size limit.

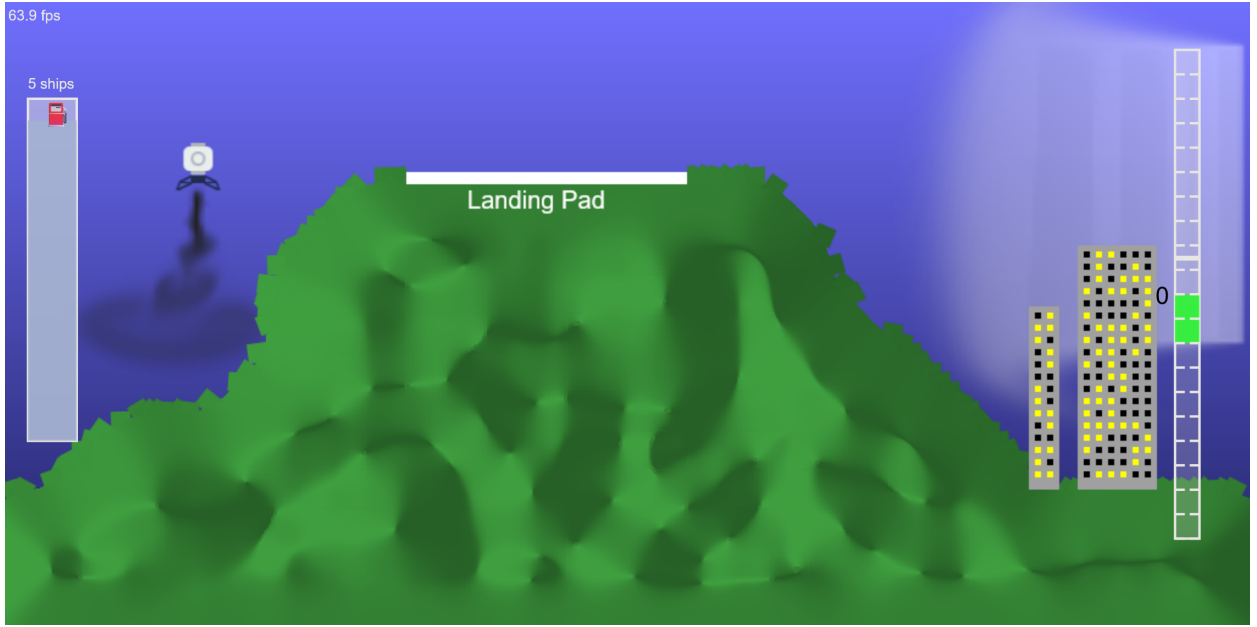


Figure 4: *Interplanetary Postal Service* by Sebastian Macke [5]

As the game's core mechanics are very simple (use WASD to power the post lander on to the landing pads), there is very little need for optimisations. This allows it to run consistently at over 60 frames per second. This demonstrates how WebGL-based simulations can deliver high performance and smooth interactivity when used for lightweight, focused experiences - which most video games aren't.

While all of these examples are incredibly impressive, they would not function well in more complicated, non-web-based video games. The first two are built as stand-alone browser-based visualisations for the purposes of aesthetics and education. Although all of these can be rewritten and ported to OpenGL-based games, there is a lot of upfront work required to do so; they do not work out-of-the-box. They are also only two-dimensional, which means further modifications would be required necessary to adapt them for 3D environments. Furthermore, for games written using pre-existing game engines such as Unity, most of the existing JavaScript simulation code would have to be rewritten into a language that is compatible with the engine, such as C#. One of the aims of this dissertation is to produce a 3D asset that is ready to use in Unity without requiring extensive modifications.

2.2.2 Unity Assets

There are a few choices on the *Unity Asset Store*[17]. However, there are a few issues with each of the available options.

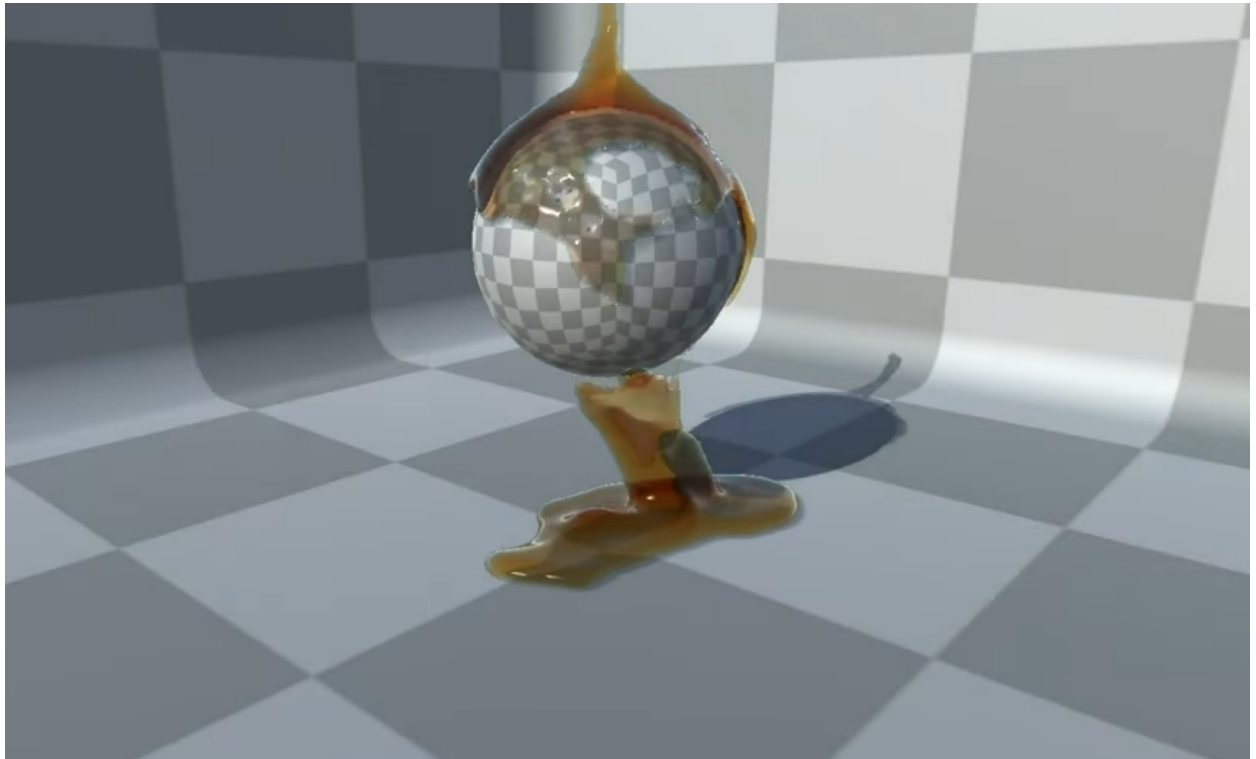


Figure 5: *Obi Fluid*, Unity Asset [6]

The most popular option appears to be *Obi Fluid*, which advertises “multi-threaded AAA quality fluid simulations” on its store page. From the screenshots and videos provided, this does appear to be the case. However, with its steep price tag, it is difficult to verify as many developers are understandably hesitant to spend over £40 on a single asset. Additionally, the store page mentions that the simulation may have performance issues in larger projects and should only be used for smaller scale projects or 2D game simulations, making it an unfit choice for 3D games or large bodies of fluid.



Figure 6: *KWS Water System Standard* [7]

Another fantastic asset is the *KWS Water System*. It has a lot of incredibly useful features, such as refraction, volumetric lighting and screen space reflections. Furthermore, it has optimisations implemented such as instanced rendering and view culling, so it is possible to simulate much larger bodies of fluid with minimal performance issues. This would be an outstanding asset for video games, if it weren't for the even steeper price tag of over £60.

In addition to these examples, there are many available assets that don't simulate actual fluid motion or behaviour, but instead create the illusion of it by only simulating the surface. This is a suitable option for games that don't require fluid interaction, but that falls outside the scope of this dissertation. One of the main motivations of this project is that the simulation is accessible to all kinds of developers, so it will be free unlike these examples.

2.2.3 Fluids in Video Games

It is also important to understand the fluid simulations that are actively present in existing video games. There aren't many games allow the player to interact with the water physically, due to the high performance cost required to implement these features.



Figure 7: *From Dust* Gameplay [8]

From Dust[24] is a god game where the player manipulates matter such as lava, soil and water. In the gameplay video[8], it is clear that the sand when placed and moved around displaces the water realistically. While the visual quality of the static sea surface may appear simplistic by modern standards, the game's real-time manipulation of large quantities of matter was groundbreaking for its era over thirteen years ago. Albeit impressive visually, there was a lot of computational resources required to run such a large scale simulation. As a result, there was quite a few complaints about the game being capped at 30 frames per second[25], which was very low even back then.



Figure 8: A screenshot of water blocked by an invisible wall in *Clair Obscur: Expedition 33*

Even nowadays there are a lot of video games that don't utilise realistic fluid flows because of their high computational resource requirement. An example of this is a game that released just this month, *Clair Obscur: Expedition 33*[26]. While the simulation is visually stunning, it is not possible to interact with the water. There is a loss of immersion here, especially considering the position of this water. It is located at the end of the prologue, after the character has left the island they have resided on their entire life to explore the abandoned mainland. The character, having never before set foot beyond their home, should be experiencing a profound sense of unfamiliarity due to a heavy environment change. The static and artificial appearance of the river diminishes this intended narrative impact, disconnecting the character from the player.



Figure 9: Helicopter physics in *Far Cry 6* [9]

A modern game that does an excellent job at fluid simulation is *Far Cry 6*. As shown in Figure 9, the wind produced by the helicopter’s turbines visibly pushes the water away from the vehicle. Furthermore, the player is able to swim and dive into the fluid, as well as observe external forces acting upon it when objects, such as explosives, are thrown into the water. This would be an ideal fluid simulation approach for many games seeking realistic water interactions. However there are a few issues with this. Since *Far Cry 6* is a proprietary, AAA game, its source code is not visible to the public, as thus the simulation is not accessible by anyone else.

Since the release of this game, the former water lead tech, Zhenyu Mao, has moved on to other projects with *Lightspeed Studios*, and has developed a new water rendering solution for games. In an interview[27], Mao mentions “Thanks to Dr. Wu’s expertise, we have developed a proprietary solution that generates natural water flow that interacts harmoniously with the environment. Our water simulation can generate accurate flow around objects, creating realistic turbulence and generating foam in the appropriate places.” This sounds incredibly promising, but is currently still a proprietary, in-house solutions available to *Lightspeed Studios* only. There is a presentation available online about the physics behind this solution[28], but that is not in the scope of this dissertation.

2.2.4 Conclusion

While there are a lot of fluid simulations available online, few are practical for use within 3D video games; they are often computationally taxing and thus would not be a feasible asset to utilise without significant prior optimisation and modifications. The options that do satisfy these conditions are usually proprietary and restricted to the studio it was developed in - or come at a premium cost inaccessible to some developers. Therefore, the motivation for this dissertation is to develop a freely accessible, efficient 3D fluid simulation that can be integrated into modern video games without significant performance trade-offs.

2.3 Software Tools

Choosing the correct set of tools is essential for an optimisation problem. They must be lightweight in nature and avoid unnecessary overhead in order to achieve the best performance possible.

2.3.1 Graphics API vs. Existing Game Engine

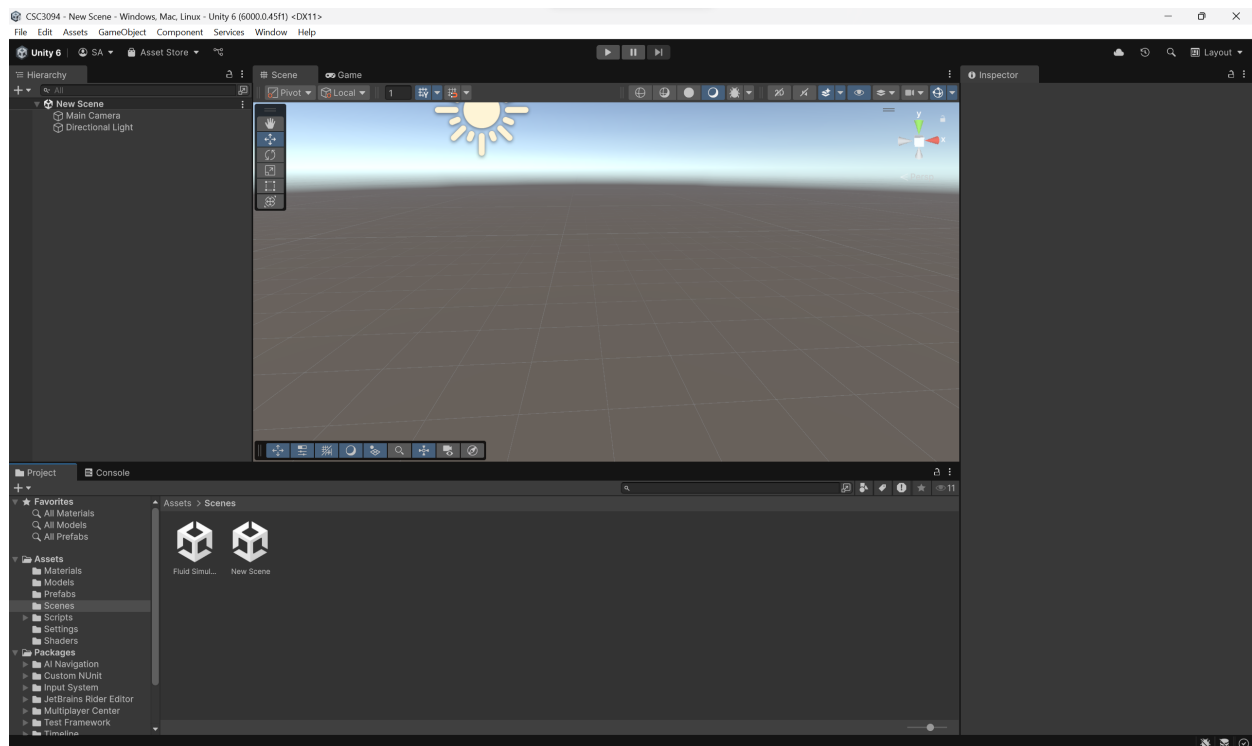


Figure 10: Empty Unity[10] scene

Game engines have the advantage of simplicity, leading to a faster development cycle. There are a lot of available pre-built tools, editors and assets that allow rapid prototyping and game development. For the purposes of this dissertation, many of these tools are not necessary. For instance, the physics engine will not be utilised as all physics will be manually coded. However, many of these tools would be beneficial for this project. For example, all linear algebra calculations related to camera depth and appearance have already been implemented. This means that by simply loading a model into the scene, it will automatically be rendered in 3D with realistic lighting. This saves the hassle of writing it all from scratch if a graphics API were to be implemented.

Game engines also benefit from large, active communities. There are plenty of tutorials, forums and online resources created by other developers. This makes it easier to find solutions to common problems, whether they involve problem solving or bug fixing. Graphics APIs are not as commonly utilised due to their increased complexity and thus have fewer resources available. However, there are two great tutorials for both *OpenGL* and *Vulkan*[29] that fully explain and provide an implementation for the setup of the graphics rendering pipeline [12][30].

Graphics APIs have the added benefit of greater control and customisation due to their lack of abstraction and increased level of understanding required. Every phase in the graphics rendering pipeline can be controlled manually, giving the developer more freedom and flexibility. There is also no overhead from the game engine, which may also slightly improve performance. Furthermore, once a project is begun within an engine, it is bound by its licenses, giving the developer less freedom.

Due to an enthusiasm to learn more about the graphics rendering pipeline and more low-level graphics interactions, it was decided at this point that a graphics API would be utilised over a game engine. Aforementioned in the project proposal, this was with the caveat that a swap to a game engine (specifically *Unity*, due to prior experience) would occur if insufficient progress was made in the strict time frame of this project. Considering the changes made to this dissertation in comparison to the project proposal, it is clear that this alteration was eventually realised.

2.3.2 OpenGL vs. Vulkan

As a graphics API was decided, the next choice was between *OpenGL* and *Vulkan*. *DirectX* was not considered due to its lack of cross-platform compatibility, as it was specifically designed for *Windows* and *XBox*. This was a relatively simple decision, as *OpenGL* is considered the beginner option, and

Vulkan is not recommended for new graphics programmers by Alexander Overvoorde, the writer of *Vulkan Tutorial*: “Vulkan is targeted at experienced graphics programmers. You should start with an easier language than *C++* and an easier API than Vulkan” [31]. Although *Vulkan* is a better choice for future-proofing (as *OpenGL* is no longer receiving updates), this reasoning was not significant justification; the project can be rewritten in the future with more time and experience. Thus, *OpenGL* was selected, accompanied by the *C++* language due to previous experience with the language.

2.4 Fluid Simulation methods

This section talks about two simulation methods involving the Navier-Stokes equations.

2.4.1 Navier-Stokes Equations

$$\frac{\partial \mathbf{u}}{\partial t} + (\mathbf{u} \cdot \nabla) \mathbf{u} = v \nabla^2 \mathbf{u} - \frac{1}{\rho} \nabla p + \mathbf{f} \quad (1)$$

Equation 1 is a non-linear partial differential equation that describes fluid motion[32]. The first term, $\frac{\partial \mathbf{u}}{\partial t}$, represents the change in velocity over time at a fixed point, where \mathbf{u} is the velocity field of the fluid. $-(\mathbf{u} \cdot \nabla) \mathbf{u}$ is called the advection term. Advection is described as “the transport of a substance or of heat by the flow of a liquid”[33]. In fluid dynamics, this may also refer to the transport of a property due to fluid flow. ∇ is a vector of partial derivatives: $\nabla = (\frac{\partial}{\partial x}, \frac{\partial}{\partial y}, \frac{\partial}{\partial z})$. Taking the dot product of \mathbf{u} , a vector, and this operator, $\mathbf{u} \cdot \nabla$, gives us a directional derivative - it describes the direction that a property is changing.

$$(\mathbf{u} \cdot \nabla) \mathbf{u} \equiv u_x \frac{\partial \mathbf{u}}{\partial x} + u_y \frac{\partial \mathbf{u}}{\partial y} + u_z \frac{\partial \mathbf{u}}{\partial z}$$

This term thus describes the advection of velocity, which is also referred to as convective acceleration, “the effect of acceleration of a flow with respect to space”[34].

There are three more terms on the right hand side of the equation: the diffusion/viscosity term, pressure and external forces. Sometimes written as $\nabla \cdot (v \nabla \mathbf{u})$, the viscosity term describes how the fluid motion is damped due to its viscosity. Fluids with a higher viscosity constant v tend to have stronger resistance, resulting in stronger smoothing and slower flows. ∇^2 is also known as the Laplacian operator. The Laplacian is obtained by summing the second partial derivative with respect to each variable component-wise:

$$\nabla^2 \mathbf{u} \equiv \left(\frac{\partial^2 u_x}{\partial x^2} + \frac{\partial^2 u_x}{\partial y^2} + \frac{\partial^2 u_x}{\partial z^2}, \frac{\partial^2 u_y}{\partial x^2} + \frac{\partial^2 u_y}{\partial y^2} + \frac{\partial^2 u_y}{\partial z^2}, \frac{\partial^2 u_z}{\partial x^2} + \frac{\partial^2 u_z}{\partial y^2} + \frac{\partial^2 u_z}{\partial z^2} \right)$$

Multiplying this value by a viscosity constant determines how much the velocity is smoothed or evened-out by viscous forces. If the Laplacian is positive, it means that the velocity is lower at that point than its neighbours, so a larger positive force is applied; a negative Laplacian applies force in the opposite direction.

Pressure is simply defined as “the amount of force acting on a certain area”[35], or force acting per unit area. As a result, a pressure gradient produces a force that pushes the fluid from areas of high pressure to areas of low pressure. This is described by the second term, $-\frac{1}{\rho} \nabla p$, where ∇p is the pressure gradient, and ρ is the density of the fluid at this position. Since gradients point in the increasing direction, the negative is taken so the fluid moves away from the direction of increasing pressure. Additionally, this gradient value gives force acting per unit volume, but the previous terms have been accelerations. This is corrected using Newton’s Second Law, $F = ma$. Since density is the mass per unit volume of the fluid, the pressure gradient is multiplied by the reciprocal of the density to obtain the acceleration. Below is a correction of the SI units to obtain acceleration.

Proof.

$$\begin{aligned} [\nabla p] &= \frac{N}{m^3} = \frac{kg \cdot ms^{-2}}{m^3} = \frac{kg}{m^2 \cdot s^2} \\ [\rho] &= \frac{kg}{m^3} \\ \frac{[\nabla p]}{[\rho]} &= \frac{kg}{m^2 \cdot s^2} \cdot \frac{m^3}{kg} = \frac{m}{s^2} \end{aligned}$$

□

The final term accounts for external forces that act on the fluid, such as gravity. These forces are included to correctly describe changes in momentum according to Newton’s Second Law.

$$\frac{\partial \rho}{\partial t} = -(\mathbf{u} \cdot \nabla) \rho + \kappa \nabla^2 \rho + S \quad (2)$$

Equation 2 has very similar structure to Equation 1, however this one is used in the calculation of a scalar quantity, density. As a result, there is no pressure force term, and external forces is replaced by an external source term S , which adds or removes density from the system. The viscosity constant

is also replaced with κ , the diffusion constant. This measures how fast the property (in this case density) diffuses through the fluid.

2.4.2 Eulerian Implementations

Eulerian, or grid-based implementations for fluid dynamics treat the fluid as a grid of cells.

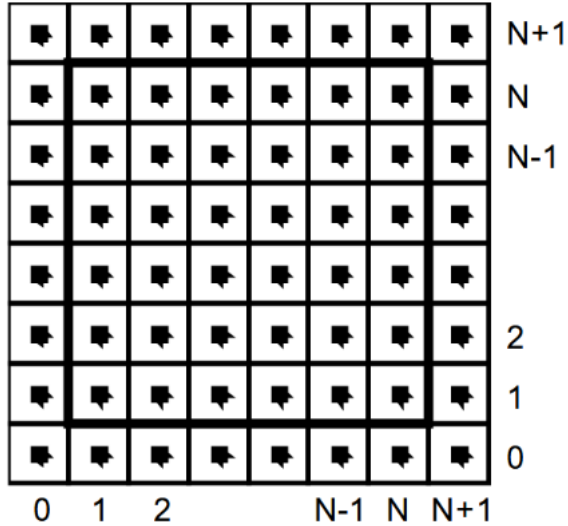


Figure 11: Computational grid with densities and velocities defined in their centres [1]

Figure 11 is a computational grid of cells by Jos Stam. There is an extra layer of cells around the grid to account for boundary conditions. This method utilises Equation 2 to produce a density diffusion solver, where each cell either adds or removes density from its neighbours. Due to distance of other cells, there is no need to include any others in this calculation, as their impact will be negligible and slow the simulation down quite considerably.

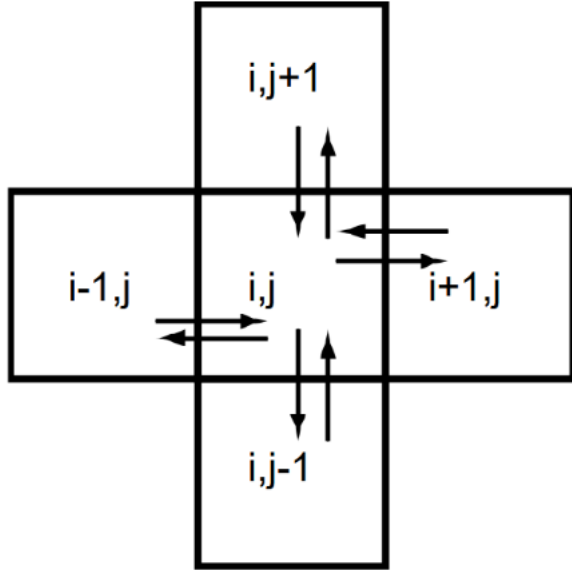


Figure 12: Density exchange through diffusion between neighbours [1]

After this diffusion has occurred, the centres of the grids are treated as sample points traced through the velocity field, similar to Lagrangian methods. In order to convert the “particles” back into grid cells, there are two grids used: a grid of cells containing the old density values and a second grid containing the new density values. The new positions are traced backwards through the velocity field to find the original grid cell, and assign this value to the new position.

Finally, there is the projection step, which ensures that the updated velocity fields are mass conserving, by enforcing the incompressibility condition:

$$\nabla \cdot \mathbf{u} = 0 \quad (3)$$

In order to perform this step, the divergence of the velocity field is computed and a Poisson equation is solved for some pressure-like field p

$$\nabla^2 p = \nabla \cdot \mathbf{u} \quad (4)$$

This is then utilised to project the velocity on to a divergence-free value

$$\mathbf{u}_{new} = \mathbf{u} - \nabla p \quad (5)$$

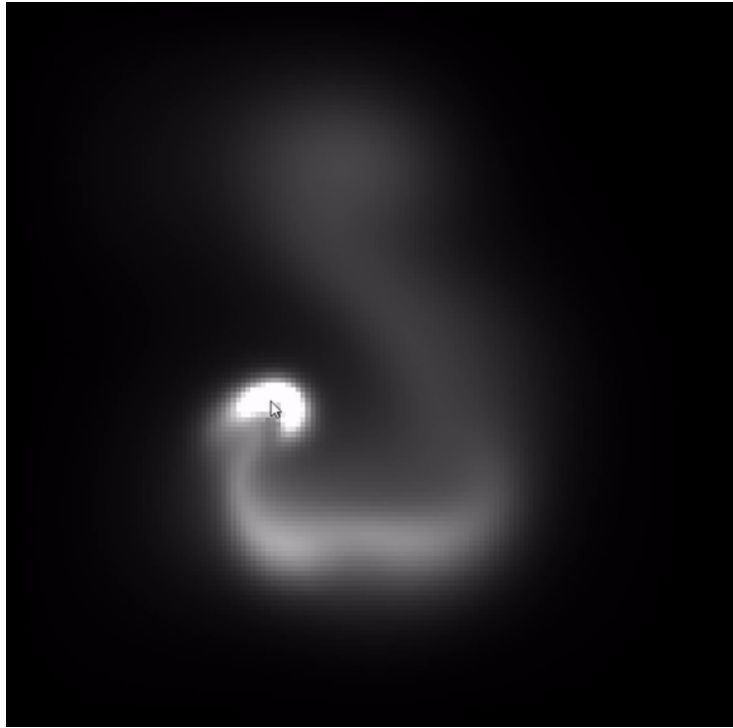


Figure 13: Eulerian simulation [11]

There are many different methods to achieve fluid flow with Eulerian implementations, but more detail is out of the scope of this dissertation.

2.4.3 Lagrangian Implementations

Lagrangian implementations of fluid flow involve treating the fluid as small parcels or particles of fluid. These particles influence their neighbours but are not confined to grid cells. As a result, more calculations are required in determining which particles are within effective range. A classic example of a Lagrangian method is Smoothed Particle Hydrodynamics (SPH).

SPH was initially developed by Gingold, Monaghan and Lucy in 1977 for the purposes of astrophysics[36]. Since the particles are independent nodes, this method is mesh-free, which improves parallelisation. Considering the expensive computations required, parallelisation is fundamental in improving performance. Furthermore, conservation of mass is guaranteed; the particles represent mass and the particles do not disappear at any stage of the simulation.

Furthermore, this method utilises the Navier-Stokes equations to produce the following generalised SPH equation:

$$A_S(\mathbf{r}) = \sum_j m_j \frac{A_j}{\rho_j} W(\mathbf{r} - \mathbf{r}_j, h) \quad (6)$$

For each particle with position \mathbf{r} , every other particle j with mass m_j , density ρ_j , position \mathbf{r}_j and property A_j is iterated through to calculate that particle's total property quantity. $W(r, h)$ is a smoothing kernel that is defined differently for each property, where r is the distance between the two points $|\mathbf{r} - \mathbf{r}_j|$ and h is the smoothing radius for each particle. After a large enough distance $r > h$, the value of the smoothing kernel becomes 0; the particle is too far away to provide any significant influence. As a result, this calculation only needs to be performed on particles that are close enough, a key optimisation step for this method. Further details regarding this method can be found in the "What Was Done and How" section of this dissertation.

2.4.4 Chosen Implementation

Due to the simpler parallelisation and streamlined process of meshfree methods, this dissertation will focus on the implementation and optimisation of a Lagrangian fluid simulation, specifically utilising Smoothed Particle Hydrodynamics.

2.5 Requirements

Using the background research, a set of functional and non-functional requirements may be produced.

2.5.1 Functional Requirements

- F.R. 1** The fluid will be rendered with particles that represent parcels of fluid.
- F.R. 2** The simulation will accurately model fluid behaviour, including properties such as viscosity, density and pressure.
- F.R. 3** The fluid will be affected by gravitational forces.
- F.R. 4** The fluid will remain within a box, which has adjustable dimensions.
- F.R. 5** The user can manipulate the fluid by dragging an object through it.

2.5.2 Non-Functional Requirements

- N.F.R. 1** The simulation will run at a high frame rate to ensure smooth gameplay.
- N.F.R. 2** There will be attempts to reduce the overall memory consumption of the simulation.
- N.F.R. 3** The simulation will be stable with minimal bugs or crashes.
- N.F.R. 4** The simulation will remain stable and flow accurately with no stuttering or jumping.
- N.F.R. 5** The simulation will run in real time, with adjustable properties that also update in real time.
- N.F.R. 6** The simulation will be modular; new fluid types and behaviours can be added in the future with ease.

3 What Was Done and How

This section talks about everything learned and implemented throughout the development process.

3.1 Ethical Considerations

This research does not involve human or animal participants and does not use sensitive or personal data of any kind. As such, there are no significant ethical concerns. All code and media are obtained from publicly available and open sources. Appropriate credit is given when required.

3.2 Software Development Model

This project adopts the agile development model. There are four core values of this method[37]:

- Individuals and Interactions over Processes and Tools
- Working Software over Comprehensive Documentation
- Customer Collaboration over Contract Negotiation
- Responding to Change over Following a Plan

While not all of these principles are directly applicable in this context, the emphasis on adaptability remains essential. Regular weekly meetings with the project supervisor supports an iterative approach and allows the scope to shift due to time constraints or technical challenges. For example, the graphics rendering method was switched from *OpenGL* to *Unity* in order to guarantee completion within the given time frame. Additionally, as the primary goal of this dissertation is optimisation, extensive documentation is unnecessary; the simulation only needs to be demonstrable and functional. Development was carried out in short iterations, with weekly goals set and versioned using *Git*.

3.3 Hardware

The following methods were implemented from a laptop with the following hardware specifications:

CPU Intel(R) Core(TM) i7-14700HX 2.10GHz

GPU NVIDIA GeForce RTX 4060 Laptop

RAM 16GB DDR5-5600MT/s

3.4 Graphics Rendering Pipeline

In order to utilise the *OpenGL* graphics library[22], it is important to first understand the API and the graphics rendering pipeline. This was achieved with the tutorials provided by the *Learn OpenGL* website created by Joey de Vries[12] as well as resources provided by the project supervisor.

The graphics pipeline takes a set of 3D coordinates as an input and transforms them into coloured 2D pixels that are displayed on the screen. Developers interact with this pipeline through the use of shaders, which are programs executed in parallel on the GPU.

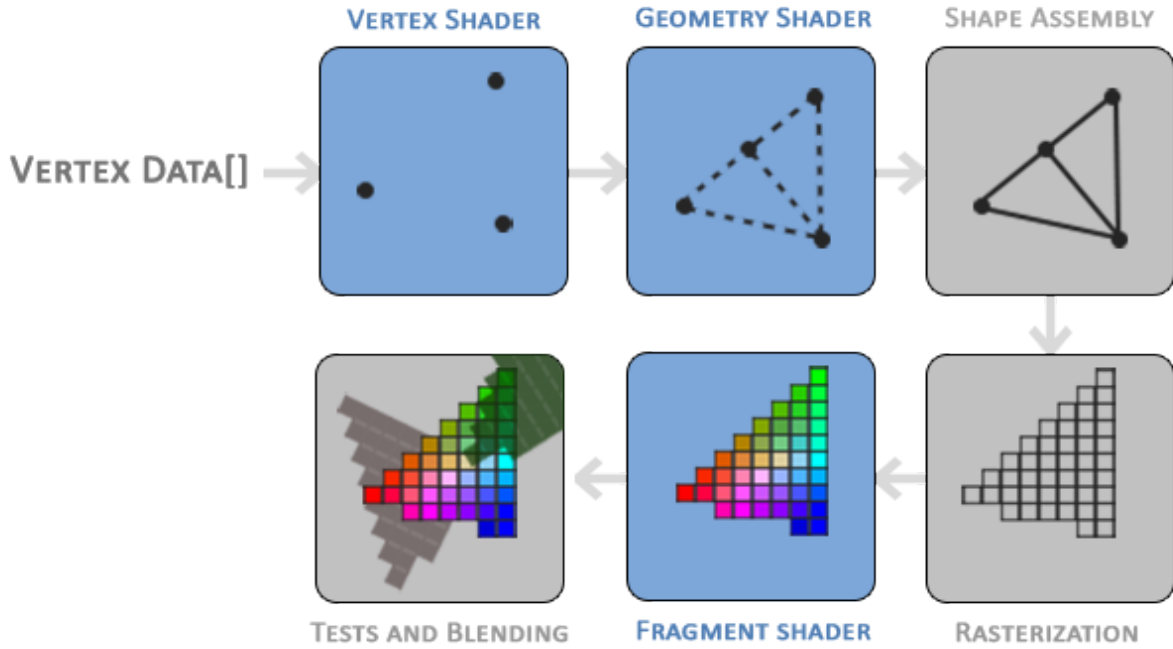


Figure 14: Graphics Rendering Pipeline [12]

3.4.1 Vertex Shader

Vertex shaders process vertices and calculates their coordinates in clip space. This tells the computer if the vertex is in camera view or if it should be discarded [38]. They can be used to perform calculations on models, such

as rotations and translations. They utilise uniform matrices, usually called model, view and projection that are passed to the shader from the main program.

Model matrices are used to represent the centre of the model being drawn by the shader, which has been transformed into the necessary position in the world. Multiplying a vertex by this value describes where the vertex exists relative to the centre of the model.

View matrices describe the camera's position and multiplying this matrix with the vertex's world position (*model · vertex*) determines the vertex's position relative to the camera.

Projection matrices describe the perspective of the camera, including variables such as fov and aspect ratio. These values can distort and scale the appearance of the model and thus need to be considered. Multiplying this matrix with the resultant calculation of the other matrices will achieve this.

An example of a very basic *OpenGL* vertex shader is shown below.

```
#version 330 core

layout (location = 0) in vec3 position;

uniform mat4 model;
uniform mat4 view;
uniform mat4 projection;

void main()
{
    gl_Position = projection * view * model *
        vec4(position, 1.0);
}
```

3.4.2 Geometry Shader

This optional shader takes a collection of vertices that form a primitive, and uses them to form other shapes. An example of this may involve producing a new vertex position that splits a triangle in half to form two smaller triangles. This step is not utilised in this project.

3.4.3 Shape Assembly

Shape assembly, or primitive assembly, uses the data from either the vertex or geometry (if used) shader to draw the primitive defined, usually a triangle.

3.4.4 Rasterization

Rasterization involves mapping the resulting primitives to the corresponding pixels on the final screen, producing fragments. A fragment is all the data required for the API to render a single pixel. Then, all fragments not within the camera view are discarded.

3.4.5 Fragment Shader

The fragment shader is used to determine the final colour of the pixels. Since only the vertices of the primitives are given, interpolation is used to calculate the colour of the pixels in between the vertices. This is done automatically by the graphics API by checking its position and distance relative to all of the primitive's vertices and determines the colour based off this value. For example, setting each vertex of a triangle primitive to a different primary light colour (red, green, blue), produces the following result:

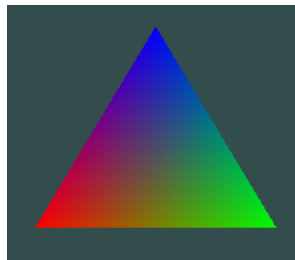


Figure 15: Rainbow Triangle rendered with OpenGL

This is done by passing the desired RGBA values of the vertices through to the vertex shader, which then passes the data through the pipeline to the fragment shader.

3.4.6 Tests and Blending

The final stage of the pipeline involves setting the opacity, or alpha of the pixels and adjusting/blending their colours appropriately. Also, if any models are overlapping, the colours of the model at the back are discarded as they should appear covered by the front model.

3.5 GLFW and GLAD

Creating an *OpenGL* context and a window to draw the graphics in are OS-specific operations. As a result, an external library is required. *GLFW*[21] is a library written in C that does all of this. Additionally, *OpenGL* is a specification. It is up to the manufacturer of the graphics card to implement the specification to a driver compatible with the card. As a result, the specific location of *OpenGL* functions are not consistent and need to be retrieved manually. *GLAD*[39] is a library that does this automatically.

3.6 Learn OpenGL

Using this knowledge of the rendering pipeline, the *OpenGL* specification and the *Learn OpenGL* website, it is now possible to render particles on to the screen and apply transformations to them. See the appendices for graphics produced from this tutorial.

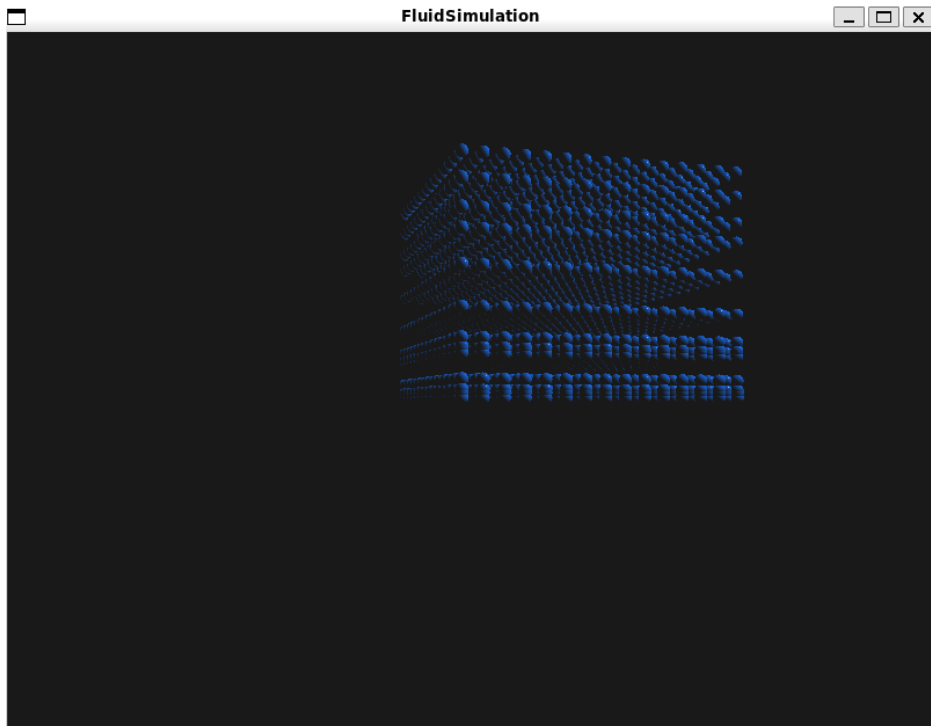


Figure 16: Final progress with OpenGL

Learning the theory behind the graphics rendering pipeline and OpenGL took longer than anticipated. It was at this point that the decision to swap

to Unity was made. Figure 16 displays the final progress achieved with *OpenGL* and *C++*. In the simulation, 1000 particles are rendered in a grid-like structure. They move downwards as a result of a gravitational force and bounce off the “floor” ($y = 0$) with slight damping. There are currently no forces calculated between the particles and as a result they move through each other.

3.7 Simulation Loop

This section provides the theory and pseudocode for the update loop of this simulation. Undefined variables that appear in the pseudocode are assumed to be defined constants outside the simulation loop. The following implementation is presented in the paper “Particle-Based Fluid Simulation for Interactive Applications”, by Matthias Müller, David Charypar and Markus Gross[36].

Algorithm 1 Simulation Loop

```

1: for all particles  $i$  do
2:   | calculate density and pressure
3: for all particles  $i$  do
4:   | compute forces
5: for all particles  $i$  do
6:   | update velocity and position
7:   | resolve collisions

```

3.7.1 Density and Pressure

Using the aforementioned generalised SPH equation, it is possible to compute the density of each particle by replacing A with ρ . Furthermore, in this simulation each particle will be the same size and mass m .

$$\rho_S(\mathbf{r}) = \sum_j m_j \frac{\rho_j}{\rho_j} W(\mathbf{r} - \mathbf{r}_j, h) \equiv m \sum_j W(\mathbf{r} - \mathbf{r}_j, h) \quad (7)$$

The chosen smoothing kernel for density is the Poly6 kernel described in the paper above[36]. This kernel is defined as:

$$W_{poly6}(\mathbf{r}, h) = \frac{315}{64\pi h^9} \begin{cases} (h^2 - r^2)^3 & \text{if } 0 \leq r \leq h \\ 0 & \text{otherwise} \end{cases} \quad (8)$$

For the purposes of speed, we use a modified version of the ideal gas equation to calculate pressure

$$p = k(\rho - \rho_0) \quad (9)$$

where k is a unique gas constant for the fluid and ρ_0 is the fluid's resting density.

The pseudocode for this calculation programatically is as follows

Algorithm 2 CALCULATEDENSITY(Particle p)

```

1: total = 0
2: for all particles  $i$  do
3:   distance = MAGNITUDE( $p.\text{position} - i.\text{position}$ )
4:   if distance  $\leq$  smoothingRadius then
5:     total += POLY6(distance)
6:    $p.\text{density} = \text{particleMass} \cdot \text{total}$ 
7:    $p.\text{pressure} = \text{gasConstant} * (\text{p.density} - \text{restDensity})$ 
```

Since the result of POLY6 is 0 when $r > h$, we save computation by skipping the calculation entirely.

3.7.2 Forces

Once all of the particles have had their properties updated, it is now possible to calculate the forces they exert on each other. The first force calculated will be the pressure force, which is a gradient property. We can take the derivative of the generalised property equation to achieve this.

$$\nabla A_S(\mathbf{r}) = \sum_j m_j \frac{A_j}{\rho_j} \nabla W(\mathbf{r} - \mathbf{r}_j, h) \quad (10)$$

For the pressure force, we use a different smoothing kernel, W_{spiky}

$$W_{spiky}(\mathbf{r}, h) = \frac{15}{\pi h^6} \begin{cases} (h - r)^3 & \text{if } 0 \leq r \leq h \\ 0 & \text{otherwise} \end{cases} \quad (11)$$

The gradient of this kernel is shown below[40]. A proof may be found in the appendices.

$$\nabla W_{spiky}(\mathbf{r}, h) = \frac{-45}{\pi h^6} \begin{cases} (h - r)^2 \cdot \frac{\mathbf{r}}{r} & \text{if } 0 \leq r \leq h \\ 0 & \text{otherwise} \end{cases} \quad (12)$$

Applying the pressure term from the Navier-Stokes equations to the general property equation produces the following calculation for pressure force

$$\mathbf{f}_i^{pressure} = - \sum_j m_j \frac{p_j}{\rho_j} \nabla W(\mathbf{r}_i - \mathbf{r}_j, h) \quad (13)$$

Note that the negative of this calculation is taken to push the particle away from the neighbour as intended. However, this force is asymmetric as the particles do not have equal pressure. There is a simple fix proposed by the paper that takes the averages of their pressures. Thus the final calculation becomes

$$\mathbf{f}_i^{pressure} = -m \sum_j \frac{p_i + p_j}{2\rho_j} \nabla W(\mathbf{r}_i - \mathbf{r}_j, h) \quad (14)$$

The pseudocode for this computation programmatically is as follows

Algorithm 3 CALCULATEPRESSUREFORCE(Particle p)

```

1: total ← [0, 0, 0]
2: for all particles  $i$  do
3:   offset ←  $p.position - i.position$ 
4:   distance = MAGNITUDE(offset)
5:   if distance < epsilon then continue
6:   direction ← offset / distance
7:   total -= ( $p.pressure + i.pressure$ ) / (2 *  $i.density$ ) * SPIKYGRADIENT(distance, direction)
return total * particleMass

```

This implementation ensures that particles do not consider themselves in the calculation (to prevent a division by zero error or the force exploding). We compare the distance to an extremely small epsilon value to account for floating point error.

Next is the viscosity force. We can use the viscosity term in Equation 1 and the generalised property equation, Equation 6, to obtain the following:

$$\mathbf{f}_i^{viscosity} = v \nabla^2 \mathbf{u} = m \sum_j \frac{\mathbf{u}_i}{\rho_j} \nabla^2 W(\mathbf{r} - \mathbf{r}_j, h) \quad (15)$$

There is another unique kernel that is used for the viscosity force, due to the requirement that velocity is always positive. Negative viscosity forces would increase the relative velocity of the particles, which is not representative of viscous behaviour.

$$W_{viscosity}(\mathbf{r}, h) = \frac{15}{2\pi h^3} \begin{cases} -\frac{r^3}{2h^3} + \frac{r^2}{h^2} + \frac{h}{2r} - 1 & \text{if } 0 \leq r \leq h \\ 0 & \text{otherwise} \end{cases} \quad (16)$$

We only utilise the Laplacian of this kernel, defined as

$$\nabla^2 W(\mathbf{r}, h) = \frac{45}{\pi h^6} (h - r) \quad (17)$$

As the initial calculations are very similar to the pressure force, the viscosity can be implemented in the same method.

Algorithm 4 CALCULATEPRESSUREANDVISCOSITYFORCE(Particle p)

```

1: totalPressure ← [0, 0, 0]
2: totalViscosity ← [0, 0, 0]
3: for all particles  $i$  do
4:   offset ←  $p.\text{position} - i.\text{position}$ 
5:   distance = MAGNITUDE(offset)
6:   if distance < epsilon then continue
7:   direction ← offset / distance
8:   totalPressure -= ( $p.\text{pressure} + i.\text{pressure}$ ) / (2 *  $i.\text{density}$ ) * SPIKY-
   GRADIENT(distance, direction)
9:   totalViscosity += VISCOSITYLAPLACIAN(distance) *
      ( $i.\text{velocity} - p.\text{velocity}$ ) /  $i.\text{density}$ 
10:   $p.\text{force} = \text{particleMass} * (\text{totalPressure} + \text{totalViscosity})$ 

```

There are also additional forces to consider, such as surface tension and external forces. Surface tension is not implemented in the CPU implementation and thus will be mentioned in the GPU section. Additionally, the only external force implemented in the CPU version is gravitational force, which is simple - just add $(0, -9.81 * \text{particleMass}, 0)$ to the total force calculation.

3.7.3 Update Velocity and Position

Now that the forces have been calculated, the SUVAT equation $v = u + a\Delta t$ can be utilised to update the final velocity. Then, Euler integration to calculate the new position $s += v\Delta t$. Δt is a small, consistent time step that can be adjusted to increase simulation stability.

Algorithm 5 MOVEPARTICLE

```

1: for all particles  $i$  do
2:    $i.\text{velocity} += i.\text{force} / \text{particleMass} * \text{deltaTime}$ 
3:    $i.\text{position} += i.\text{velocity} * \text{deltaTime}$ 

```

3.7.4 Resolve Collisions

This step is straightforward. The particles are confined to a box to prevent the particles from spreading out infinitely. To implement this, a range is defined in all three directions. If the new particle position would exceed this range, it instead becomes the value it is closest to. Then, a small dampening is applied and the velocity direction is flipped. An example implementation can be found in the appendices. To prevent stuttering at the boundaries, it is recommended to calculate the new velocity and position values in temporary variables first, resolve any collisions, and then assign these final values to the particle.

3.8 Spawn and Move Particles

The following section describes the process taken to render particles in *Unity* using the CPU and the GPU.

The first step to simulating a fluid using Smoothed Particle Hydrodynamics is to create a grid of particles to represent the fluid. Their properties will be stored in a struct. Each particle struct will contain the following properties: a unique identification number, the current forces being applied to it, velocity, position, density and pressure.

3.8.1 CPU

```
private void SpawnParticles()
{
    int counter = 0;
    for (int i = -HALF_ROW; i < HALF_ROW; i++)
    {
        for (int j = -HALF_ROW; j < HALF_ROW; j++)
        {
            for (int k = -HALF_ROW; k < HALF_ROW; k++)
            {

                Vector3 particlePosition = SPAWN_POINT + SPAWN_VARIANCE * (new Vector3(i, j, k) + Random.onUnitSphere);

                GameObject particleInit = Instantiate(particleObj, particlePosition, Quaternion.identity);
                particleInit.hideFlags = HideFlags.HideInHierarchy;

                ParticleCPU particleInst = new()
                {
                    ID = counter,
                    position = particlePosition,
                    gameObject = particleInit,
                    currentForce = new(0.0f, PARTICLE_MASS * GRAVITY, 0.0f)
                };

                particles[counter] = particleInst;
                counter++;
            }
        }
    }
}
```

Figure 17: Particle instantiation

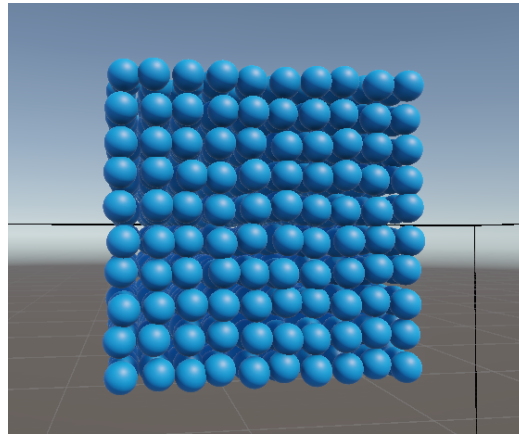


Figure 18: First frame of the simulation using prefabs

For convenience, the game object associated with the particle is initially included in the struct for quick position assignment, which may cause performance issues due to high memory usage when the struct is passed frequently

in function calls. In the CPU implementation, the highest number of particles tested was 1000.

Next, the particles need to be rendered on to the screen. This is easily done in *Unity* by creating a prefab of the built-in sphere object and instantiating the prefab many times. In order to make the simulation more realistic, a slight variance is added to the particles' starting positions, while maintaining the grid structure. For each instantiation, a particle struct is created and the game object is assigned to it. This struct is then added to a particles array, which contains every particle.

Once the particles were spawned and bouncing due to gravitational forces, the simulation loop described above was written in *C#*. See the appendices for methods and calculations. However, the performance and frame rate of the simulation had dropped significantly, to around 2 frames per second.

3.8.2 GPU

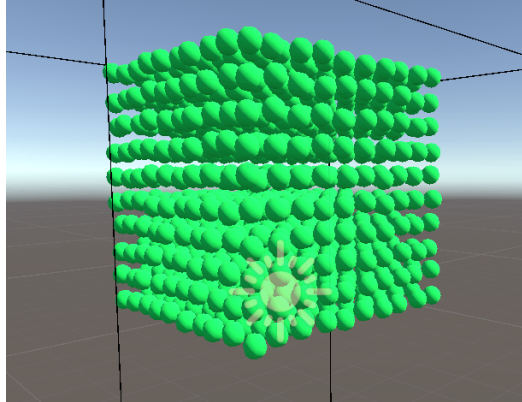


Figure 19: First frame of the simulation using GPU instancing

In order to render particles using the GPU, a technique called GPU Instancing is used. This is when all the models are rendered simultaneously with a single draw call. Initially, a surface shader found online was used in this project in order to speed up the process[41]. This is eventually rewritten into a vertex and fragment shader that will be explained later in this paper. The rendering logic used is from the same repository. See the appendices for code snippets. Furthermore, another optimisation to note is that the mesh utilised in this method is not the built in sphere object, but rather a low-poly sphere with a lot less triangles, to further enhance performance.

With this technique, we use a compute shader and HLSL to perform the calculations. We then redraw the particles in their new positions using another single draw call every update frame. For 1000 particles, the same amount of particles as the CPU implementation, this method achieves over 600 frames per second with the same hardware. Furthermore, once we increase the particle count further, performance remains high, maintaining over 500 frames per second for approximately 32,000 particles.

3.9 Spatial Hashing

The reason the simulation is so slow at this point is because each particle is comparing itself with every other particle in every update step. This is an $O(n^2)$ algorithm and is too slow for large particle counts. The first optimisation involves the aforementioned idea that only the particle's neighbours influence it. The number of calculations performed can thus be considerably reduced with Spatial Hashing.

Spatial Hashing is a technique that divides a space into a hash table. The table contains hashes that correspond to a small section of the space, a cell, and all the items or particles within that cell[42]. This reduces the number of calculations as only the cell that the particle is in and its neighbouring cells need to be considered for each particle.

This algorithm is used at the beginning of each simulation loop. Then, instead of iterating through every particle, each process only needs to check the particles in the neighbour array. There are two slight variants of this method utilised in this project, one for the CPU and one for the GPU.

3.9.1 Spatial Hash CPU

This section describes the processes involved in the spatial hash used for the C# and CPU implementation. A lot of this method is inspired by a pre-existing implementation found online[43].

Algorithm 6 PARTIALSPATIALHASHCPU

```

1: for all particles  $i$  do
2:   calculate which cell  $i$  is in
3:   find the hash/key for that cell
4: for all particles  $i$  do
5:   update the table
6: for all particles  $i$  do
7:   find neighbours and store their IDs in  $i.neighbours$ 
```

This method is an improvement as each particle ends up with its own array of neighbours, which is only calculated once at the start of each update loop. The neighbours are stored in a vector within the particle struct and is unique to each particle. This is a huge improvement from before, where each particle calculated its neighbours independently, every update. However, this is at the cost of a lot more storage, as each particle stores their neighbours independently and can introduce repeated data. In regards to performance, the frame rate improves significantly from 2 frames to 15 frames per second on average with 1000 particles still.

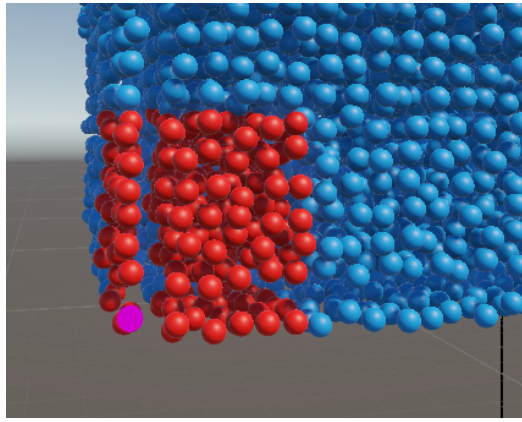


Figure 20: Visualisation of neighbour array for pink particle

There are still issues with larger particle counts in this implementation due to large memory consumption and the multiple draw calls. In Figure 20, this method was tested with 8000 particles, but the frame rate averaged around 0.5 frames per second. Due to this, the decision was made to move the calculations to the GPU and no further work was completed on this version.

3.9.2 Spatial Hash GPU

The algorithm used for the GPU is more complete. It was a lot easier to debug and improve this version due to the increased performance of the particle rendering. This implementation is created with the aid of multiple online resources[13][43][44][45].

This version differs from the incomplete implementation described above in that it avoids storing a vector of neighbours within each particle structure. Instead, it employs a more efficient approach using a single lookup table. After computing hash keys for all particles, the array of particles is sorted based on these keys. The lookup table then stores the starting index in the

Algorithm 7 SpatialHashGPU

```
1: for all particles  $i$  do
2:   | calculate which cell  $i$  is in
3:   | find the hash key for that cell
4: for all particles  $i$  do
5:   | sort the particles by hash key
6: for all particles  $i$  do
7:   | update the lookup table
```

sorted array for each unique hash key, allowing for quick access to particles in the same spatial cell. This reduces memory overhead and improves cache coherence. Figure 21 provides a visual explanation of this method created by Sebastian Lague[13].

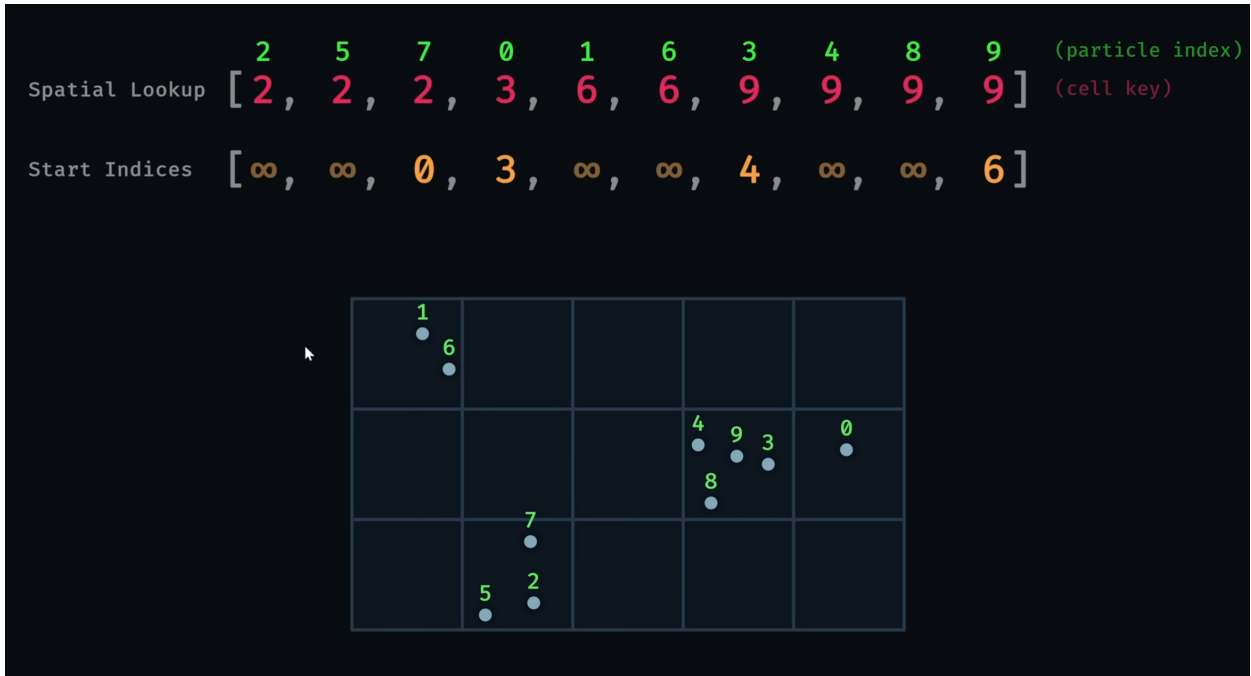


Figure 21: Spatial Hash Visualisation [13]

3.9.3 Cell Calculation

The following sections will explain how to implement each step of the algorithm. The code snippets are all in HLSL.

The space that the particle can occupy (the volume within the bounds of the box) is divided into cells with dimensions equal to a value greater than

or equal to the smoothing radius of the particles. This is to guarantee that any neighbouring particles that will provide an influence on this position is either within the same cell or in directly adjacent cells. The simplest way to do this is to divide the current position of the particle by the smoothing radius and return either the floor or ceiling of this - so cells within the same cell have the same cell coordinate.

```
inline int3 FindCell(in float3 position)
{
    return int3(floor(position / smoothingRadius));
}
```

Figure 22: FindCell HLSL

3.9.4 Hash Key Calculation

The cell coordinates produced are integer vectors with three entries. This is inefficient for memory and inconvenient for fast lookups; one integer comparison is better than three. In order to convert these vectors into a single integer with minimal overlap, each integer is multiplied by a large hash value and the results are combined using the bitwise XOR operation. Then the hash value is wrapped around the length of the array so that it can be used as an index.

```
inline uint FindHash(int3 cell)
{
    return (
        cell.x * 73856093 ^
        cell.y * 19349663 ^
        cell.z * 83492791
    ) % particleCount;
}
```

Figure 23: FindHash HLSL

3.9.5 Storing the Hash Keys

As these are inline methods, a function that will perform these operations and then store the obtained values in an array needs to be defined. The

array begins unsorted with each index being equal to the particle's unique ID. The thread group size attribute is declared at the top of the method. In this implementation, there are 256 threads in each thread group. This means that 256 threads will be launched and use shared resources simultaneously. A power of two is chosen here due to the nature of the sorting algorithm that is used in the next step.

```
[numthreads(256,1,1)]
void HashParticles(int3 id: SV_DISPATCHTHREADID)
{
    _lookupTable[id.x] = 0xFFFFFFFF;
    uint particleIndex = _particleIndices[id.x];
    _cellIndices[particleIndex] = FindHash(FindCell(_particles[particleIndex].position));
}
```

Figure 24: HashParticles HLSL

3.9.6 Bitonic Sort

Bitonic Sequence “A data-set is bitonic if there exists an index i for which all elements less than or equal to i are in increasing order, and all elements greater than or equal to i are in decreasing order” [44].

Something to note is that this definition is valid for sequences that are also entirely increasing or entirely decreasing. As a result, any collection of numbers can be split into a series of bitonic sequences by reducing it down into smaller lists of length 2. This sorting algorithm therefore does not work on lists with a length that is not equal to a power of 2, hence why a thread group of size 256 is used.

Bitonic Sort “A comparison-based sorting algorithm which sorts a data-set by converting the list of numbers into a bitonic sequence. The list is then sorted using a merge function” [44].

The pseudocode will be presented below, with the following variables

- arr = the data-set being sorted
- lowIndex = the lowest index of the array or sub-array
- count = the number of elements in the array or sub-array

- direction = whether the bitonic sequence should be increasing or decreasing, 1 = increasing and 0 = decreasing

Algorithm 8 BitonicMerge(arr, lowIndex, count, direction)

```

1: if count > 1 then
2:   set k = count / 2
3:   for (i = lowIndex; i <= lowIndex + k; i++) do
4:     if direction == (arr[i] > arr[i+k]) then
5:       swap arr[i] and arr[i+k]
6:   BITONICMERGE(arr, lowIndex, k, direction)
7:   BITONICMERGE(arr, lowIndex + k, k, direction)

```

Algorithm 9 BitonicSort(arr, lowIndex, count, direction)

```

1: if count > 1 then
2:   set k = count / 2
3:   BITONICSORT(arr, lowIndex, k, 1)
4:   BITONICSORT(arr, lowIndex + k, k, 0)
5:   BITONICMERGE(arr, lowIndex, count, direction)

```

The reason that a Bitonic Sort is chosen as our sorting algorithm is because it is a parallel algorithm. This means that multiple operations required in the algorithm can be computed simultaneously. For example, the sequential recursive BITONICSORT and BITONICMERGE calls do not depend on each other and can therefore be computed in parallel. This is perfect for a GPU based implementation as parallelisation can occur through threading.

This paper adopts a parallelised version of the Bitonic Sort found in a YouTube tutorial online[45].

```

// parallelise bitonic sort
1 reference
private void SortParticles()
{
    for (var dim = 2; dim <= ParticleCount; dim <= 1)
    {
        computeShader.SetInt("dim", dim);
        for (var block = dim >> 1; block > 0; block >>= 1)
        {
            computeShader.SetInt("block", block);
            computeShader.Dispatch(BitonicSortKernel, ParticleCount / 256, 1, 1);
        }
    }
}

```

Figure 25: C# parallelisation

```

[numthreads(256,1,1)]
void BitonicSort(int3 id: SV_DISPATCHTHREADID)
{
    uint i = id.x + id.y * 256 * 1024;
    uint j = i ^ block;

    if(j <= i || i >= particleCount || j >= particleCount) return;

    uint keyI = _particleIndices[i];
    uint keyJ = _particleIndices[j];

    float valueI = _cellIndices[keyI];
    float valueJ = _cellIndices[keyJ];

    float diff = (valueI - valueJ) * ((i & dim) == 0 ? 1 : -1);

    if (diff > 0)
    {
        _particleIndices[i] = keyJ;
        _particleIndices[j] = keyI;
    }
}

```

Figure 26: Bitonic Sort computation HLSL

3.9.7 Update Lookup Table

Now that the particles have been sorted according to their hash key values, the lookup table needs to be updated with the changes.

```
[numthreads(256,1,1)]
void FillLookupTable(uint3 id: SV_DISPATCHTHREADID)
{
    uint particleIndex = _particleIndices[id.x];
    uint cellIndex = _cellIndices[particleIndex];

    InterlockedMin(_lookupTable[cellIndex], id.x);
}
```

Figure 27: FillLookupTable HLSL

This method iterates through every particle and finds which cell it is in. Then it compares the index of the particle with the starting index currently stored in the table. If this is the first particle in this cell, the value of `_lookupTable[cellIndex]` will be an incredibly large number, otherwise it'll be the index of the first particle in that cell. Therefore, when `INTERLOCKEDMIN(_lookupTable[cellIndex], id.x)` is called, if this is the first particle of the cell, its index will be lower than the large default number and will replace this value, otherwise it will remain unchanged.

3.9.8 Using the Spatial Hash

Once the spatial hash has been implemented, it needs to be integrated into the simulation loop. Note that finding the neighbour-finding logic is moved into the calculation methods.

Algorithm 10 Simulation Loop With Spatial Hashing

```
1: reset lookup table
2: for all particles  $i$  do
3:    $\lfloor$  calculate the cell and its hash key
4:   SORTPARTICLES()
5:   for all particles  $i$  do
6:      $\lfloor$  update lookup table
7:     for all particles  $i$  do
8:        $\lfloor$  calculate density and pressure
9:     for all particles  $i$  do
10:     $\lfloor$  compute forces
11:    for all particles  $i$  do
12:       $\lfloor$  update velocity and position
13:       $\lfloor$  resolve collisions
```

By eliminating non-neighbouring particles and using a lookup table to store previously computed comparisons, the algorithm's complexity is reduced to $O(n)$ complexity. The worst case scenario is still $O(n^2)$ (if all the particles are within the same cell or neighbouring cells), but this should never be the case due to the forces they exert on each other.

With these changes, the simulation achieved frame rates ranging between 250 and 320 for approximately 32,000 particles, a huge improvement to the 15 frames before.

3.10 More Forces

Two additional forces have not been implemented thus far due to the challenges associated with debugging, stemming from suboptimal optimization. This is no longer an issue thanks to the spatial hash. This section describes their implementations.

3.10.1 Surface Tension

This section describes an integration of surface tension also given by the aforementioned paper[36].

Molecules in a fluid experience attractive forces from their neighbours. When they are surrounded by neighbours in all directions (when they are not at the surface), these forces are equal in all directions; the net force is **0**. They are unbalanced at the surface and act in the direction of the surface normal towards the fluid. The effect of this force depends on the two fluids

present at the surface (for example water and air), resulting in a tension coefficient σ .

To find which particles are on the surface of the fluid, we use the generalised property equation to produce a colour field. The field is 1 in locations a particle is present and 0 otherwise.

$$c_S(\mathbf{r}) = \sum_j m_j \frac{1}{\rho_j} W(\mathbf{r} - \mathbf{r}_j, h) \quad (18)$$

The smoothing kernel used in these calculations is the previously mentioned Poly6 kernel. The gradient of this colour field is denoted as \mathbf{n} , and it represents the surface normal field pointing into the fluid. Its divergence $\nabla \cdot \mathbf{n} \equiv \nabla^2 c_S$ measures the curvature of the surface. To obtain these two values, the gradient and Laplacian of the Poly6 kernel are required. Their derivations can be found in the appendices.

$$\nabla W_{poly6}(\mathbf{r}, h) = \frac{315}{63\pi h^9} \begin{cases} -6(h^2 - r^2)^2 \mathbf{r} & 0 \leq r \leq h \\ 0 & \text{otherwise} \end{cases} \quad (19)$$

$$\nabla^2 W_{poly6}(\mathbf{r}, h) = \frac{315}{63\pi h^9} \begin{cases} -6(3h^4 - 10h^2r^2 + 7r^4) & 0 \leq r \leq h \\ 0 & \text{otherwise} \end{cases} \quad (20)$$

The direction is reversed by taking the negative as the force is trying to flatten the surface.

$$\kappa = \frac{-\nabla^2 c_S}{|\mathbf{n}|} \quad (21)$$

Putting this all together, the following surface force calculation is derived

$$\mathbf{f}_i^{surface} = \sigma \kappa \mathbf{n} = -\sigma \nabla^2 c_S(\mathbf{r}_i) \frac{\mathbf{n}}{|\mathbf{n}|} \quad (22)$$

There arises a numerical issue when $|\mathbf{n}|$ is too small. To fix this, a threshold is predetermined; the calculations are only considered if this value is greater than the threshold. Similar to the viscosity force, these force calculations can be performed in the same loop as the pressure force.

Algorithm 11 CALCULATEFORCES(Particle p)

```
1: totalPressure ← [0, 0, 0]
2: totalViscosity ← [0, 0, 0]
3: surfaceForce ← [0, 0, 0]
4: colorFieldGradient ← [0, 0, 0]
5: coloeFieldLaplacian = 0
6: for all neighbour particles  $i$  do
7:   offset ←  $p.\text{position} - i.\text{position}$ 
8:   distance = MAGNITUDE(offset)
9:   if distance < epsilon then continue
10:  direction ← offset / distance
11:  totalPressure -= ( $p.\text{pressure} + i.\text{pressure}$ ) / (2 *  $i.\text{density}$ ) * SPIKY-
    GRADIENT(distance, direction)
12:  totalViscosity += VISCOSITYLAPLACIAN(distance) *
    ( $i.\text{velocity} - p.\text{velocity}$ ) /  $i.\text{density}$ 
13:  colorFieldGradient += POLY6GRADIENT(distance, direction)
    /  $i.\text{density}$ 
14:  colorFieldLaplacian += POLY6LAPLACIAN(distance) /  $i.\text{density}$ 
15:  colorFieldGradient *= particleMass
16:  colorFieldLaplacian *= particleMass
17:  colorFieldGradientLength = LENGTH(colorFieldGradient)
18:  if colorFieldGradientLength > threshold then
19:    curvature = -colorFieldLaplacian / colorFieldGradientLength
20:    surfaceForce = -tensionCoefficient * curvature
      * NORMALIZE(colorFieldGradient)
21:   $p.\text{force} = \text{particleMass} * (\text{totalPressure} + \text{totalViscosity}) + \text{surfaceForce}$ 
```

3.10.2 External Forces

Although gravity has already been applied, the fluid should be pushed away and interact with objects within the simulation. If the object comes into contact with the particle, it should push the particle in the opposite direction. In this simulation, a single sphere game object was added to the scene; moving it into the box pushes the fluid away. See the appendices for the implementation.

3.10.3 Performance

These additional calculations have little impact on the overall frame rate of the simulation, it consistently remains within the 250 to 320 frame rate

described beforehand for approximately 32,000 particles.

3.11 Pre-Computed Constants

Another optimisation made at this point involved constants and reducing the overall number of calculations made.

The first change involves distance checking. Instead of using `(distance)()` and comparing this to the smoothing radius, we instead compare the squared distance with the squared smoothing radius, only square rooting when needed. This is because calculating the square root is a very expensive computation and should only be done when needed. This can also be extended by pre-computing the squared smoothing radius and storing it in a variable, as this is a value that will not change during runtime.

There are other constants that can be pre-computed also. For example, each smoothing kernel involves multiplication of a fraction that depends on h , the smoothing radius. As h is a constant, these can also be calculated and passed to the compute shader once, as shown below.

```
// calculate kernel constants once, improved optimisation
float radius3 = particleRadius * particleRadius * particleRadius;
float radius5 = radius3 * particleRadius * particleRadius;

float polyMult = 315 / (64 * Mathf.PI * radius3);
float polyGradMult = -945 / (32 * Mathf.PI * radius5);
float polyLapMult = -945 / (32 * Mathf.PI * radius5 * radius3 * particleRadius);
float spikyGradMult = -45 / (Mathf.PI * radius3);
float viscLapMult = 45 / (Mathf.PI * radius5);

computeShader.SetFloat("polyMult", polyMult);
computeShader.SetFloat("polyGradMult", polyGradMult);
computeShader.SetFloat("polyLapMult", polyLapMult);
computeShader.SetFloat("spikyGradMult", spikyGradMult);
computeShader.SetFloat("viscLapMult", viscLapMult);
```

Figure 28: Pre-computed Variables [14]

This improvement increased the consistency of the frame rate; it remains within 280 to 340 frames per second.

3.12 Circles

It was at this point that the rendering shader was rewritten. Thanks to the *OpenGL* learned at the beginning, it was possible to rewrite the Surface shader into a Vertex and Fragment shader. See the appendices for the new shader code. The reason for this was to change the mesh that was being rendered.

Previously, a low-poly sphere was being used, consisting of 60 triangles. Instead of a 3D mesh, a quad may be utilised instead, which consists of only 2 triangles. In order to maintain the 3D appearance, the vertex shader was rewritten to ensure that the meshes were constantly facing the camera. This was done using a tutorial found online[14].

The snippet below positions a quad in world space and orients it to always face the camera by performing the following steps:

- Start with the quad's world position as the centre
- Scale the vertex coordinates to determine visual dimensions
- Extract the camera's right and up directions; the x and y axes in world space
- Offset the quad's vertices using these vectors, making sure the quad remains perpendicular to the camera's forward direction

```
float3 worldCentre = p.position;
float2 vertOffset = v.vertex.xy * _size * 2;

float3 camUp = unity_CameraToWorld._m01_m11_m21;
float3 camRight = unity_CameraToWorld._m00_m10_m20;

float3 vertPosWorld = worldCentre + camRight * vertOffset

o.pos = mul(UNITY_MATRIX_VP, float4(vertPosWorld, 1));
o.worldPos = vertPosWorld;

float3 worldNormal = UnityObjectToWorldNormal(v.normal);
o.worldNormal = normalize(worldNormal);
o.velocity = length(p.velocity);
```

Figure 29: Camera Logic Vertex Shader [14]

In order to maintain a spherical appearance, the corners of the quad need to be discarded. This is done by the Fragment Shader:

- Shift the UV coordinates so that the quad's centre is (0,0)
- Scale the coordinates to range between -1 and 1
- Compute the squared distance from the centre using the dot product $x^2 + y^2$
- Discards the fragment if this value is greater than 1 (the circle's radius)

```
float2 centreOffset = (i.uv - 0.5) * 2;
float sqrDst = dot(centreOffset, centreOffset);
if (sqrDst > 1) discard;
```

Figure 30: Circle Logic Fragment Shader [14]

For any fragments not discarded, the colour of the circle is set based on the particle's velocity. A rainbow gradient was chosen for the purposes of the demonstration but is easily adjustable due to the formula used[15].

```
// color helper function
float3 palette(in float t, in float3 a, in float3 b, in float3 c, in float3 d)
{
    return a + b * cos(2 * PI * (c * t + d));
}
```

Figure 31: Colour Palette Formula [15]

The rainbow gradient is achieved with the following values:

- a = (0.50, 0.50, 0.50)
- b = (0.50, 0.50, 0.50)
- c = (1.00, 1.00, 1.00)
- d = (0.00, 0.33, 0.67)

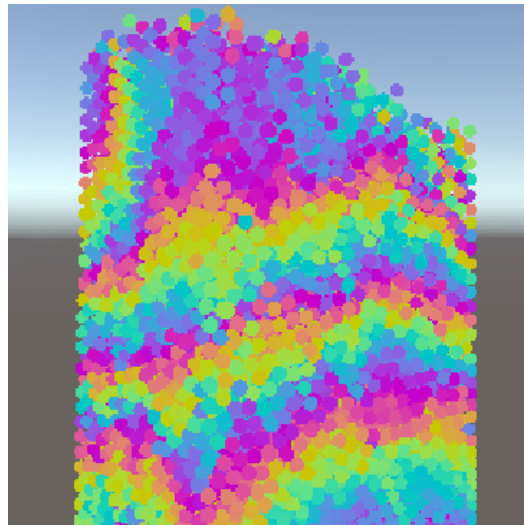


Figure 32: Rainbow gradient and circle particles

With this optimisation, the simulation's frame rate improved from 340 frames to around 400 frames with approximately 40,000 particles. This was the final product of this dissertation.

4 Results and Evaluation

This project produced three simulations with varying levels of completion, illustrating the iterative nature of the Agile development process.

4.1 Agile Development

One of the key strengths of employing the Agile methodology in this project was the flexibility it offered in adapting to the strict time frame presented. The iterative nature allowed quick changing of software and tools, without the constraints of a more rigid development plan. This was especially helpful when the decision to swap over completely from *OpenGL* to *Unity* was made; there was no pause or replanning required. Furthermore, this allowed for a more self-directed workflow, due to independent development and research. However, there was still access to a supervisor if required. Overall, there was a more efficient and responsive development process due to the balance between independence and guidance provided.

Despite these advantages, there were also a few issues with this method. Due to the encouraged autonomy, too much independence led to lacking time structure, especially in the absence of external accountability. Supervisor support should have been utilised more than it was. Additionally, progress could have definitely been documented or recorded better; some *Git* commits contained a large number of changes, which made it difficult to track specific modifications and the affect on the frame rate as a result of them.

Overall, Agile development provided significant contributions to the adaptability and progress of the project. While it was suited for dynamic and evolving projects such as this one, the methodology was very dependent on the discipline of the people utilising it.

4.2 OpenGL Simulation

One of the “simulations” produced in this dissertation was the previously mentioned grid of cubes developed using *C++* and *OpenGL*. Due to the lack of features and the use of shaders and GPU-based rendering, the simulation achieved a consistently high frame rate. However, it did not portray realistic fluid behaviour, as the particles were only influenced by a gravitational force and experienced no inter-particle interactions (they passed through each other in straight lines with minimal collision detection at a boundary).

Although this method was ultimately abandoned, it still proved to be very beneficial from a learning perspective. A lot of the overall technical knowledge gained from this project was from the initial research required

to use the *OpenGL* graphics API. Hands-on experience with the graphics rendering pipeline through the use of *OpenGL* and custom shaders provided key insights into low-level rendering processes and enabled improvements in the *Unity* implementation. For example, the rendering shader was rewritten independently with this acquired knowledge. Furthermore, the process of learning compute shaders was greatly simplified and sped up the development process of this simulation significantly. Overall, it was a very important part of this project as acquiring low-level graphics programming skills improved technical confidence and enabled both this project and future projects.

In hindsight, while appreciative of the knowledge gained from this implementation, if supervisor support were further utilised, the decision to swap software could have been made a lot earlier. Due to the significant portion of development time occupied, there was a lot less time allocated to the final implementation as a whole. More time could have been allocated to optimisation techniques if the simulation’s physics were completed at an earlier stage. Learning to balance exploration and knowledge with results is an important skill to improve in the future.

4.3 Unity CPU Simulation

The next simulation produced in this project was a CPU-based implementation with *C#* and *Unity*. This achieved the same things that the previous simulation did, a grid of particles that moved due to gravitational forces, but had a lower frame rate, starting at around 300 frames per second for 1000 particles. This is not a large particle count, but larger numbers decreased this value quite significantly, so this was the initial count chosen. After the physics was implemented, the performance had dropped, peaking at 2 frames per second. With the first optimisation technique, spatial hashing, this was improved by over 20 times, achieving a consistent frame rate of over 15 frames per second for 1000 particles. However, this was nowhere near the desired number of particles, and increasing the count still produced detrimental performance reduction. Thus, the next optimisation was to switch to a GPU-based implementation.

An advantage of this CPU implementation was prior experience with *Unity* from a full *C#*-based perspective. This reduced the learning curve significantly and thus greatly reduced the amount of time required to reach this point in development. Due to the familiarity of the environment, faster and more confident prototyping was possible. Moreover, confidence in the programming language facilitated the process of translating the academic papers used, from physics equations into executable code. Concepts such as Object-Oriented Programming and *Unity*’s MonoBehavior scripts were

already well understood, further enhancing efficiency and accuracy within the implementation. As a result, a focus on particle behaviour and performance optimisation was possible.

There were unfortunately still a number of issues with this implementation. There was a lot of problems with memory, as the algorithm developed involved passing through entire structs between functions, causing repeated data to be recreated as copies, leading to significant performance overhead. Furthermore, this repeated copying was not cache-friendly, leading to slower data access. An improvement on this would have been to either pass the information to the methods by reference, or to rewrite the logic in a way that did not involve entire particle structs being passed through every step of the algorithm. Such a small particle count producing a low frame rate caused the debugging process to be quite frustrating, due to the difficulty of efficiently testing changes, hindering the ability to identify bottlenecks within the code logic.

There were a lot more optimisations that could have been implemented to improve these issues. For example, multithreading is supported in *C#*. However, the CPU has significantly less threads than the GPU and is not as good at performing calculations quickly. As a result, it was deemed unnecessary to implement threading on this version of the project; it was more time efficient to move on to the GPU implementation immediately.

The combination of these issues and the limited time frame contributed to the decision of abandoning this second implementation and continuing to a fully GPU-based implementation within Unity, though the initial programming required to produce this was beneficial in simplifying and speeding up the GPU implementation process.

4.4 Unity GPU Simulation

The final simulation produced in this project was a GPU-based implementation with *HLSL* and Compute Shaders with *Unity*. When this version reached the same development point as the OpenGL implementation - a grid of particles affected by gravitational forces - it also achieved very high frame rates, averaging around 600 frames per second for 1,000 particles. When the physics was initially applied with no optimisations, the frame rate decreased to around 300 frames per second for 1,000 particles and less than 100 for 32,000 particles. Integrating the spatial hash algorithm into this simulation improved the average frame rate, achieving results between 250 to 320 frames per second for 32,000 particles. Manually pre-computing and setting constant values into the simulation further improved the frame rate, to around 280-340 frames per second due to the significant reduction in the number of calcula-

tions performed. Finally, making the particles 2D circles that maintain their 3D appearance improved the overall frame rate even further to around 400 frames for 32,000 particles.

However, at this point when testing the impact of higher particle counts, there was an issue noticed regarding the box bounds that the particles were contained in. In the first frame, the particles were not forming a full grid as the grid was too large for the box bounds. This may have caused issues in the first few frames of the simulation but the particles quickly rectified this error and returned to a stable fluid flow.

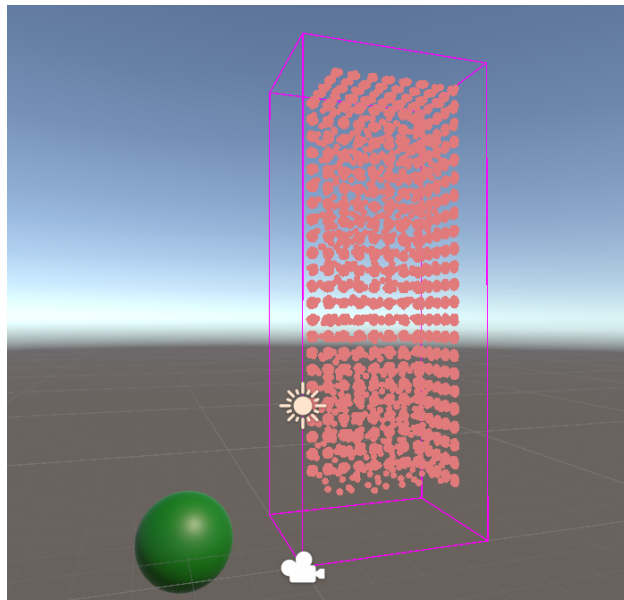


Figure 33: First Frame Small Box

When the box bound was increased before running the simulation, the frame rate consistently remained in the 600s. The underlying reasoning is uncertain, but it is believed that it may be due to the collision resolution calculations. This was noticed too late in the development stage and further investigation could not be performed. The remaining results for this simulation will however involve box dimensions that satisfy the entire grid formation.

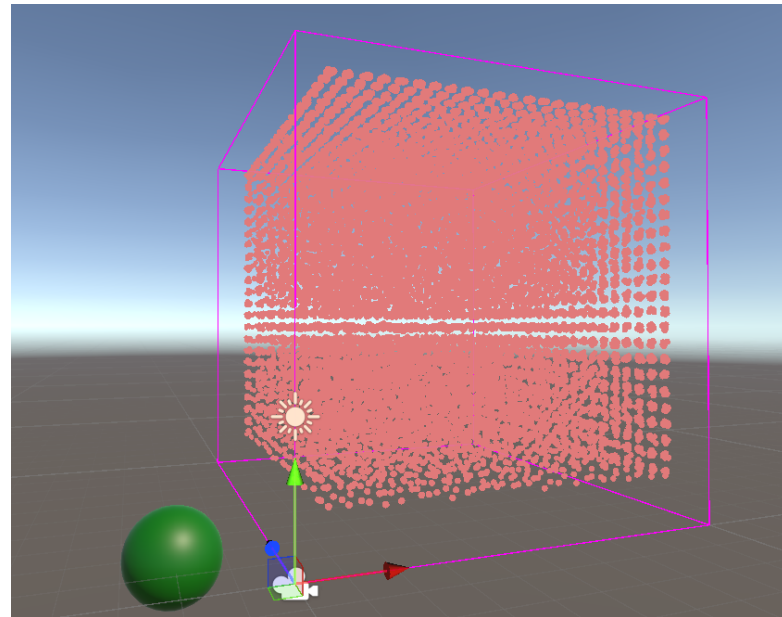


Figure 34: First Frame Big Box

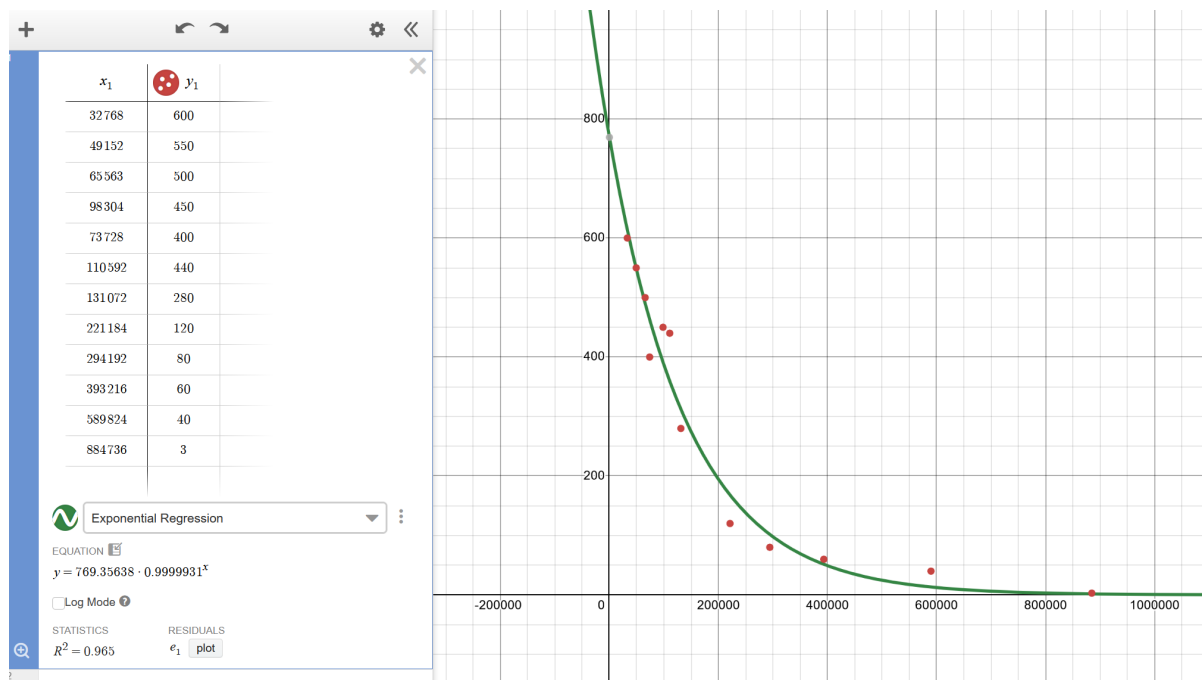


Figure 35: Particle Count vs. Frame Rate [16]

Figure 35 shows the frame rates obtained for different particle counts. This graph was created using Desmos, an online graphing calculator[16]. There appears to be an exponential relationship between frame rate and particle count for this simulation. In the case of a video game, 60 frames per second is usually the target to maintain a smooth gameplay experience, and this simulation achieves a remarkable count of over 390,000 particles at this FPS.

A slight error noticed when testing larger particle counts was that some particles remained in the grid structure for a longer time than anticipated.

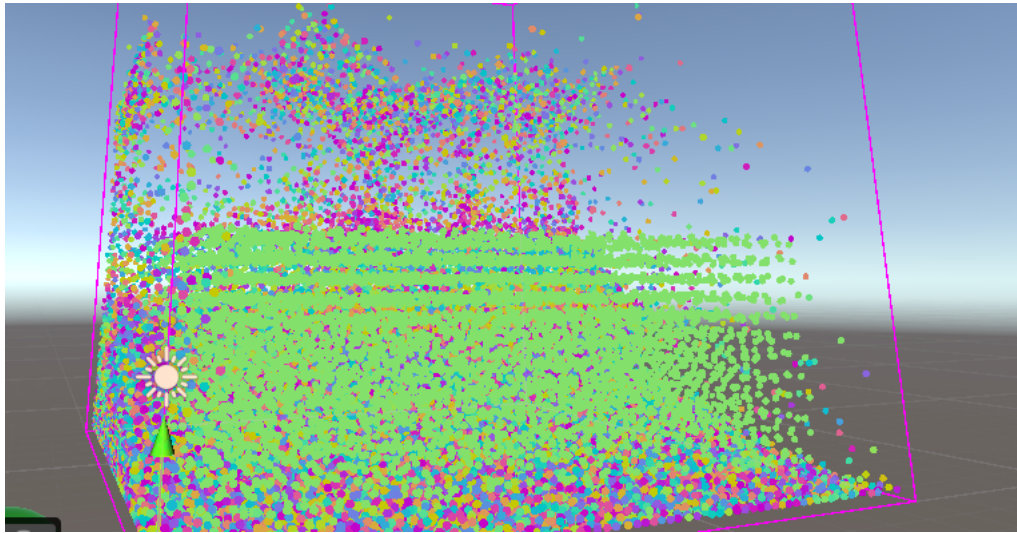


Figure 36: Grid Simulation Issues

There has not been a fix implemented and therefore, although this issue is eventually resolved automatically, it is not recommended to use this simulation for larger particle counts.

This simulation offers several improvements over the previous two versions. Most notably, it is more complete and can handle more than 1,000 particles. This significant improvement in performance is partly due to the improved memory management; it does not copy structs across methods and involves multi-threading, unlike the CPU implementation. This change also allows it to handle substantially greater particle counts with little trouble.

This simulation does suffer from a few issues. At the moment, it is just a demonstration of fluid physics. More code is required to make the fluid fully interactable; it is currently only affected by the sphere within the scene. Furthermore, it is not currently possible to create two different fluids simultaneously without writing more code. There is also the aforementioned issue

with the reduced frame rate issues when the grid does not fit fully inside the initial box, and the delay in particle movement for larger particle counts. This heavily affects its scalability and needs further work to improve. Finally, it still looks like a collection of particles rather than a full body of liquid. Although this was out of the scope of this project, there is definitely more work that could be done in this area.

Overall, this is a satisfying result for an initial project in the area of fluid simulation. Achieving a fluid flow that exhibits a high degree of realism is a gratifying outcome.

4.5 Requirements

Functional requirements 1-5 were satisfied: the fluid simulation is rendered with particles that represent parcels of fluid - this is the SPH approach that was consistently used throughout the paper. The calculations involved consider the fluid's viscosity, density and pressure, satisfying functional requirement 2. It is also affected by the position of the sphere object within the scene and by gravitational forces, satisfying functional requirements 3 and 5. Finally, the fluid does not leave the assigned box dimensions, and are affected by the box changing dimensions. This satisfies the final functional requirement, number 4.

Non-functional requirements 1, 2, 5 and 6 were satisfied: the simulation achieves an average frame rate of 600 for over 32,000 particles, and maintains over 60 frames for up to 390,000 particles, satisfying non-functional requirement 1. Evidence of memory reductions are described through the lookup table improvement in the spatial hashing algorithm and the struct-copying issues mentioned in the CPU implementation. This satisfies non-functional requirement 2. The properties of the fluid can be adjusted in the Unity inspector in real time, and the fluid reacts to these changes with no delay. This satisfies non-functional requirement 5. Although more code is required to implement new fluid types, the simple modifiability of the fluid properties mentioned earlier will make future implementation of other fluids easier. This satisfies non-functional requirement 6.

When the box dimensions are changed, the program does sometimes stutter slightly. This does not satisfy non-functional requirement 4. The aforementioned issue with large particle count grids dissatisfies non-functional requirement 3. These issues could not be rectified in the given time frame, but are possible in future work.

4.6 Hardware Statistics

This section uses HWiNFO[46] to display the CPU core temperatures and core usages and GPU statistics when the laptop is idle, with just HWiNFO and the Unity Editor open, and when both the simulations are running.

4.6.1 Idle

| | | | | | |
|---|--------------------|--------|-------|--------|--------|
| ✓ | Core Usage | 1.9 % | 0.0 % | 62.4 % | 3.2 % |
| | P-core 0 T0 Usage | 1.5 % | 0.0 % | 31.9 % | 2.4 % |
| | P-core 0 T1 Usage | 5.0 % | 0.0 % | 47.0 % | 1.9 % |
| | P-core 1 T0 Usage | 4.0 % | 0.0 % | 49.4 % | 3.4 % |
| | P-core 1 T1 Usage | 0.0 % | 0.0 % | 47.2 % | 2.7 % |
| | P-core 2 T0 Usage | 0.0 % | 0.0 % | 49.4 % | 2.5 % |
| | P-core 2 T1 Usage | 0.4 % | 0.0 % | 47.9 % | 3.2 % |
| | P-core 3 T0 Usage | 0.0 % | 0.0 % | 48.8 % | 2.5 % |
| | P-core 3 T1 Usage | 0.4 % | 0.0 % | 37.8 % | 1.1 % |
| | P-core 4 T0 Usage | 0.0 % | 0.0 % | 51.7 % | 10.5 % |
| | P-core 4 T1 Usage | 15.0 % | 0.0 % | 62.4 % | 14.3 % |
| | P-core 5 T0 Usage | 8.5 % | 0.0 % | 54.7 % | 11.3 % |
| | P-core 5 T1 Usage | 0.0 % | 0.0 % | 53.5 % | 12.4 % |
| | P-core 6 T0 Usage | 0.0 % | 0.0 % | 50.5 % | 2.1 % |
| | P-core 6 T1 Usage | 0.4 % | 0.0 % | 45.6 % | 1.4 % |
| | P-core 7 T0 Usage | 0.6 % | 0.0 % | 49.0 % | 2.5 % |
| | P-core 7 T1 Usage | 0.4 % | 0.0 % | 46.8 % | 1.2 % |
| | E-core 8 T0 Usage | 0.0 % | 0.0 % | 55.3 % | 2.1 % |
| | E-core 9 T0 Usage | 1.3 % | 0.0 % | 49.7 % | 1.3 % |
| | E-core 10 T0 Usage | 0.3 % | 0.0 % | 33.6 % | 1.3 % |
| | E-core 11 T0 Usage | 0.0 % | 0.0 % | 47.7 % | 0.9 % |
| | E-core 12 T0 Usage | 6.4 % | 0.0 % | 48.7 % | 2.6 % |
| | E-core 13 T0 Usage | 0.0 % | 0.0 % | 46.4 % | 0.9 % |
| | E-core 14 T0 Usage | 0.0 % | 0.0 % | 33.2 % | 0.8 % |
| | E-core 15 T0 Usage | 0.0 % | 0.0 % | 33.2 % | 0.8 % |
| | E-core 16 T0 Usage | 8.0 % | 0.0 % | 26.0 % | 1.2 % |
| | E-core 17 T0 Usage | 0.4 % | 0.0 % | 14.7 % | 0.5 % |
| | E-core 18 T0 Usage | 0.4 % | 0.0 % | 49.7 % | 1.6 % |
| | E-core 19 T0 Usage | 0.0 % | 0.0 % | 30.3 % | 0.9 % |

Figure 37: CPU core usage IDLE

| CPU [#0]: Intel Core i7-14700HX: DTS | | | | | |
|--------------------------------------|-------------------|-------|-------|-------|-------|
| | Core Temperatures | 40 °C | 34 °C | 52 °C | 41 °C |
| P-core 0 | 38 °C | 36 °C | 47 °C | 39 °C | |
| P-core 1 | 41 °C | 38 °C | 52 °C | 42 °C | |
| P-core 2 | 40 °C | 38 °C | 45 °C | 40 °C | |
| P-core 3 | 41 °C | 38 °C | 47 °C | 41 °C | |
| P-core 4 | 37 °C | 34 °C | 50 °C | 38 °C | |
| P-core 5 | 40 °C | 34 °C | 52 °C | 39 °C | |
| P-core 6 | 40 °C | 38 °C | 46 °C | 40 °C | |
| P-core 7 | 40 °C | 36 °C | 45 °C | 40 °C | |
| E-core 8 | 40 °C | 40 °C | 44 °C | 41 °C | |
| E-core 9 | 40 °C | 40 °C | 44 °C | 41 °C | |
| E-core 10 | 41 °C | 39 °C | 44 °C | 41 °C | |
| E-core 11 | 41 °C | 39 °C | 44 °C | 41 °C | |
| E-core 12 | 42 °C | 42 °C | 46 °C | 44 °C | |
| E-core 13 | 44 °C | 42 °C | 46 °C | 44 °C | |
| E-core 14 | 44 °C | 42 °C | 46 °C | 44 °C | |
| E-core 15 | 44 °C | 42 °C | 46 °C | 44 °C | |
| E-core 16 | 38 °C | 37 °C | 41 °C | 39 °C | |
| E-core 17 | 38 °C | 37 °C | 41 °C | 39 °C | |
| E-core 18 | 38 °C | 37 °C | 41 °C | 39 °C | |
| E-core 19 | 38 °C | 37 °C | 41 °C | 39 °C | |
| > Core Distance to TjMAX | 60 °C | 48 °C | 66 °C | 59 °C | |
| | GPU Power | 16.26 | 16.26 | 59.26 | 16.26 |

Figure 38: CPU core temperatures IDLE

| GPU [#1]: NVIDIA GeForce RTX 4060 Laptop | | | | | |
|--|-----------------|-----------|-------------|-----------|---------|
| | GPU Temperature | 40.3 °C | 39.6 °C | 41.7 °C | 40.2 °C |
| GPU Memory Junction Temperature | 50.0 °C | 48.0 °C | 54.0 °C | 50.0 °C | |
| GPU Hot Spot Temperature | 47.7 °C | 47.0 °C | 48.8 °C | 47.7 °C | |
| GPU Thermal Limit | 75.0 °C | 75.0 °C | 75.0 °C | 75.0 °C | |
| GPU Core Voltage | 0.630 V | 0.630 V | 0.940 V | 0.636 V | |
| > GPU Rail Voltages | | 17.328 V | 20.631 V | | |
| GPU Power | 1.959 W | 1.929 W | 16.402 W | 2.239 W | |
| > GPU Rail Powers | | 0.000 W | 13.485 W | | |
| GPU Clock | 210.0 MHz | 210.0 MHz | 2,370.0 MHz | 252.4 MHz | |
| GPU Memory Clock | 101.2 MHz | 101.2 MHz | 2,000.2 MHz | 137.7 MHz | |
| GPU Video Clock | 765.0 MHz | 765.0 MHz | 2,055.0 MHz | 790.0 MHz | |
| GPU Effective Clock | 13.2 MHz | 11.8 MHz | 2,370.0 MHz | 47.8 MHz | |
| GPU Crossbar Clock | 825.0 MHz | 825.0 MHz | 2,085.0 MHz | 849.2 MHz | |
| GPU Core Load | 0.0 % | 0.0 % | 8.0 % | 0.1 % | |
| GPU Memory Controller Load | 0.0 % | 0.0 % | 52.0 % | 0.5 % | |
| GPU Video Engine Load | 0.0 % | 0.0 % | 0.0 % | 0.0 % | |
| GPU Bus Load | 0.0 % | 0.0 % | 3.0 % | 0.0 % | |
| GPU Memory Usage | 5.8 % | 5.8 % | 6.4 % | 5.9 % | |
| > GPU D3D Usages | | 0.0 % | 2.9 % | | |
| > GPU Performance Limiters | Yes | No | Yes | 100 % | |
| GPU Memory Available | 7,710 MB | 7,668 MB | 7,710 MB | 7,702 MB | |
| GPU Memory Allocated | 478 MB | 478 MB | 520 MB | 486 MB | |
| GPU D3D Memory Dedicated | 251 MB | 251 MB | 294 MB | 260 MB | |
| GPU D3D Memory Dynamic | 7 MB | 7 MB | 42 MB | 26 MB | |
| PCIe Link Speed | 2.5 GT/s | 2.5 GT/s | 16.0 GT/s | 2.8 GT/s | |

Figure 39: GPU statistics IDLE

4.6.2 CPU

| | | | | |
|----------------------|--------|--------|--------|--------|
| Core Usage | 6.2 % | 0.0 % | 72.0 % | 3.5 % |
| P-core 0 T0 Usage | 3.1 % | 0.0 % | 31.9 % | 2.4 % |
| P-core 0 T1 Usage | 44.0 % | 0.0 % | 47.0 % | 1.8 % |
| P-core 1 T0 Usage | 5.3 % | 0.0 % | 49.4 % | 3.5 % |
| P-core 1 T1 Usage | 0.5 % | 0.0 % | 48.2 % | 2.7 % |
| P-core 2 T0 Usage | 1.8 % | 0.0 % | 49.4 % | 2.7 % |
| P-core 2 T1 Usage | 0.0 % | 0.0 % | 47.9 % | 3.3 % |
| P-core 3 T0 Usage | 0.8 % | 0.0 % | 48.8 % | 3.0 % |
| P-core 3 T1 Usage | 0.0 % | 0.0 % | 37.8 % | 1.7 % |
| P-core 4 T0 Usage | 33.3 % | 0.0 % | 68.0 % | 13.2 % |
| P-core 4 T1 Usage | 0.0 % | 0.0 % | 65.5 % | 13.6 % |
| P-core 5 T0 Usage | 60.4 % | 0.0 % | 72.0 % | 13.2 % |
| P-core 5 T1 Usage | 0.0 % | 0.0 % | 70.3 % | 13.4 % |
| P-core 6 T0 Usage | 13.3 % | 0.0 % | 50.5 % | 2.5 % |
| P-core 6 T1 Usage | 0.0 % | 0.0 % | 47.6 % | 1.9 % |
| P-core 7 T0 Usage | 8.9 % | 0.0 % | 49.0 % | 2.7 % |
| P-core 7 T1 Usage | 0.0 % | 0.0 % | 49.5 % | 1.6 % |
| E-core 8 T0 Usage | 0.6 % | 0.0 % | 55.3 % | 1.8 % |
| E-core 9 T0 Usage | 0.3 % | 0.0 % | 49.7 % | 1.1 % |
| E-core 10 T0 Usage | 0.1 % | 0.0 % | 33.6 % | 1.1 % |
| E-core 11 T0 Usage | 0.0 % | 0.0 % | 47.7 % | 0.9 % |
| E-core 12 T0 Usage | 0.9 % | 0.0 % | 48.7 % | 2.4 % |
| E-core 13 T0 Usage | 0.0 % | 0.0 % | 46.4 % | 0.8 % |
| E-core 14 T0 Usage | 0.0 % | 0.0 % | 33.2 % | 0.8 % |
| E-core 15 T0 Usage | 0.0 % | 0.0 % | 33.2 % | 0.8 % |
| E-core 16 T0 Usage | 0.7 % | 0.0 % | 26.0 % | 1.2 % |
| E-core 17 T0 Usage | 0.4 % | 0.0 % | 23.6 % | 0.6 % |
| E-core 18 T0 Usage | 0.2 % | 0.0 % | 49.7 % | 1.4 % |
| E-core 19 T0 Usage | 0.1 % | 0.0 % | 30.3 % | 0.8 % |
| Max CPU/Thread Usage | 60.4 % | 10.2 % | 72.0 % | 31.6 % |

Figure 40: CPU core usage CPU IMPL

| | Core Temperatures | 49 °C | 33 °C | 81 °C | 41 °C |
|--------------------------|-------------------|-------|-------|-------|-------|
| P-core 0 | 44 °C | 35 °C | 48 °C | 39 °C | |
| P-core 1 | 49 °C | 38 °C | 68 °C | 43 °C | |
| P-core 2 | 48 °C | 37 °C | 51 °C | 41 °C | |
| P-core 3 | 57 °C | 37 °C | 61 °C | 42 °C | |
| P-core 4 | 52 °C | 34 °C | 78 °C | 40 °C | |
| P-core 5 | 69 °C | 33 °C | 81 °C | 42 °C | |
| P-core 6 | 49 °C | 38 °C | 69 °C | 41 °C | |
| P-core 7 | 49 °C | 34 °C | 74 °C | 41 °C | |
| E-core 8 | 46 °C | 40 °C | 49 °C | 41 °C | |
| E-core 9 | 46 °C | 40 °C | 48 °C | 41 °C | |
| E-core 10 | 46 °C | 39 °C | 48 °C | 41 °C | |
| E-core 11 | 46 °C | 39 °C | 48 °C | 41 °C | |
| E-core 12 | 50 °C | 41 °C | 51 °C | 44 °C | |
| E-core 13 | 50 °C | 42 °C | 51 °C | 44 °C | |
| E-core 14 | 50 °C | 42 °C | 51 °C | 44 °C | |
| E-core 15 | 50 °C | 42 °C | 51 °C | 44 °C | |
| E-core 16 | 44 °C | 37 °C | 46 °C | 39 °C | |
| E-core 17 | 44 °C | 37 °C | 45 °C | 39 °C | |
| E-core 18 | 44 °C | 37 °C | 45 °C | 39 °C | |
| E-core 19 | 44 °C | 37 °C | 45 °C | 39 °C | |
| > Core Distance to TjMAX | 51 °C | 19 °C | 67 °C | 59 °C | |
| CPU Package | 69 °C | 48 °C | 81 °C | 51 °C | |
| Core Max | 69 °C | 42 °C | 81 °C | 47 °C | |

Figure 41: CPU core temperatures CPU IMPL

| GPU [#1]: NVIDIA GeForce RTX 4060 Laptop | | | | | |
|--|-----------|-----------|-------------|-----------|--|
| GPU Temperature | 43.1 °C | 39.6 °C | 43.3 °C | 40.6 °C | |
| GPU Memory Junction Temperature | 52.0 °C | 48.0 °C | 56.0 °C | 50.4 °C | |
| GPU Hot Spot Temperature | 50.6 °C | 47.0 °C | 50.7 °C | 48.1 °C | |
| GPU Thermal Limit | 75.0 °C | 75.0 °C | 75.0 °C | 75.0 °C | |
| ⚡ GPU Core Voltage | 0.630 V | 0.630 V | 0.940 V | 0.637 V | |
| > ⚡ GPU Rail Voltages | | 17.328 V | 20.631 V | | |
| ⚡ GPU Power | 3.083 W | 1.929 W | 16.481 W | 2.465 W | |
| > ⚡ GPU Rail Powers | | 0.000 W | 13.485 W | | |
| ⌚ GPU Clock | 210.0 MHz | 210.0 MHz | 2,370.0 MHz | 258.9 MHz | |
| ⌚ GPU Memory Clock | 101.2 MHz | 101.2 MHz | 2,000.2 MHz | 142.6 MHz | |
| ⌚ GPU Video Clock | 765.0 MHz | 765.0 MHz | 2,055.0 MHz | 793.8 MHz | |
| ⌚ GPU Effective Clock | 134.8 MHz | 11.8 MHz | 2,370.0 MHz | 77.7 MHz | |
| ⌚ GPU Crossbar Clock | 825.0 MHz | 825.0 MHz | 2,085.0 MHz | 852.6 MHz | |
| ⌚ GPU Core Load | 13.0 % | 0.0 % | 20.0 % | 2.4 % | |
| ⌚ GPU Memory Controller Load | 0.0 % | 0.0 % | 52.0 % | 0.5 % | |
| ⌚ GPU Video Engine Load | 0.0 % | 0.0 % | 0.0 % | 0.0 % | |
| ⌚ GPU Bus Load | 3.0 % | 0.0 % | 6.0 % | 0.5 % | |
| ⌚ GPU Memory Usage | 6.1 % | 5.8 % | 6.6 % | 6.0 % | |
| > ⌚ GPU D3D Usages | | 0.0 % | 14.1 % | | |
| > ⌚ GPU Performance Limiters | Yes | No | Yes | 100 % | |
| ⌚ GPU Memory Available | 7,691 MB | 7,650 MB | 7,716 MB | 7,699 MB | |
| ⌚ GPU Memory Allocated | 497 MB | 472 MB | 538 MB | 489 MB | |
| ⌚ GPU D3D Memory Dedicated | 271 MB | 245 MB | 312 MB | 262 MB | |
| ⌚ GPU D3D Memory Dynamic | 44 MB | 7 MB | 67 MB | 28 MB | |
| ⌚ PCIe Link Speed | 2.5 GT/s | 2.5 GT/s | 16.0 GT/s | 2.8 GT/s | |

Figure 42: GPU statistics CPU IMPL

4.6.3 GPU

| Sensor | Current | Minimum | Maximum | Average |
|----------------------|---------|---------|---------|---------|
| Core Usage | 13.6 % | 0.0 % | 72.0 % | 4.1 % |
| P-core 0 T0 Usage | 40.9 % | 0.0 % | 42.7 % | 4.5 % |
| P-core 0 T1 Usage | 1.7 % | 0.0 % | 47.0 % | 2.2 % |
| P-core 1 T0 Usage | 38.5 % | 0.0 % | 56.3 % | 5.2 % |
| P-core 1 T1 Usage | 1.6 % | 0.0 % | 48.2 % | 3.2 % |
| P-core 2 T0 Usage | 29.8 % | 0.0 % | 49.8 % | 4.5 % |
| P-core 2 T1 Usage | 1.4 % | 0.0 % | 47.9 % | 2.4 % |
| P-core 3 T0 Usage | 23.2 % | 0.0 % | 49.5 % | 4.1 % |
| P-core 3 T1 Usage | 1.4 % | 0.0 % | 37.8 % | 1.3 % |
| P-core 4 T0 Usage | 60.9 % | 0.0 % | 68.0 % | 15.9 % |
| P-core 4 T1 Usage | 2.9 % | 0.0 % | 65.5 % | 13.5 % |
| P-core 5 T0 Usage | 60.1 % | 0.0 % | 72.0 % | 17.1 % |
| P-core 5 T1 Usage | 1.5 % | 0.0 % | 70.3 % | 13.3 % |
| P-core 6 T0 Usage | 23.5 % | 0.0 % | 50.5 % | 4.0 % |
| P-core 6 T1 Usage | 2.1 % | 0.0 % | 50.1 % | 2.1 % |
| P-core 7 T0 Usage | 24.9 % | 0.0 % | 49.0 % | 4.6 % |
| P-core 7 T1 Usage | 1.6 % | 0.0 % | 49.5 % | 1.8 % |
| E-core 8 T0 Usage | 8.9 % | 0.0 % | 55.3 % | 1.9 % |
| E-core 9 T0 Usage | 3.3 % | 0.0 % | 49.7 % | 1.2 % |
| E-core 10 T0 Usage | 2.9 % | 0.0 % | 33.6 % | 1.3 % |
| E-core 11 T0 Usage | 2.7 % | 0.0 % | 47.7 % | 1.1 % |
| E-core 12 T0 Usage | 16.2 % | 0.0 % | 48.7 % | 2.4 % |
| E-core 13 T0 Usage | 5.2 % | 0.0 % | 49.2 % | 1.2 % |
| E-core 14 T0 Usage | 2.4 % | 0.0 % | 33.4 % | 1.0 % |
| E-core 15 T0 Usage | 2.1 % | 0.0 % | 49.1 % | 1.0 % |
| E-core 16 T0 Usage | 9.7 % | 0.0 % | 49.1 % | 1.7 % |
| E-core 17 T0 Usage | 5.4 % | 0.0 % | 35.1 % | 0.9 % |
| E-core 18 T0 Usage | 3.2 % | 0.0 % | 49.7 % | 1.5 % |
| E-core 19 T0 Usage | 3.0 % | 0.0 % | 30.3 % | 0.9 % |
| Max CPU/Thread Usage | 60.9 % | 10.2 % | 72.0 % | 34.7 % |
| Total CPU Usage | 13.6 % | 0.9 % | 13.7 % | 4.1 % |

Figure 43: CPU core usage GPU IMPL

| Sensor | Current | Minimum | Maximum | Average |
|--|---------|---------|---------|---------|
| ⌚ Total CPU Utility | 23.7 % | 0.7 % | 28.5 % | 4.2 % |
| > ⌚ Core Ratios | 38.6 x | 4.0 x | 55.0 x | 18.1 x |
| ⌚ Uncore Ratio | 38.0 x | 8.0 x | 48.0 x | 17.8 x |
| ▼ 🖥 CPU [#0]: Intel Core i7-14700HX: DTS | | | | |
| ↳ Core Temperatures | | | | |
| P-core 0 | 57 °C | 33 °C | 81 °C | 42 °C |
| P-core 1 | 56 °C | 35 °C | 59 °C | 40 °C |
| P-core 2 | 58 °C | 38 °C | 69 °C | 44 °C |
| P-core 3 | 61 °C | 37 °C | 63 °C | 42 °C |
| P-core 4 | 59 °C | 36 °C | 64 °C | 43 °C |
| P-core 5 | 66 °C | 34 °C | 78 °C | 41 °C |
| P-core 6 | 68 °C | 33 °C | 81 °C | 43 °C |
| P-core 7 | 59 °C | 38 °C | 69 °C | 42 °C |
| P-core 8 | 57 °C | 34 °C | 74 °C | 41 °C |
| E-core 8 | 55 °C | 38 °C | 55 °C | 42 °C |
| E-core 9 | 55 °C | 38 °C | 55 °C | 42 °C |
| E-core 10 | 55 °C | 38 °C | 55 °C | 42 °C |
| E-core 11 | 55 °C | 39 °C | 55 °C | 42 °C |
| E-core 12 | 57 °C | 41 °C | 57 °C | 44 °C |
| E-core 13 | 57 °C | 41 °C | 57 °C | 44 °C |
| E-core 14 | 57 °C | 41 °C | 57 °C | 44 °C |
| E-core 15 | 57 °C | 41 °C | 57 °C | 44 °C |
| E-core 16 | 53 °C | 36 °C | 53 °C | 40 °C |
| E-core 17 | 53 °C | 36 °C | 53 °C | 40 °C |
| E-core 18 | 53 °C | 36 °C | 53 °C | 40 °C |
| E-core 19 | 53 °C | 36 °C | 53 °C | 40 °C |
| > Core Distance to TjMAX | 43 °C | 19 °C | 67 °C | 58 °C |
| CPU Package | 68 °C | 48 °C | 81 °C | 52 °C |
| Core Max | 68 °C | 41 °C | 81 °C | 48 °C |

Figure 44: CPU core temperatures GPU IMPL

| Sensor | Current | Minimum | Maximum | Average |
|--|-------------|------------|-------------|------------|
| ⌚ Write Rate | 0.006 MB/s | 0.000 MB/s | 5.592 MB/s | 0.097 MB/s |
| ⌚ Read Total | 94,052 MB | 94,021 MB | 94,052 MB | |
| ⌚ Write Total | 99,938 MB | 99,788 MB | 99,938 MB | |
| ▼ 🖥 GPU [#1]: NVIDIA GeForce RTX 4060 Laptop | | | | |
| ↳ GPU Temperature | 56.4 °C | 39.5 °C | 56.4 °C | 41.7 °C |
| ↳ GPU Memory Junction Temperature | 66.0 °C | 48.0 °C | 66.0 °C | 51.4 °C |
| ↳ GPU Hot Spot Temperature | 62.2 °C | 46.8 °C | 62.2 °C | 49.0 °C |
| ↳ GPU Thermal Limit | 75.0 °C | 75.0 °C | 75.0 °C | 75.0 °C |
| ↳ GPU Core Voltage | 1.010 V | 0.630 V | 1.010 V | 0.672 V |
| > GPU Rail Voltages | | 17.317 V | 20.631 V | |
| ↳ GPU Power | 31.779 W | 1.929 W | 37.117 W | 5.207 W |
| > GPU Rail Powers | | 0.000 W | 70.965 W | |
| ⌚ GPU Clock | 2,565.0 MHz | 210.0 MHz | 2,580.0 MHz | 482.5 MHz |
| ⌚ GPU Memory Clock | 2,000.2 MHz | 101.2 MHz | 2,000.2 MHz | 324.3 MHz |
| ⌚ GPU Video Clock | 2,190.0 MHz | 765.0 MHz | 2,205.0 MHz | 927.7 MHz |
| ⌚ GPU Effective Clock | 2,562.4 MHz | 11.8 MHz | 2,577.1 MHz | 320.4 MHz |
| ⌚ GPU Crossbar Clock | 2,220.0 MHz | 825.0 MHz | 2,235.0 MHz | 983.9 MHz |
| ⌚ GPU Core Load | 60.0 % | 0.0 % | 61.0 % | 7.3 % |
| ⌚ GPU Memory Controller Load | 0.0 % | 0.0 % | 57.0 % | 0.5 % |
| ⌚ GPU Video Engine Load | 0.0 % | 0.0 % | 0.0 % | 0.0 % |
| ⌚ GPU Bus Load | 20.0 % | 0.0 % | 22.0 % | 2.2 % |
| ⌚ GPU Memory Usage | 6.0 % | 5.8 % | 6.6 % | 6.0 % |
| > GPU D3D Usages | | 0.0 % | 35.6 % | |
| > GPU Performance Limiters | Yes | No | Yes | 100 % |
| ⌚ GPU Memory Available | 7,694 MB | 7,650 MB | 7,716 MB | 7,696 MB |
| ⌚ GPU Memory Allocated | 494 MB | 472 MB | 538 MB | 492 MB |
| ⌚ GPU D3D Memory Dedicated | 268 MB | 245 MB | 312 MB | 265 MB |
| ⌚ GPU D3D Memory Dynamic | 47 MB | 7 MB | 67 MB | 30 MB |
| ⌚ PCIE Link Speed | 16.0 GT/s | 2.5 GT/s | 16.0 GT/s | 4.1 GT/s |

Figure 45: GPU statistics GPU IMPL

4.6.4 Hardware Evaluation

Comparing the CPU core usage values, it is evident that the full C# version uses fewer cores than the compute shader version at any given time. This is expected considering multithreading was not implemented and likely contributes to performance issues in this version due to bottlenecking. Additionally, none of the cores ever reach maximum capacity, indicating significant room for improvement and optimisation, as described above.

As most of the computation is supposed to be offloaded on to the GPU, it is expected for the compute shader version to not tax the CPU heavily. This is confirmed by these statistics; the C# version shows negligible GPU utilisation whereas the final version appropriately offloads a lot of the work to the GPU.

Temperature readings also support these claims and confirm that thermal conditions are stable and consistent. This is also evidence that the operating system is dynamically reallocating tasks between the cores to balance thermal load. Although some of the cores reach temperatures as high as 81 deg *C*, their average is nearly half of this, indicating they are short bursts of heat rather than consistent values.

In conclusion, the data suggests that the C# implementation underutilises the CPU, leading to performance bottlenecks. This is due to a lack of multithreading and optimised resource allocation. In contrast, the compute shader version correctly offloads computations to the GPU and efficiently utilises it as shown by its average clock speed increasing. These results highlight the importance of proper task delegation between the hardware and demonstrates attempts to optimise performance this way.

5 Conclusion

This section discusses the original aim and objectives and whether they were satisfied. It also talks about the knowledge gained from this project and future work that may be done.

5.1 Aim and Objectives

5.1.1 Aim

This project produced an accurate fluid simulation that utilised Smoothed Particle Hydrodynamics. Evidence of the final fluid can be seen in the appendices below. The general SPH equations are formed using the Navier-Stokes equations as explained in Background Review. Furthermore, the frame rate of the simulation was consistently measured and there were successful attempts to optimise it. From an original performance of 2 frames per second, this was improved by over 300 times this amount, to a consistent 600 frames per second. The resulting code is a 3D fluid flow that works within Unity. Although it is not yet available as an asset, this will be possible in the future.

5.1.2 Objectives

1. **Explore Existing Fluid Simulations** - There was a thorough analysis of existing fluid simulations both available online and already implemented within video games. There were a lot of issues identified, such as availability, cost of assets and quality due to performance requirements. Benefits involved high visual quality and some interactivity.
2. **Navier-Stokes and SPH** - There was a thorough explanation of the Navier-Stokes equations and what they mean. There was no description of their derivation, which could have been included but deemed unnecessary. Eulerian and Lagrangian implementations of these equations were described and explained with examples for each given: a grid-based solution by Jos Stam and Smoothed Particle Hydrodynamics. A conclusion was drawn regarding which implementation was selected for this paper.
3. **OpenGL and C++/GLFW** - There was a thorough explanation of the rendering graphics pipeline as a result of the *OpenGL* research performed. The reasoning for its selection was also highlighted in the Background Review section of the paper. Furthermore, the issues experienced due to lack of time were also explained.

4. **Unity and Compute Shaders** - There was a thorough description of two implementation methods using *Unity*, a CPU implementation with just *C#* and a GPU implementation including compute shaders. This paper describes the methods used to produce fluid flow behaviours with both, with a main focus on the compute shader version.
5. **Frame Rate and Performance Investigations** - There were sufficient performance optimisations made throughout the paper. Starting from an extremely low frame rate of 2 frames per second, the simulation was eventually improved to 600 frames. Additionally, each action taken to improve the frame rate was described with the implementation presented. There are still a few issues with the simulation fluidity, but this is an area for future work.

5.2 What Was Learned

There was a lot learned throughout the course of this dissertation. Using *OpenGL* for the first time deepened understanding on lower level graphics programming and the fundamentals of graphics rendering. Exploring the graphics rendering pipeline and how developers can interact with it through the use of shaders was also challenging but very rewarding. Evaluating the available options and assessing their project suitability improved development and planning skills. Before this project, experience with graphics and shaders was limited to the use of Shader Graphs in *Unity*, a node-based approach similar to coding environments like *Scratch*. This did not provide a thorough understanding of what shaders did and how they functioned; it was a high level abstraction that simplified the technical learning required. By the end of this project, it is now possible to write shaders without these simplifications, using *GLSL* and *HLSL*.

Furthermore, experience with fluid dynamics was minimal and based mostly on foundational concepts covered in an introductory module, *MSP2803: “Fluid Dynamics 1”* at Newcastle University. There was also a brief understanding of grid-based simulations due to the Paper Review in *CSC2034: “Introducing Contemporary Topics in Computing”*, a module taught in this degree; the paper chosen to review was the Stam paper mentioned in this dissertation[1]. As a result, a lot more research was required to fully understand the physics in computational fluid dynamics and to learn how to implement smoothed particle hydrodynamics in this simulation.

Previous projects were not reliant on optimisation, so there was little initial knowledge on techniques that could be used to improve a program’s performance. An example of this would be through the use of structs. Through

research, it was discovered that passing structs through methods caused all the data to be copied, which can cause huge performance and storage issues in much larger programs. The ability to use references is something that should have been known due to past experience with *C++* but was not considered until actively searching for optimisation techniques.

Learning about how a program can interact with the GPU through the use of shaders also increased understanding of computer architecture elements, such as threads and cores. Switching to the GPU-based computation for all of the calculations was something not practised before and produced a significant performance increase. Although this is not required for smaller projects, it will be very helpful for future simulation tasks or larger programs.

Additionally, a number of new algorithms and their computational implementations were learned. Neighbour-finding techniques such as spatial hashing have a number of uses outside of fluid simulations and video games in general and will be a useful tool for a developer to be able to use. Parallel algorithms, specifically Bitonic sort were also discovered through the course of this paper. Though it is simple to identify where parts of an algorithm are not reliant on each other (and can thus be executed in parallel), it is not as easy to automate the process. This will be a useful tool in the future for optimisation problems also as the computation can be offloaded to other threads and performed simultaneously.

5.3 Future Work

There are a lot of areas where the existing simulation can be improved. The previously mentioned stuttering and collision logic causing frame drops are examples of this. Identifying the causes for these issues and then correcting them are examples of future work that can be done.

Collision logic could also be further improved to consider terrain and other objects that are rendered into the scene. As of now, the particles interact with the box due to it being drawn in the same position as the bounds set. For the sphere, its position is updated in the shader and then collisions are checked - which is a very slow and poorly scaled implementation - performance would suffer as more interactable objects were implemented this way. Custom RigidBodies or advanced collision logic can be developed in the future to account for all objects that may be in the scene.

In addition, the simulation is still a collection of particles. In the future, methods can be used to hide the particles and achieve a more realistic fluid appearance, by visually smoothing them or rendering them with surface reconstruction techniques such as ray-marching or screen spacing. Also, the simulation currently only supports one type of fluid at a time. In the fu-

ture this simulation should be able to simulate the interactions between two different fluids, such as oil and water.

As both the *OpenGL* and CPU implementations were ultimately abandoned, it would be great to revisit them and improve them even further. Although the CPU version may not achieve as high frame rates as the other two, it can still be optimised well enough to be realistic and run with at least 60 frames per second. The *OpenGL* version, however, could be improved to a state where it may become slightly superior to the GPU implementation with *Unity*, due to the lack of overhead present from a graphics API as opposed to an entire game engine.

Further optimisations can be made in addition to the ones currently implemented in the final version. Since performance decreases at an exponential rate, there is a lot more work that can be done to reduce these effects and maintain a high frame count for larger particle quantities. An eventual goal would be to make the simulation smooth and consistent for 1,000,000 particles at 60 frames per second, though this is still quite far out of reach for now. This may be possible with more recent studies and discoveries made in computational fluid dynamics - the papers used in this dissertation are quite outdated by now (Stam's and Müller's papers was written in 2003) but were great tools for making a start in CFDs.

More future work would involve integrating the completed fluid into an actual video game environment. This would be to ensure that the fluid does not affect the performance of other assets built into a scene with it and does not reduce the overall frame rate of the game to a suboptimal value.

6 References

References

- [1] J. Stam, “Real-Time Fluid Dynamics for Games,” <https://damassets.autodesk.net/content/dam/autodesk/www/autodesk-reasearch/Publications/pdf/realtime-fluid-dynamics-for.pdf>, 2003, paper, last accessed February 18, 2025.
- [2] T. Sze and Y. Liu, “Online Gantt,” <https://www.onlinegantt.com/#/gantt>, online software, last accessed February 19, 2025.
- [3] PavelDoGreat, <https://paveldogreat.github.io/WebGL-Fluid-Simulation/>, web-based fluid simulation, last accessed January 28, 2025.
- [4] G. Kot, “Viscoelastic WebGL Fluid Simulation,” <https://grantkot.com/ll/>, web-based fluid simulation, last accessed January 29, 2025.
- [5] S. Macke, “Interplanetary Postal Service,” <https://play.js13kgames.com/interplanetary-postal-service/>, web-based game, last accessed April 26, 2025.
- [6] V. Method, “Obi Fluid,” <https://assetstore.unity.com/packages/tools/physics/obi-fluid-63067>, unity asset, last accessed April 26, 2025.
- [7] Kripto289, “KWS Water System standard,” <https://assetstore.unity.com/packages/tools/particles-effects/kws-water-system-standard-rendering-191771>, unity asset, last accessed April 26, 2025.
- [8] deluxe.mp4, “From Dust Gameplay (PC HD),” <https://www.youtube.com/watch?v=gk4hRWD6BT8>, YouTube, video, last accessed April 24, 2025.
- [9] D. A. Gaming, “Incredible Water Physics and Details in Far Cry 6,” <https://www.youtube.com/watch?v=BNispn46eAw>, YouTube, 2022, video, last accessed February 18, 2025.
- [10] “Unity,” <https://unity.com/>, Unity Technologies, game engine, last accessed March 1, 2025.
- [11] aobu, “Eulerian implementation of fluid simulation,” <https://github.com/aobu/FluidSim>, GitHub repository, last accessed April 29.

- [12] J. de Vries, “Learn OpenGL,” <https://learnopengl.com/>, 2014, tutorial website, last accessed April 27, 2025.
- [13] S. Lague, “Coding Adventures: Simulating Fluids,” <https://www.youtube.com/watch?v=rSKMYc1CQHE>, YouTube, 2024, video, last accessed May 1.
- [14] ——, “Coding Adventures: Rendering Fluids,” <https://www.youtube.com/watch?v=kOkfC5fLfgE>, YouTube, 2024, video, last accessed May 1.
- [15] I. Quilez, “palettes - 1999,” <https://iquilezles.org/articles/palettes/>, website tutorial, last accessed May 3.
- [16] Desmos, “Desmos Graphing Calculator,” <https://www.desmos.com/calculator/>, graphing calculator, last accessed May 5.
- [17] “Unity Asset Store,” <https://assetstore.unity.com/>, Unity Technologies, asset store, last accessed March 2, 2025.
- [18] Eyratrin, “Stylized Water URP,” <https://assetstore.unity.com/packages/vfx/shaders/stylized-water-upr-shader-277311>, unity asset, last accessed April 26, 2025.
- [19] “Computational Fluid Dynamics (CFD) Market Size, Share, Growth, and Industry Analysis, By Type (Personal and Commercial), By Application (Aerospace and Defense, Automotive Industry, Electrical and Electronics, and Others), Regional Insights and Forecast From 2025 To 2033,” <https://www.businessresearchinsights.com/market-reports/computational-fluid-dynamics-cfd-market-111787>, Business Research Insights, 2025, article, last accessed February 18, 2025.
- [20] “Far Cry 6,” <https://www.ubisoft.com/en-gb/game/far-cry/far-cry-6>, Ubisoft, 2021, video game, last accessed April 25, 2025.
- [21] “GLFW,” <https://www.glfw.org/>, window creation API, last accessed February 1, 2025.
- [22] “OpenGL,” <https://www.opengl.org/>, Khronos Group, graphics API, last accessed February 1, 2025.
- [23] “WebGL,” <https://en.wikipedia.org/wiki/WebGL>, Wikipedia, last accessed April 25, 2025.

- [24] Éric Chahi, “From Dust,” <https://store.ubisoft.com/uk/from-dust/56c4948588a7e300458b4766.html>, Ubisoft Montpellier, 2011, video game.
- [25] J. Papadopoulos, “From Dust PC is capped at 30fps and requires you to be online; No AA or VSync options,” Dark Side of Gaming, Tech. Rep., 2011, tech report.
- [26] S. Interactive, “Clair Obscur: Expedition 33,” Kepler Interactive, 2025, video game.
- [27] A. Sergeev, “The Photon Water System: Developing a Next-Gen Water Rendering Solution for Games,” <https://80.lv/articles/developing-a-next-gen-water-rendering-solution-for-games/>, April 2023, interview.
- [28] Z. Wu and K. Wu, “Photon Water System: Open world water rendering and real-time simulation,” <https://gdcvault.com/play/1028829/Advanced-Graphics-Summit-Open-World>, Lightspeed Studios, March 2023.
- [29] “Vulkan,” <https://www.vulkan.org/>, Khronos Group, graphics API, last accessed April 27, 2025.
- [30] A. Overvoorde, “Vulkan Tutorial,” <https://vulkan-tutorial.com/>, tutorial website, last accessed April 27, 2025.
- [31] ——, <https://vulkan-tutorial.com/#comment-2809900518>, comment on tutorial website, last accessed April 27, 2025.
- [32] Mia John, “Animation of fluids,” https://www.slideserve.com/Mia_John/animation-of-fluids, September 2011, lesson slides, last accessed April 28.
- [33] C. Dictionary, “Advection,” <https://dictionary.cambridge.org/dictionary/english/advection>, dictionary definition, last accessed April 28.
- [34] Wikipedia, “Navier-stokes equations,” https://en.wikipedia.org/wiki/Navier%20%93Stokes_equations, wikipedia, last accessed April 28.
- [35] BBC, “Pressure in fluids,” <https://www.bbc.co.uk/bitesize/articles/zv7ybqt#zwv4cmn>, KS3 physics resource, last accessed April 24.

- [36] D. C. Matthias Müller and M. Gross, “Particle-based fluid simulation for interactive applications,” <https://matthias-research.github.io/pages/publications/sca03.pdf>, 2003, paper, last accessed April 20.
- [37] GeeksForGeeks, “Agile software development – software engineering,” <https://www.geeksforgeeks.org/software-engineering-agile-software-development/>, March 2024, educational website, last accessed April 29.
- [38] sabarnac, “Gpu shader tutorial,” <https://shader-tutorial.dev/basics/vertex-shader/>, shader tutorial, last accessed April 29.
- [39] Dav1dde, “Glad,” <https://github.com/Dav1dde/glad>, multi-language loader-generator for graphics APIs, last accessed April 29.
- [40] R. L. Guy, “Smoothed Particle Hydrodynamics Fluid Simulation,” <https://rlguy.com/sphfluidsim/>, 2015, website, last accessed April 30.
- [41] A. Venkat, “Gridparticle shader,” <https://github.com/AJTech2002/Smoothed-Particle-Hydrodynamics/blob/youtube-part-1/Assets/Shaders/GridParticle.shader>, GitHub repository, last accessed April 20.
- [42] P. D., “Implementing Spatial Hashing For Efficient Collision Detection In 3d Environments,” <https://peerdh.com/blogs/programming-insights/implementing-spatial-hashing-for-efficient-collision-detection-in-3d-environments>, 2024.
- [43] E. Nicol, “SPH-Fluid-Simulator,” <https://github.com/lijenicol/SPH-Fluid-Simulator/tree/master>, GitHub repository, last accessed March 10.
- [44] NullPointer Exception, “Bitonic Sort - Sorting Algorithms Mini-Series (Episode 9),” <https://www.youtube.com/watch?v=uEfieI0MumY>, YouTube, 2021, video, last accessed May 1.
- [45] A. Venkat, “Coding a Realtime Fluid Simulation in Unity [Pt. 2],” <https://www.youtube.com/watch?v=9M72KrGhYuE>, YouTube, 2024, video, last accessed May 1.
- [46] M. Malík, “Hwinfo,” <https://www.hwinfo.com/>, system information and diagnostics tool, last accessed May 6.

A Unity Asset Store

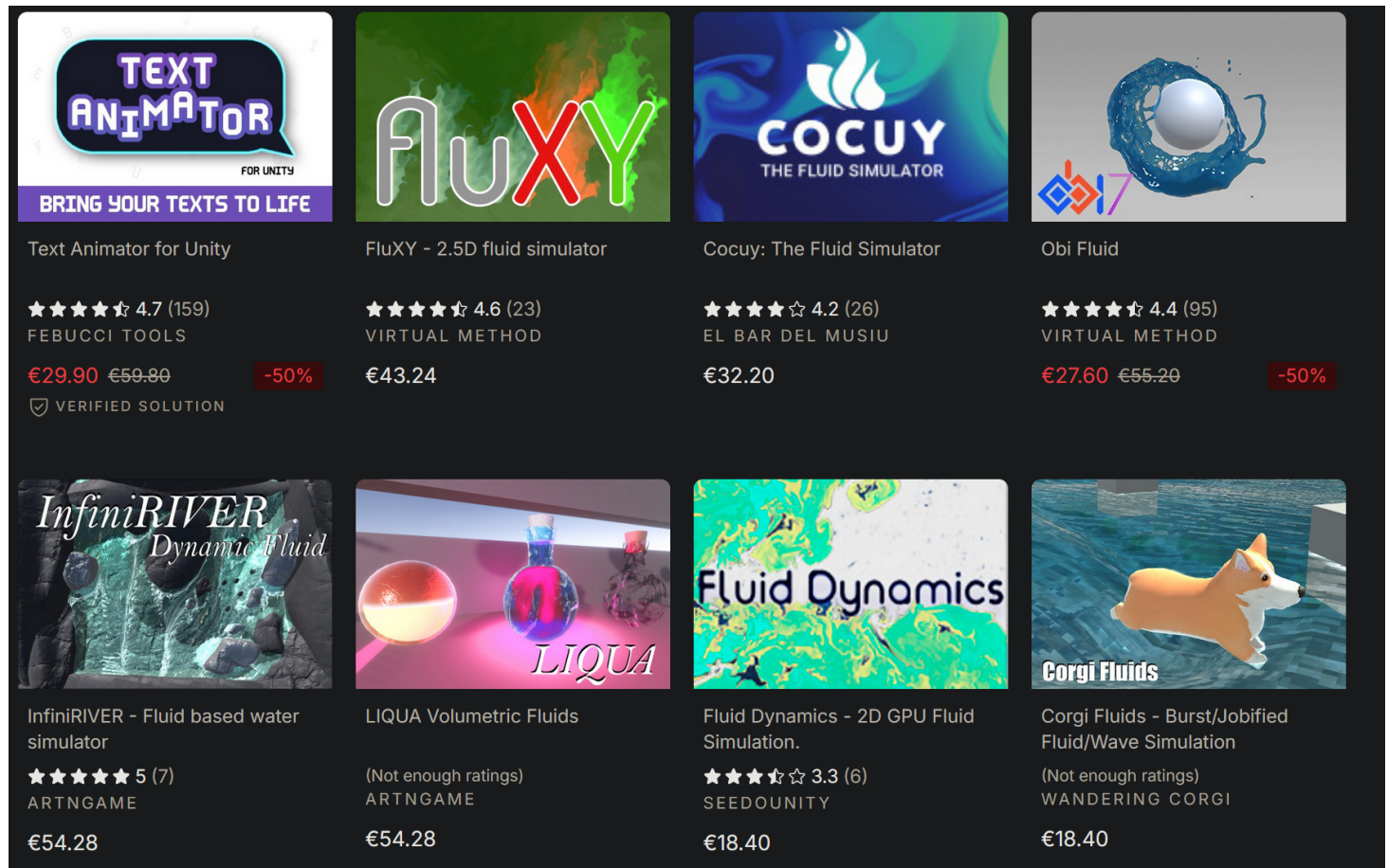


Figure 46: Most popular results for "fluid simulation" [17]

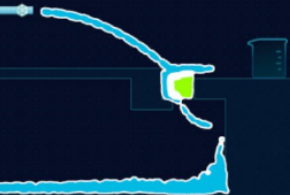
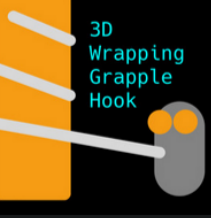
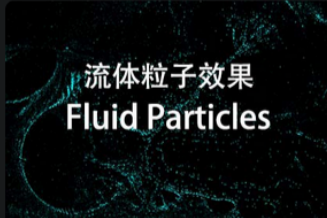
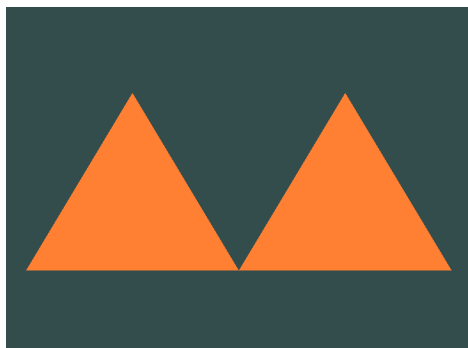
| | | | |
|--|--|---|---|
|  |  |  |  |
| Easy Camera: RTS & Top-Down (Not enough ratings) KAGEBANA PRODUCTION Free | Kinematic Character Controller ★★★★★ 4.8 (189) PHILIPPE ST-AMAND Free | Multi-State Character Controller ★★★★☆ 3.7 (7) IMITATION STUDIOS Free | Soft2D for Unity ★★★☆☆ 2.3 (6) TAICHI GRAPHICS Free |
|  |  |  |  |
| Zibra Effects: VR/AR Solution (Subscription) ★★★★☆ 3 (24) ZIBRA AI Free | FlexiCamTool - Camera Controller (Not enough ratings) GLITCH & GIGGLE GAMES €4.59 | Ready-2-Use Character Controller (Not enough ratings) AZTECH GAMES €4.59 | 3D Wrapping Grapple Hook (Not enough ratings) A TRILLION GAMES LTD €4.59 |
|  |  |  |  |
| Fluid Particles (Not enough ratings) MAYTHING STUDIO €5.51 | Screen Space Fluids ★★★★☆ 4.2 (17) DR KORZEN €6.44 | Spice Up: Rain (Not enough ratings) FRONKON GAMES €9.19 | Idle Anim Set (Not enough ratings) MOTIONDEZIRE €9.19 |

Figure 47: Cheapest results for "fluid simulation" [17]

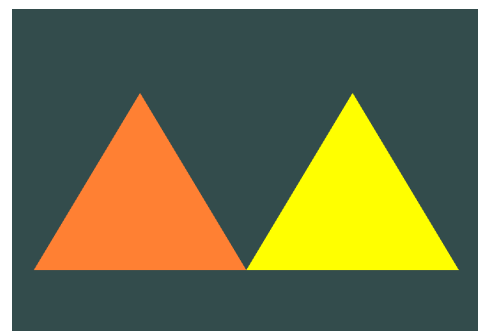


Figure 48: Example of surface-only Unity asset [18]

B Learn OpenGL and graphics

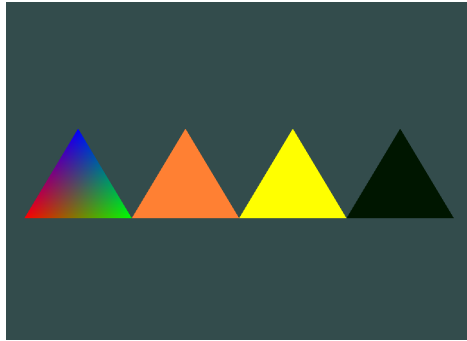


(a) Rendering two triangles with the same shader in OpenGL

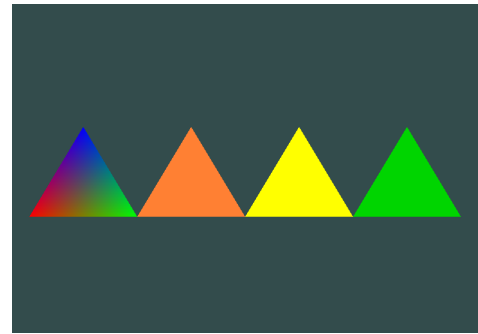


(b) Rendering two triangles with different shaders in OpenGL

Figure 49: Initial Triangle Rendering

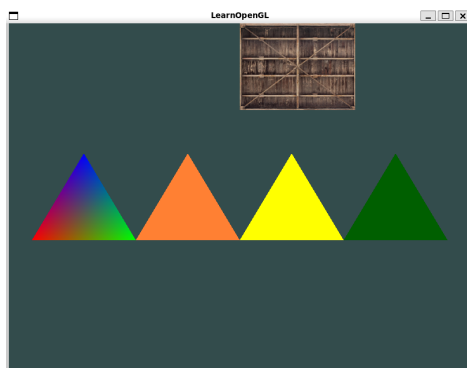


(a) Colour-changing triangle dark

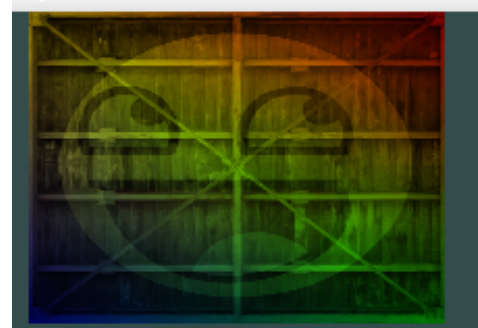


(b) Colour-changing triangle light

Figure 50: Rainbow Triangle and Colour-changing triangle

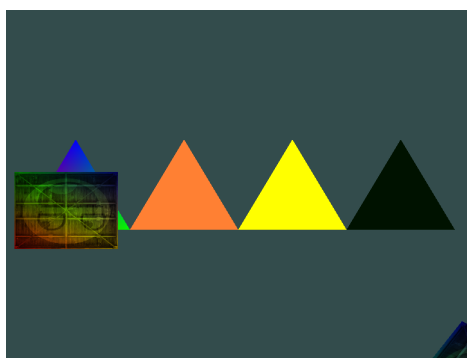


(a) Texture Rendering

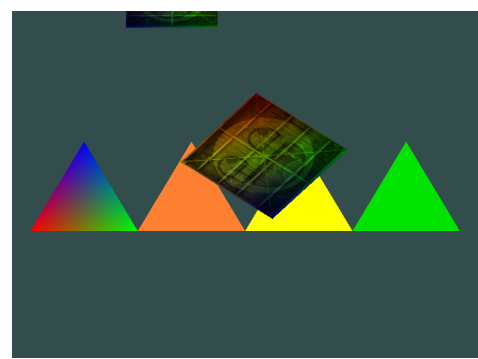


(b) Colours and textures applied over a texture

Figure 51: Textures



(a) First position



(b) Second position

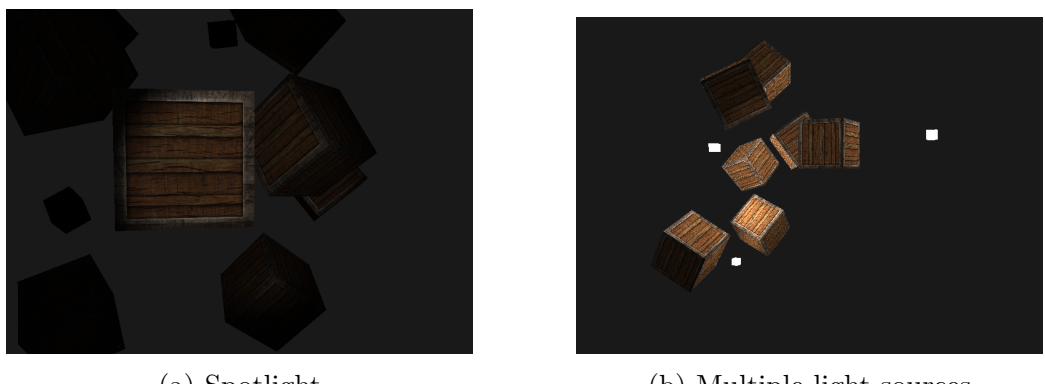
Figure 52: Graphics moving with time



(a) Light in top right corner

(b) Light on the right

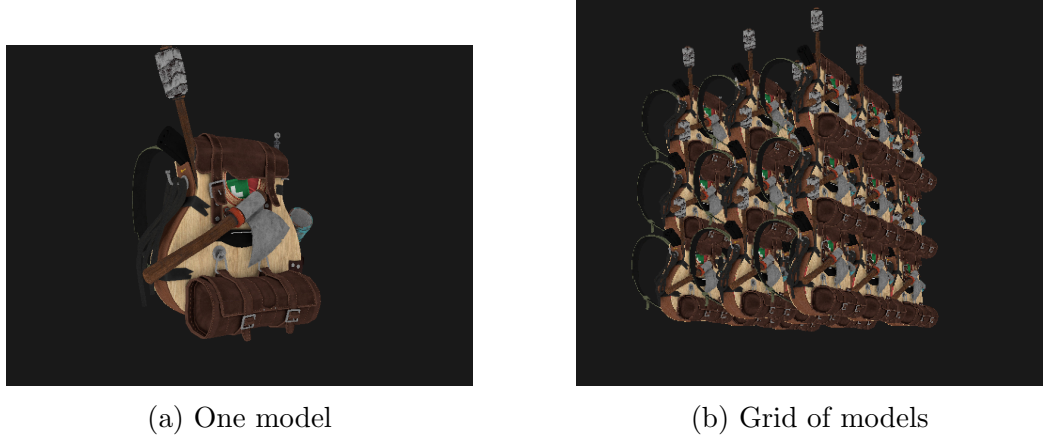
Figure 53: Phong Lighting and moveable light source



(a) Spotlight

(b) Multiple light sources

Figure 54: More lighting



(a) One model

(b) Grid of models

Figure 55: Rendering Object Files

C CPU Implementation with Unity

```
1 reference
public void ResolveCollisions(int boxSize)
{
    float particleRadius = ParticleManagerCPU.PARTICLE_RADIUS;
    float damping = -0.3f;

    if (position.y <= particleRadius)
    {
        position.y = particleRadius;
        velocity.y *= damping;
    }
    else if (position.y >= boxSize)
    {
        position.y = boxSize;
        velocity.y *= damping;
    }

    if (position.x <= particleRadius)
    {
        position.x = particleRadius;
        velocity.x *= damping;
    }
    else if (position.x >= boxSize)
    {
        position.x = boxSize;
        velocity.x *= damping;
    }

    if (position.z <= particleRadius)
    {
        position.z = particleRadius;
        velocity.z *= damping;
    }
    else if (position.z >= boxSize / 2)
    {
        position.z = boxSize / 2;
        velocity.z *= damping;
    }
}
```

Figure 56: CPU collision detection C#

```

private void Update()
{
    //apply gravity
    for (int i = 0; i < PARTICLE_COUNT; i++)
    {
        particles[i].velocity += DELTA_TIME * GRAVITY * Vector3.down;
        //particles[i].position += particles[i].velocity * DELTA_TIME;
    }

    //update spatial hash and keys
    for (int i = 0; i < PARTICLE_COUNT; i++)
    {
        particles[i].cell = SpatialHashCPU.CalculateCell(particles[i].position);
        particles[i].hash = SpatialHashCPU.CalculateCellHash(particles[i].cell);
    }

    //update neighbour table
    neighbourTable = SpatialHashCPU.NeighbourTable(particles);

    for (int i = 0; i < PARTICLE_COUNT; i++)
    {
        particles[i].neighbours = SpatialHashCPU.GetNeighbours(neighbourTable, particles[i], particles);
    }

    //calculate density and pressure
    for (int i = 0; i < PARTICLE_COUNT; i++)
    {
        particles[i] = CalculateDensityPressure(particles[i]);
    }

    //apply forces
    for (int i = 0; i < PARTICLE_COUNT; i++)
    {
        /*particles[i] = ComputeForces(particles[i]);*/

        particles[i].velocity += RECIPROCAL_MASS * DELTA_TIME * particles[i].currentForce;
        particles[i].position = particles[i].gameObject.transform.position;
        particles[i].position += particles[i].velocity * DELTA_TIME;
        Vector3 pressureForce = CalculatePressureForce(particles[i].position, particles[i]);
        Vector3 pressureAcceleration = pressureForce / particles[i].density;
        particles[i].velocity += pressureAcceleration * DELTA_TIME;

        Vector3 viscosityForce = CalculateViscosityForce(particles[i]);
        Vector3 viscosityAcceleration = viscosityForce / particles[i].density;
        particles[i].velocity += viscosityAcceleration * DELTA_TIME;
    }

    // apply actual position
    for (int i = 0; i < PARTICLE_COUNT; i++)
    {
        particles[i].position += particles[i].velocity * DELTA_TIME;
        particles[i].ResolveCollisions(BOX_SIZE);

        particles[i].gameObject.transform.position = particles[i].position; //make the actual particle move now
    }
}

```

Figure 57: Simulation Loop

```

1 reference
public static Dictionary<uint, List<int>> NeighbourTable(ParticleCPU[] particles)
{
    Dictionary<uint, List<int>> neighbourTable = new();

    for (int i = 0; i < particles.Length; i++)
    {
        uint hash = particles[i].hash;

        if (!neighbourTable.ContainsKey(hash))
        {
            neighbourTable[hash] = new List<int>();
        }

        neighbourTable[hash].Add(i);
    }

    return neighbourTable;
}

```

Figure 58: Neighbour Table

```

public ParticleCPU CalculateDensityPressure(ParticleCPU particle)
{
    float sum = 0;

    foreach (int otherID in particle.neighbours)
    {
        ParticleCPU other = particles[otherID]; //foreach(otherID in particle.neighbours) Particle other = particles[otherID];

        float dist = (particle.position - other.position).magnitude;
        float distSquared = dist * dist;

        if (distSquared < PARTICLE_EFFECT_RADIUS_SQUARED)
            sum += Poly6(distSquared * 0.004f);
    }

    sum += Poly6(0.0f); //add own density

    particle.density = sum * PARTICLE_MASS + EPSILON; //add small value to prevent division by 0;
    particle.pressure = GAS_CONSTANT * (particle.density - TARGET_DENSITY);

    return particle;
}

```

Figure 59: Density and Pressure

```
1 reference
public static HashSet<int> GetNeighbours(Dictionary<uint, List<int>> neighbourTable, ParticleCPU particle, ParticleCPU[] particles)
{
    HashSet<int> neighbours = new();

    for (int dx = -1; dx <= 1; dx++)
    {
        for (int dy = -1; dy <= 1; dy++)
        {
            for (int dz = -1; dz <= 1; dz++)
            {
                Vector3Int neighbourCell = particle.cell + new Vector3Int(dx, dy, dz);
                uint neighbourHash = CalculateCellHash(neighbourCell);

                if (neighbourTable.TryGetValue(neighbourHash, out var indices))
                {
                    foreach (int index in indices)
                    {
                        if (particles[index].ID != particle.ID)
                        {
                            neighbours.Add(particles[index].ID);
                        }
                    }
                }
            }
        }
    }

    return neighbours;
}
```

Figure 60: Get Neighbours

```

1 reference
public Vector3 CalculatePressureForce(Vector3 position, ParticleCPU particle)
{
    Vector3 pressureForce = Vector3.zero;

    foreach (int otherID in particle.neighbours)
    {
        ParticleCPU other = particles[otherID];
        if (particle.ID == other.ID) continue;

        Vector3 offset = other.position - position;
        float dist = offset.magnitude;

        if (dist < EPSILON) continue;

        Vector3 dir = offset / dist;
        pressureForce += (particle.pressure + other.pressure) / (2 * other.density) * PARTICLE_MASS * SpikyKernelGradient(dist, dir);
    }

    return pressureForce;
}

1 reference
public Vector3 CalculateViscosityForce(ParticleCPU particle)
{
    Vector3 viscosityForce = Vector3.zero;

    foreach (int otherID in particle.neighbours)
    {
        ParticleCPU other = particles[otherID];
        if (particle.ID == other.ID) continue;

        float dist = (particle.position - other.position).magnitude;
        viscosityForce += (other.velocity - particle.velocity) * ViscosityLaplacianKernel(dist);
    }

    return viscosityForce * VISCOSITY;
}

```

Figure 61: Pressure and Viscosity Forces

D GPU Implementation with Unity

D.1 Rendering Logic

```
[System.Serializable]
[StructLayout(LayoutKind.Sequential, Size = 44)] //maintain order of data
4 references
public struct ParticleGPU
{
    0 references
    public float pressure;
    0 references
    public float density;

    0 references
    public Vector3 forces;
    0 references
    public Vector3 velocity;
    1 reference
    public Vector3 position;
}
```

Figure 62: Particle struct sent to shader

```
private void Update()
{
    // render the particles
    material.SetFloat(SizeProperty, particleRenderSize);
    material.SetBuffer(ParticlesBufferProperty, _particlesBuffer);

    if (!showSpheres) return;

    Graphics.DrawMeshInstancedIndirect
    (
        particleMesh,
        0,
        material,
        new Bounds(Vector3.zero, boxDimensions),
        _argsBuffer,
        castShadows: UnityEngine.Rendering.ShadowCastingMode.Off
    );
}
```

Figure 63: Update loop to render the particles

```

[Header("Properties")]
1 reference
private static readonly int SizeProperty = Shader.PropertyToID("_size");
1 reference
private static readonly int ParticlesBufferProperty = Shader.PropertyToID("_particlesBuffer");
0 references
private void Awake()
{
    if (!GetComponent<CORG>().gpu) return;

    SpawnParticles();

    // setup buffers
    uint[] args =
    {
        particleMesh.GetIndexCount(0),
        (uint)ParticleCount,
        particleMesh.GetIndexStart(0),
        particleMesh.GetBaseVertex(0),
        0
    };

    _argsBuffer = new ComputeBuffer(1, args.Length * sizeof(uint), ComputeBufferType.IndirectArguments);
    _argsBuffer.SetData(args);

    _particlesBuffer = new ComputeBuffer(ParticleCount, 44);
    _particlesBuffer.SetData(particles);

    _particleIndicesBuffer = new ComputeBuffer(ParticleCount, 4);
    _cellIndicesBuffer = new ComputeBuffer(ParticleCount, 4);
    _lookupTableBuffer = new ComputeBuffer(ParticleCount, 4);

    //initial indices setup
    uint[] particleIndices = new uint[ParticleCount];
    for (uint i = 0; i < ParticleCount; i++) particleIndices[i] = i;
    _particleIndicesBuffer.SetData(particleIndices);

    SetUpComputeBuffers();
}

```

Figure 64: Buffer setup for shaders

```

1 reference
private void SpawnParticles()
{
    List<ParticleGPU> _particles = new();

    // spawn particles in a grid - removed triple for loop but might actually worsen performance due to additional calculations
    for (int i = 0; i < rowCount.x * rowCount.y * rowCount.z; i++)
    {
        int x = i / (rowCount.x * rowCount.y);
        int y = i / rowCount.x % rowCount.y;
        int z = i % rowCount.x;

        Vector3 spawnPos = spawnPoint + 2 * particleRadius * new Vector3(x, y, z);
        spawnPos += jitter * particleRadius * Random.onUnitSphere;

        ParticleGPU particle = new();
        {
            position = spawnPos
        };

        _particles.Add(particle);
    }

    particles = _particles.ToArray();
}

```

Figure 65: Render the grid of particles with slight jitter

D.2 Sphere Collider Logic

Note: the sphere's position and radius is passed through to the shader every update loop.

```

// collision external force
float3 collisionDir = _particles[particleIndex].position - collisionPosition;
float distance2 = dot(collisionDir, collisionDir);

if (distance2 < collisionRadius * collisionRadius + smoothingRadius)
{
    // only square root if needed; expensive operation
    float distance = sqrt(distance2);
    float3 normalizeDir = collisionDir / distance;
    float falloff = 1 - (distance / collisionRadius);
    _particles[particleIndex].forces += normalizeDir * collisionForce * falloff;
}

```

Figure 66: Sphere Collider Logic

D.3 Collision Resolution

```
[numthreads(256,1,1)]
void MoveParticles(int3 id: SV_DISPATCHTHREADID)
{
    const float damping = -0.3;

    float3 vel = _particles[id.x].velocity + deltaTime * _particles[id.x].forces / particleMass; //v = u + at, F = ma
    float3 pos = _particles[id.x].position + vel * deltaTime;

    // box collision resolutions
    if (pos.x - smoothingRadius < 0)
    {
        pos.x = smoothingRadius;
        vel.x *= damping;
    }
    else if (pos.x + smoothingRadius > boxDimensions.x)
    {
        pos.x = boxDimensions.x - smoothingRadius;
        vel.x *= damping;
    }

    if (pos.y - smoothingRadius < 0)
    {
        pos.y = smoothingRadius;
        vel.y *= damping;
    }
    else if (pos.y + smoothingRadius > boxDimensions.y)
    {
        pos.y = boxDimensions.y - smoothingRadius;
        vel.y *= damping;
    }

    if (vel.y < 0.1) vel.y == 0;

    if (pos.z - smoothingRadius < 0)
    {
        pos.z = smoothingRadius;
        vel.z *= damping;
    }
    else if (pos.z + smoothingRadius > boxDimensions.z)
    {
        pos.z = boxDimensions.z - smoothingRadius;
        vel.z *= damping;
    }

    _particles[id.x].velocity = vel;
    _particles[id.x].position = pos;
}
```

Figure 67: Particle movement and collision resolution in the same method

D.4 Rewritten Shader

```
Shader "Instanced/GridTestParticleShader"
{
    Properties
    {
        _Glossiness("Smoothness", Range(0,1)) = 0.5
        _Metallic("Metallic", Range(0,1)) = 0.0
        _Color("Color", Color) = (0.25, 0.5, 0.5, 1)
        _DensityRange ("Density Range", Range(0,500000)) = 1.0
    }

    SubShader
    {
        Tags { "RenderType" = "Opaque" }
        LOD 200

        Pass
        {

            CGPROGRAM
            #pragma vertex vert
            #pragma fragment frag
            #pragma multi_compile_instancing
            #pragma instancing_options procedural:setup

            #include "UnityCG.cginc"

            float _Glossiness;
            float _Metallic;
            float3 _Color;
            float _DensityRange;
            float _size;

            #define PI 3.141592654

            struct Particle
            {
                float pressure;
                float density;
                float3 force;
                float3 velocity;
                float3 position;
            };
        
```

Figure 68: setup and Particle struct

```

struct appdata
{
    float3 vertex : POSITION;
    float3 normal : NORMAL;
    UNITY_VERTEX_INPUT_INSTANCE_ID
};

struct v2f
{
    float4 pos : SV_POSITION;
    float3 worldPos : TEXCOORD0;
    float3 worldNormal : TEXCOORD1;
    float velocity : TEXCOORD2;
    UNITY_VERTEX_INPUT_INSTANCE_ID
};

StructuredBuffer<Particle> _particlesBuffer;

void setup() {}

v2f vert(appdata v)
{
    v2f o;

    UNITY_SETUP_INSTANCE_ID(v);

    Particle p = _particlesBuffer[unity_InstanceID];

    float3 pos = p.position;
    float scale = _size;
    float3 worldPos = pos + v.vertex * scale;

    o.pos = UnityObjectToClipPos(float4(worldPos, 1.0));
    o.worldPos = worldPos;

    float3 worldNormal = UnityObjectToWorldNormal(v.normal);
    o.worldNormal = normalize(worldNormal);

    o.velocity = length(p.velocity);

    UNITY_TRANSFER_INSTANCE_ID(v, o);

    return o;
}

```

Figure 69: appdata, v2f structs and vertex shader

```

// color helper function
float3 palette(in float t, in float3 a, in float3 b, in float3 c, in float3 d)
{
    return a + b * cos(2 * PI * (c * t + d));
}

fixed4 frag(v2f i) : SV_TARGET
{
    float3 a = float3(0.5, 0.5, 0.5);
    float3 b = float3(0.5, 0.5, 0.5);
    float3 c = float3(1.0, 1.0, 1.0);
    float3 d = float3(0.0, 0.33, 0.67);

    float3 colNoLight = palette(i.velocity, a, b, c, d);

    float3 lightDir = normalize(_WorldSpaceLightPos0.xyz);
    float dotProduct = max(0, dot(i.worldNormal, lightDir));

    float3 colLight = colNoLight * (dotProduct + 0.2);

    return float4(colLight, 1.0);
}
ENDCG
}
}
}

```

Figure 70: Fragment Shader and Palette method

D.5 Final Result

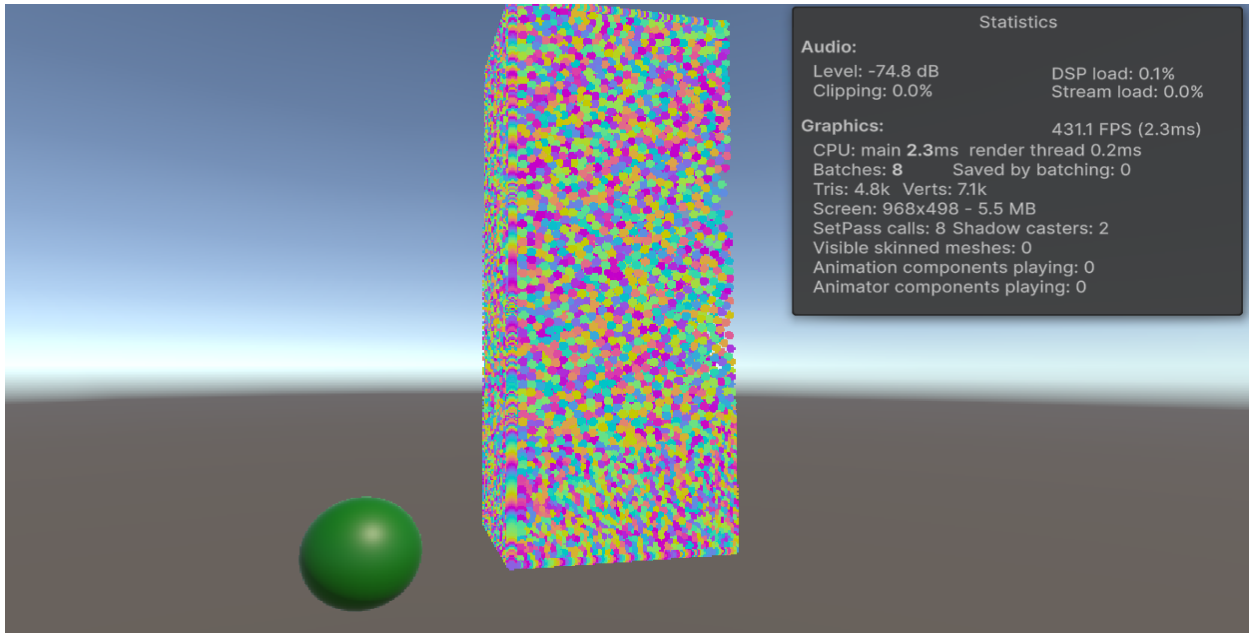


Figure 71: Small box, first few seconds

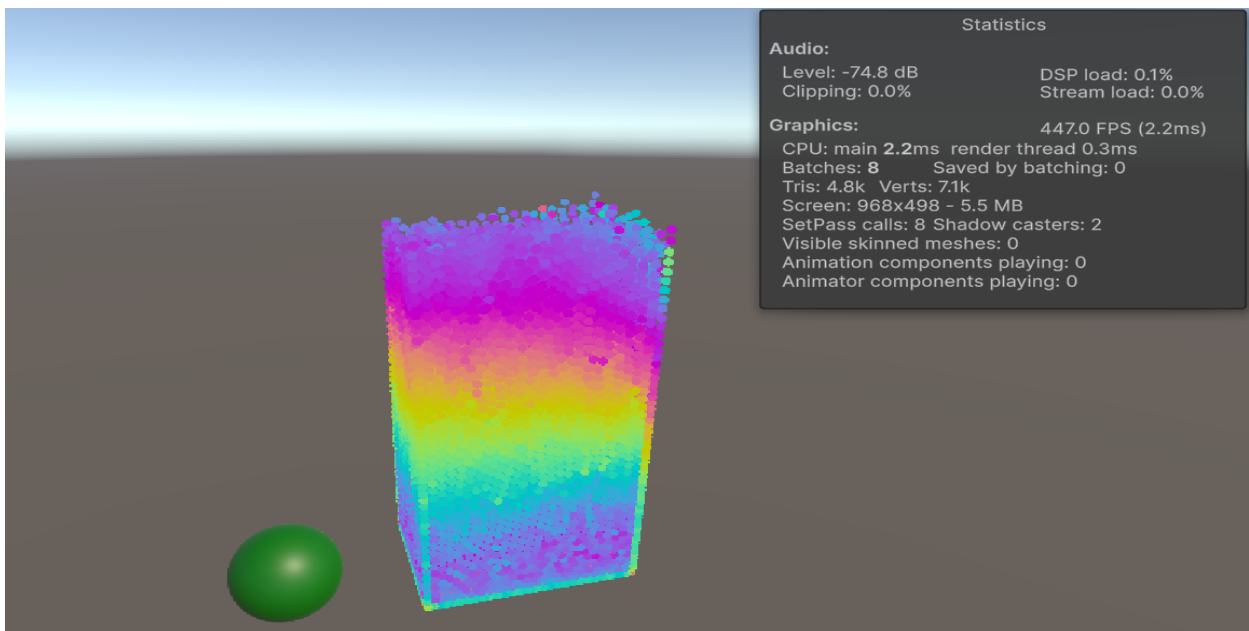


Figure 72: Small box, slowed down

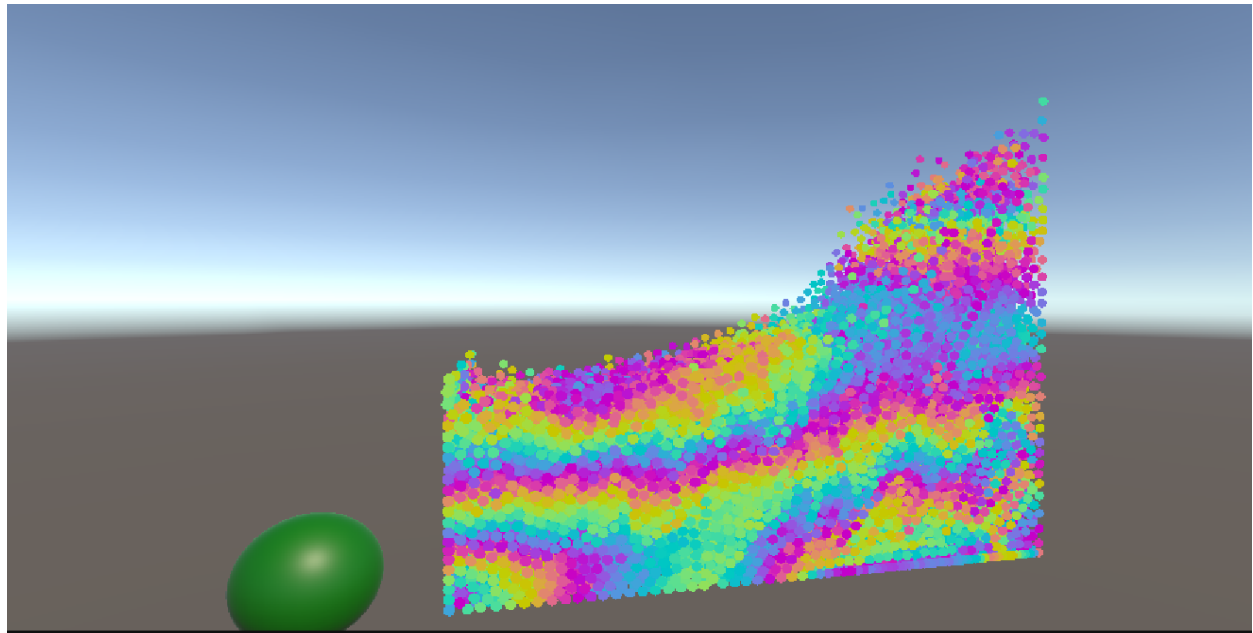


Figure 73: Box X-dimension increase

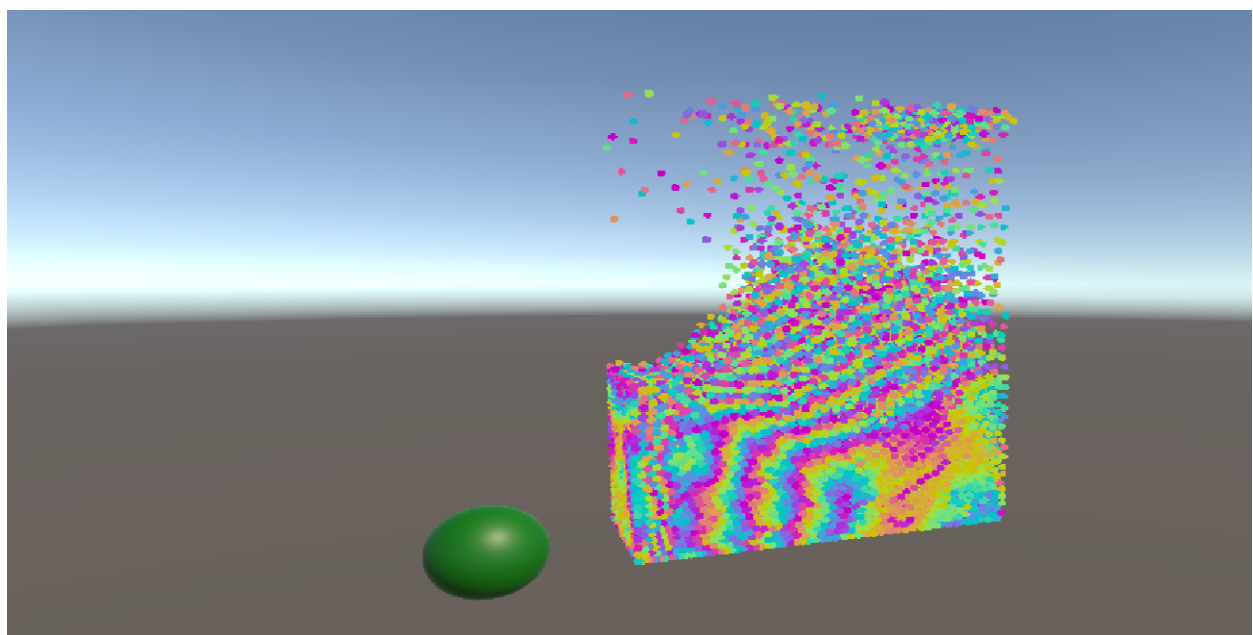


Figure 74: Box X-dimension abruptly decreased

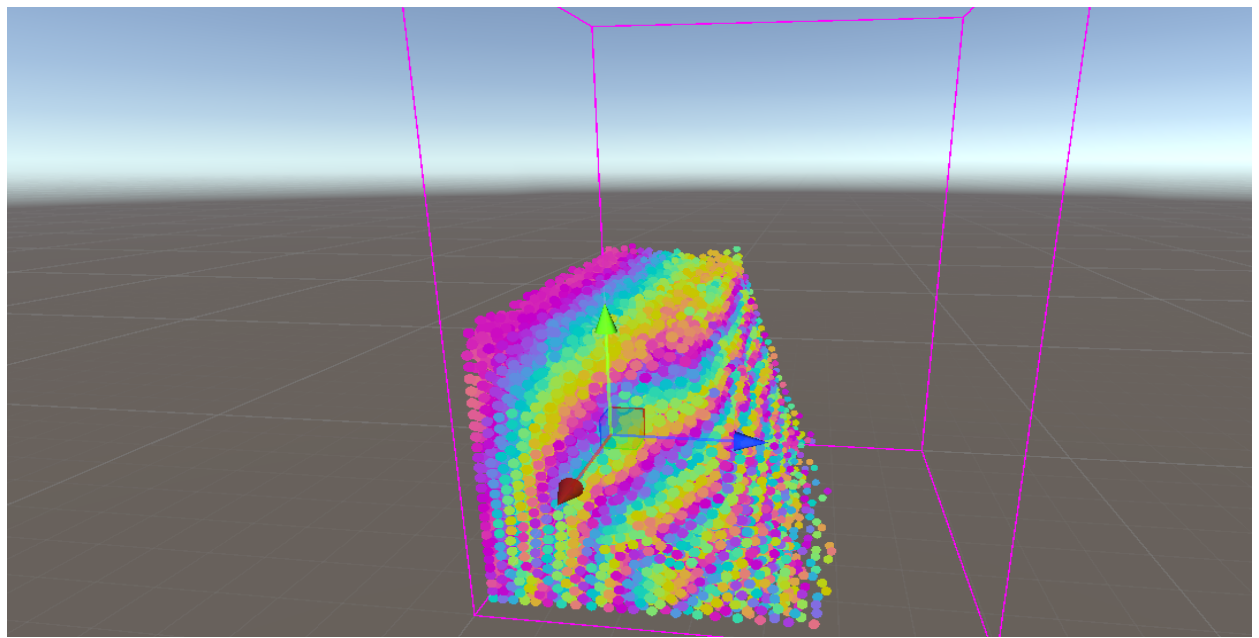


Figure 75: Box Z-dimension increase

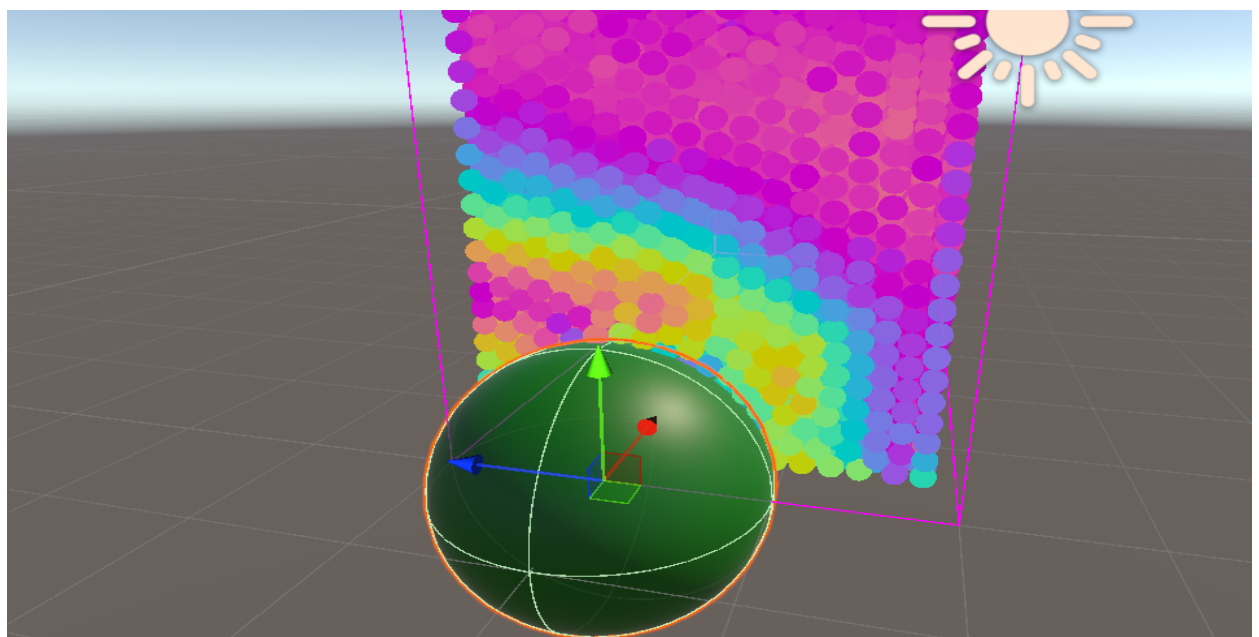


Figure 76: Ripples as particles pushed away by sphere

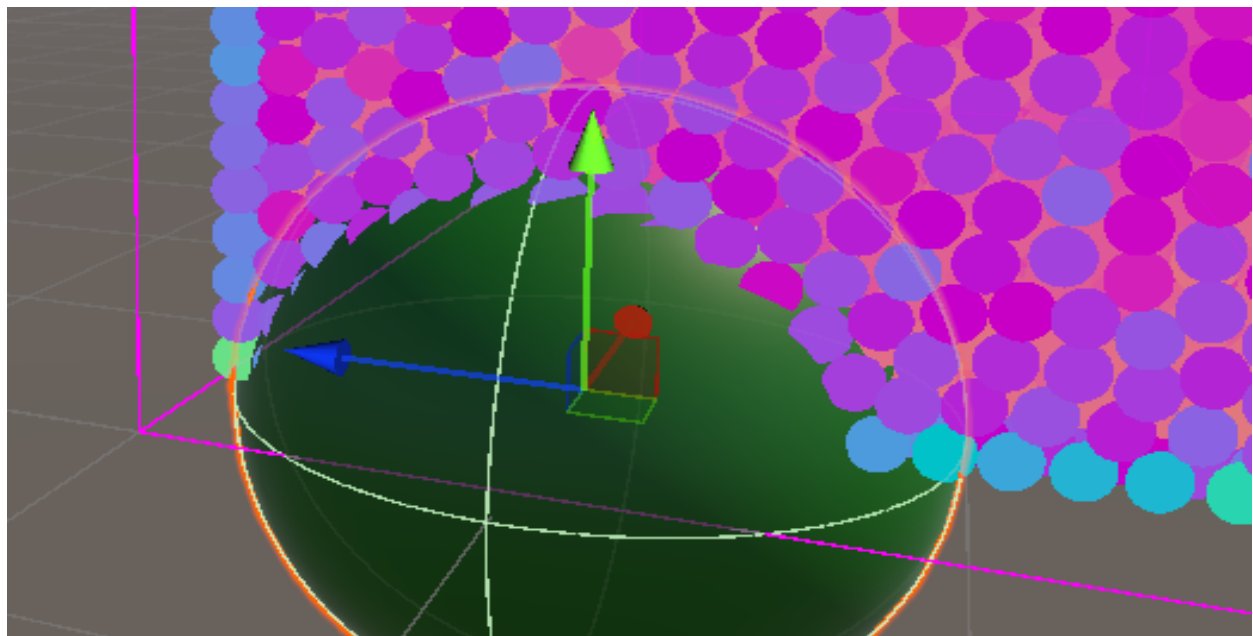


Figure 77: Sphere displacement



Figure 78: No particles inside the sphere radius

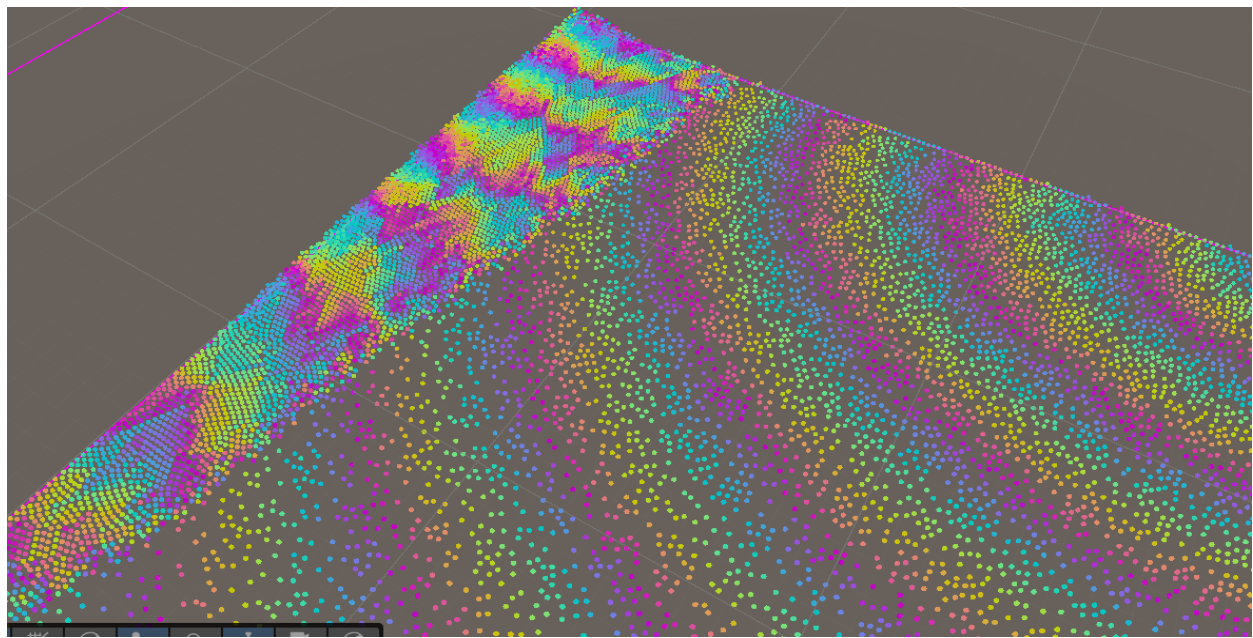


Figure 79: Box X-dimension increase then Z-dimension increase

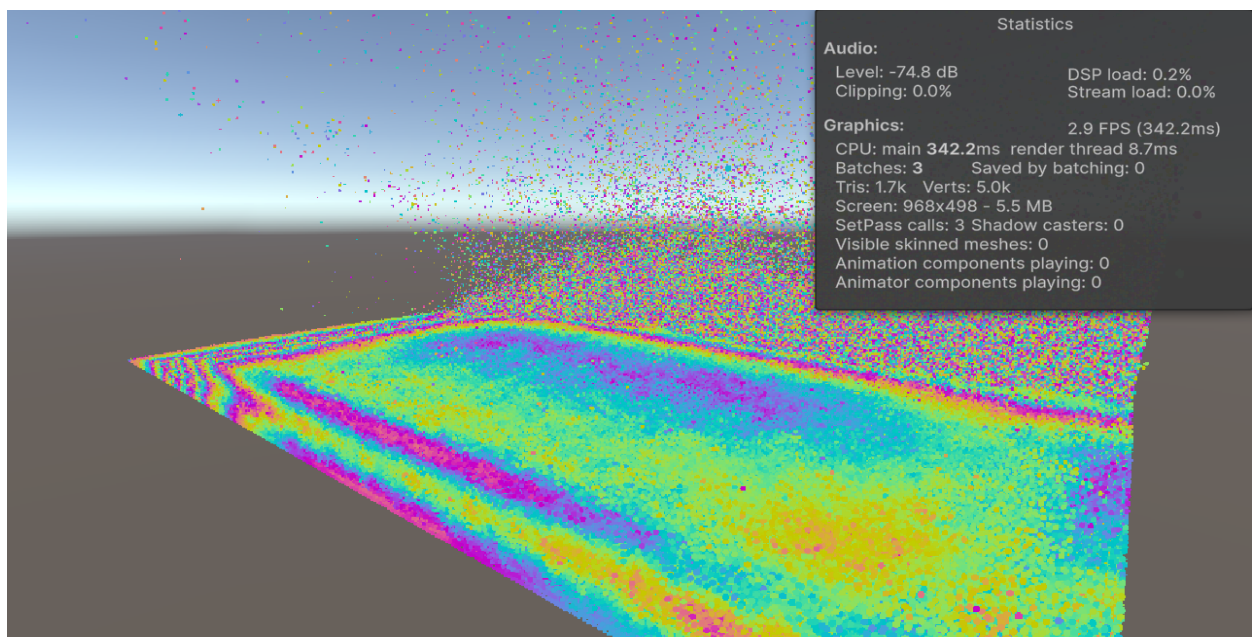


Figure 80: 3 FPS and instability with 884736 particles

E Kernel Derivations

E.1 Spiky Kernel Gradient

Proof. Spherical Gradient is defined as

$$\nabla f = \frac{\partial f}{\partial r} \mathbf{e}_r + \frac{1}{r} \frac{\partial f}{\partial \theta} \mathbf{e}_\theta + \frac{1}{r \sin \theta} \frac{\partial f}{\partial \phi} \mathbf{e}_\phi$$

where $\mathbf{e}_r, \mathbf{e}_\theta, \mathbf{e}_\phi$ are the unit direction vectors in the radial, polar and azimuthal directions respectively.

Due to the radial symmetry of smoothing kernels, this is simplified to

$$\nabla f = \frac{\partial f}{\partial r} \mathbf{e}_r$$

$$\nabla W_{spiky}(\mathbf{r}, h) = \frac{\partial W}{\partial r} \cdot \frac{\mathbf{r}}{r}$$

$$\frac{\partial W}{\partial r} = \frac{15}{\pi h^6} \cdot \frac{\partial}{\partial r} (h - r)^3$$

Applying the chain rule

$$\frac{\partial}{\partial r} (h - r)^3 = 3 \cdot (h - r)^2 \cdot (-1) = -3(h - r)^2$$

Therefore

$$\nabla W_{spiky}(\mathbf{r}, h) = \frac{15}{\pi h^6} \cdot -3(h - r)^2 \cdot \frac{\mathbf{r}}{r} = \frac{-45}{\pi h^6} \begin{cases} (h - r)^2 \cdot \frac{\mathbf{r}}{r} & 0 \leq r \leq h \\ 0 & otherwise \end{cases}$$

□

E.2 Poly6 Gradient

Proof. Using the spherical gradient from E.1

$$\nabla W_{poly6}(r, h) = \frac{\partial W}{\partial r} \cdot \frac{\mathbf{r}}{r}$$

$$\frac{\partial W}{\partial r} = \frac{315}{64\pi h^9} \cdot \frac{\partial}{\partial r} (h^2 - r^2)^3$$

Applying the chain rule

$$\frac{\partial}{\partial r} (h^2 - r^2)^3 = 3 \cdot (h^2 - r^2)^2 \cdot (-2r) = 6r(h^2 - r^2)^2$$

Therefore

$$\begin{aligned}\nabla W_{poly6}(\mathbf{r}, h) &= \frac{315}{64\pi h^9} \cdot 6(h^2 - r^2)^2 \cdot r \cdot \frac{\mathbf{r}}{r} \\ &= \frac{315}{64\pi h^9} \begin{cases} 6(h^2 - r^2)^2 \cdot \mathbf{r} & 0 \leq r \leq h \\ 0 & otherwise \end{cases}\end{aligned}$$

□

E.3 Poly6 Laplacian

Proof. Spherical Laplacian is defined as

$$\nabla^2 f = \frac{1}{r^2} \frac{\partial}{\partial r} \left(r^2 \frac{\partial f}{\partial r} \right) + \frac{1}{r^2 \sin \theta} \frac{\partial}{\partial \theta} \left(\sin \theta \frac{\partial f}{\partial \theta} \right) + \frac{1}{r^2 \sin^2 \theta} \left(\frac{\partial^2 f}{\partial \phi^2} \right)$$

Due to the radial symmetry of the kernel functions, this is simplified to

$$\nabla^2 f = \frac{1}{r^2} \frac{\partial}{\partial r} \left(r^2 \frac{\partial f}{\partial r} \right)$$

Using the chain rule

$$\begin{aligned}\frac{\partial}{\partial r} \left(r^2 \frac{\partial f}{\partial r} \right) &= 2r \cdot \frac{\partial f}{\partial r} + r^2 \cdot \frac{\partial^2 f}{\partial r^2} \\ \frac{1}{r^2} \left(2r \cdot \frac{\partial f}{\partial r} + r^2 \cdot \frac{\partial^2 f}{\partial r^2} \right) &= \frac{2}{r} \cdot \frac{\partial f}{\partial r} + \frac{\partial^2 f}{\partial r^2}\end{aligned}$$

Therefore

$$\nabla^2 W(\mathbf{r}, h) = 2r \cdot \frac{\partial f}{\partial r} + \frac{\partial^2 f}{\partial r^2}$$

Using the result from E.2, let $C = \frac{315}{64\pi h^9}$

$$\begin{aligned}
\frac{\partial W^2}{\partial r^2} &= \frac{\partial}{\partial r} (-6C(h^2 - r^2)^2 r) \\
&= -6C \cdot \frac{\partial}{\partial r} [(h^2 - r^2)^2 \cdot r] \\
&= -6C \cdot \left[(h^2 - r^2)^2 \cdot \frac{d}{dr}(r) + r \cdot \frac{d}{dr}(h^2 - r^2)^2 \right] \\
&= -6C \cdot \left[(h^2 - r^2)^2 \cdot 1 + r \cdot 2(h^2 - r^2) \cdot (-2r) \right] \\
&= -6C \cdot \left[(h^2 - r^2)^2 - 4r^2(h^2 - r^2) \right] \\
&= -6C \cdot (h^2 - r^2) \cdot \left[(h^2 - r^2) - 4r^2 \right]
\end{aligned}$$

Combining these results

$$\begin{aligned}
\frac{2}{r} \cdot \frac{\partial f}{\partial r} + \frac{\partial^2 f}{\partial r^2} &= \frac{2}{r} \cdot (-6Cr(h^2 - r^2)^2) + (-6C \cdot (h^2 - r^2) \left[(h^2 - r^2) - 4r^2 \right]) \\
&= -12C \cdot (h^2 - r^2)^2 - 6C \cdot (h^2 - r^2) \cdot \left[(h^2 - r^2) - 4r^2 \right] \\
&= -6C \cdot (h^2 - r^2) \left[2(h^2 - r^2) + (h^2 - r^2 - 4r^2) \right] \\
&= -6C \cdot (h^2 - r^2) \left[3(h^2 - r^2) - 4r^2 \right] \\
&= -6C \cdot (h^2 - r^2) \cdot (3h^2 - 7r^2) \\
&= -6C \cdot (3h^4 - 10h^2r^2 + 7r^4) \\
&= C \cdot [-6(3h^4 - 10h^2r^2 + 7r^4)]
\end{aligned}$$

Therefore

$$\nabla^2 W(\mathbf{r}, h) = \frac{315}{64\pi h^9} \begin{cases} -6(3h^4 - 10h^2r^2 + 7r^4) & 0 \leq r \leq h \\ 0 & otherwise \end{cases}$$

□